NASA CR - 167914

NASA

EXHAUST EMISSIONS REDUCTION FOR INTERMITTENT COMBUSTION AIRCRAFT ENGINES

FINAL REPORT

BY
BERNARD J. REZY
KENNETH J. STUCKAS
J. RONALD TUCKER
JAY E. MEYERS

TELEDYNE CONTINENTAL MOTORS
Aircraft Products Division

PREPARED FOR
NATIONAL AERONAUTICS AND SPACE ADMINISTRATION

NASA LEWIS RESEARCH CENTER
CLEVELAND, OHIO 44135
CONTRACT NAS3-19755

1. Report No.	2. Government Accession No.	3. Recipient's Catalog No.
NASA CR-167914		

4. Title and Subtitle	5. Report Date
Exhaust Emissions Reduction For Intermittent Combustion Aircraft Engines	May 1982
	6. Performing Organization Code
7. Author(s)	8. Performing Organization Report No.
B. J. Rezy, K. J. Stuckas, J. R. Tucker, J. E. Meyers	
	10. Work Unit No.
9. Performing Organization Name and Address	
Teledyne Continental Motors Aircraft Products Division P. O. Box 90 Mobile, AL 36601	11. Contract or Grant No. NAS3-19755
	13. Type of Report and Period Covered Contractor Final Report
12. Sponsoring Agency Name and Address	
National Aeronautics and Space Administration Washington, D.C. 20546	14. Sponsoring Agency Code

15. Supplementary Notes

Project Manager, Kaleel L. Abdalla
NASA Lewis Research Center
Cleveland, OH

16. Abstract

Exhaust emissions standards promulgated by the U. S. Environmental Protection Agency for aircraft piston engines, rising fuel prices and the possibility of reduced fuel availability generated the need for research aimed at reducing exhaust emissions while at the same time improving the fuel economy of General Aviation aircraft piston engines.

Projected benefits from exploratory testing and analytical predictions have resulted in this effort to investigate and develop three concepts which, when applied to an aircraft piston engine, provide reductions in exhaust emissions of hydrocarbons and carbon monoxide while simultaneously improving fuel economy.

The three chosen concepts, (1) an improved fuel injection system, (2) an improved cooling cylinder head, and (3) exhaust air injection, when combined, show a synergistic relationship in achieving these goals.

In addition, the benefits of variable ignition timing were explored and both dynamometer and flight testing of the final engine configuration were accomplished.

17. Key Words (Suggested by Author(s))	18. Distribution Statement
Aircraft Piston Engine Spark-Ignition Engine Exhaust Emissions	

19. Security Classif. (of this report)	20. Security Classif. (of this page)	21. No. of Pages	22. Price*
Unclassified	Unclassified	54	

* For sale by the National Technical Information Service, Springfield, Virginia 22161

TABLE OF CONTENTS

LIST OF ILLUSTRATIONS

LIST OF TABLES

SECTION 1.0
SUMMARY

Exhaust emissions standards promulgated by the U. S. Environmental Protection Agency for aircraft piston engines, rising fuel prices and the possibility of reduced fuel availability generated the need for research aimed at reducing exhaust emissions while at the same time improving the fuel economy of General Aviation aircraft piston engines.

Projected benefits from exploratory testing and analytical predictions have resulted in this effort to investigate and develop three concepts which, when applied to an aircraft piston engine, provide reductions in exhaust emissions of hydrocarbons and carbon monoxide while simultaneously improving fuel economy.

The three chosen concepts, (1) an improved fuel injection system, (2) an improved cooling cylinder head, and (3) exhaust air injection, when combined, show a synergistic relationship in achieving these goals.

In addition, variable ignition timing was explored and a flight test was conducted on a prototype engine containing all the improvements.

The results show that a flightworthy engine can be designed to reduce emissions of carbon monoxide and hydrocarbons to levels well within the former EPA standards, while at the same time showing improvements in fuel economy of over 6 percent on a typical flight profile and 27 percent on the LTO cycle.

SECTION 2.0
INTRODUCTION

The Aircraft Products Division of Teledyne Continental Motors (TCM) has been actively engaged in research aimed at improving the fuel economy and reducing exhaust emissions of its General Aviation aircraft piston engines. The requirement for this work came from two sources. First, the U. S. Environmental Protection Agency (EPA), under provisions of Section 231 of the Clean Air Act set exhaust emissions standards for aircraft and aircraft engines (1)*. This regulation, published in 1973, included standards for aicraft piston engines which were to go into effect after December 31, 1979. Second, recent awareness of the need for reduced energy consumption by the various sectors of private and public transportation led to efforts to improve the fuel economy of General Aviation aircraft piston engines. This effort was given impetus by the reality of increased fuel prices and the possibility of reduced fuel availability.

The work presented here was done under Contract NAS3-19755 funded jointly by NASA Lewis Research Center and Teledyne Continental Motors.

SECTION 3.0
FUEL ECONOMY AND THE AIRCRAFT PISTON ENGINE

The fuel economy of the modern air-cooled aircraft piston engine depends to a great extent on a number of considerations not directly related to the efficiency of the combustion process. Engine cooling, pilot fuel management technique, material limitations, engine acceleration, detonation and cold starting all play a part in the overall fuel economy of the engine throughout its operating range.

A generalized mixture ratio curve presented in Figure 1 shows the effect that fuel-air ratio has on fuel economy, power, cylinder head temperature (CHT) and exhaust gas temperature (EGT). While the absolute values of these parameters change with engine power, the relationship shown here is approximately true for operation over the normal flight regime of the engine from 40 - 100% power. Best power occurs at about 0.076 fuel-air ratio, peak cylinder head temperature at 0.067 which is the stoichiometric (chemically correct) fuel-air ratio, peak exhaust gas temperature at 0.062, and best economy at 25 F° lean of peak EGT at a fuel-air ratio in the vicinity of 0.059.

Beyond best economy, a point exists where the EGT begins to increase before the lean misfire limit is reached. This increase in EGT is thought to be the result of retarded flame propagation from the flame kernel initiated by one or both of the two spark plugs in the combustion chamber. As the mixture is leaned beyond this point, the retardation of flame propagation increases, delaying complete combustion to a point later in the expansion stroke. The result is higher EGT, lower CHT, lower power and poorer fuel economy. Taken to an extreme where one magneto is turned off so that only one spark plug fires, the same effect can be demonstrated except increases in EGT of about 250 F° can occur.

While the "lean misfire limit" has been variously defined (2-5), it will be defined here as a point at which the engine operator detects audible roughness in engine operation. This point is characterized by a sudden decrease in EGT and usually occurs between fuel-air ratios of .052 and .042 depending on the engine, ignition timing and fuel system.

From Figure 1 it is easy to postulate a fuel schedule for maximum economy, disregarding any additional practical considerations. When full power is desired, the engine must be operated at wide open throttle and best power fuel-air ratio. Between full power and closed throttle the engine should be operated at best economy fuel-air ratio. At closed throttle, regardless of engine speed, the leanest possible fuel-air ratio which will

* Numbers in parenthesis designate references at end of paper.

maintain steady combustion will yield minimum fuel consumption. The latter flight condition can be visualized as a closed throttle, high speed descent where the airflow across the propeller is overdriving the engine.

However, when practical engine operation is considered, limitations to this ideal fuel schedule must be taken into account as shown in Figure 2. The IO-520 engine is the basis for the work done in this study and its specifications are presented in Table 1. TCM continuous flow fuel system normally used on this engine is a simple, low cost, reliable system which responds only to variations in throttle angle and engine speed (6). Because this type of fuel injection system is insensitive to variations in ambient air density, nominal full rich fuel flow is set at a value which provides a margin for adequate performance. The production tolerance band permits the full rich fuel flow to fall anywhere within these limits for standard day conditions. Manual leaning is permitted only within the shaded area.

This restricted manual leaning region is intended to provide adequate cooling and detonation free operation at maximum rated power (105% of maximum continuous power), as well as in the climb power region from 75% to 100% power. Variable geometry cowl flaps also aid in cooling the engine during climb, reducing the requirement for further enrichening the fuel-air mixture to maintain cylinder head temperatures below the allowable limit of 460° F.

At 75% power - that is, a manifold pressure and RPM which gives 75% power at full rich fuel flow - leaning is permitted to peak EGT long enough to determine its value so that enrichening to 50 F° rich of peak EGT is possible. This limitation is set to provide exhaust valve and valve guide durability as well as a detonation margin. The leaning limit of 50 F° rich of peak EGT applies to cruise operation in the 65% to 75% power range.

At 65% power or below, leaning to peak EGT or below is allowed, as the value of peak EGT is below that which occurs at the 75% maximum cruise power point when set 50 F° rich of peak EGT (7).

From Figure 2 then, it can be seen that the fuel economy potential of this engine can be fully realized only in operation at or below 65% of maximum continuous power.

While the fuel economy potential of the engine itself is important, overall aircraft fuel economy is dictated by airframe aerodynamic efficiency. The 7500-foot density altitude cruise performance of a typical General Aviation single-engine aircraft is shown in Figure 3. Maximum economy for the aircraft occurs at 55% power giving a savings of 19.5% in fuel used per mile over cruise at 75% power at the expense of 18.5% more time in cruise. If operation at best economy were permitted at 75% power, a fuel savings of 9% would be possible over operation at 75% power and 50 F° rich of peak EGT. In order for operation at best economy and 75% power to be permitted, the obstacles of exhaust valve and valve stem durability would have to be overcome.

Of course, fuel economy during the non-cruise modes of operation can also be improved. Below the normal minimum cruise power level of about 42% of maximum continuous power fuel savings can be achieved

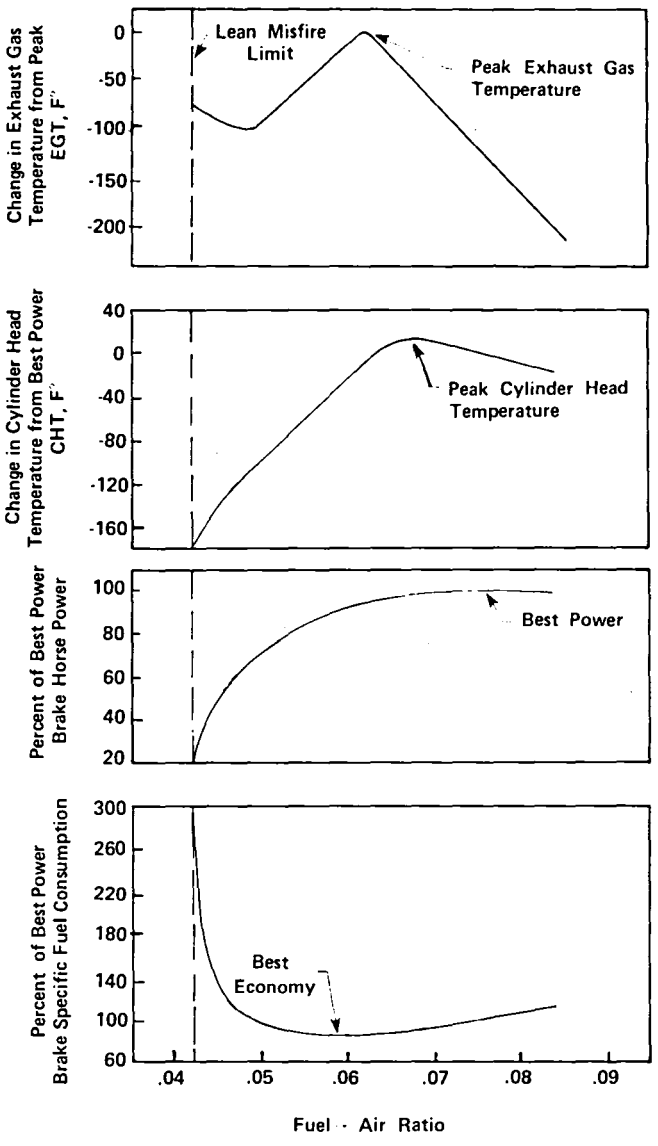

Fig. 1 - Effect of fuel-air ratio on power, brake specific fuel consumption, cylinder head temperature and exhaust gas temperature at constant engine speed, manifold pressure and spark timing.

Table 1 - IO-520 Engine Specification

Manufacturer	Teledyne Continental Motors
Model	IO-520
Cylinder Arrangement	Six Cylinder Horizontally Opposed
Compression Ratio	8.5:1
Bore (inches)	5.25
Stroke (inches)	4.00
Piston Displacement (cu. in.)	520
BRAKE HORSEPOWER	
Rated Maximum Takeoff	300 @ 2850 RPM
Rated Maximum Continuous	285 @ 2700 RPM
Maximum Cruise	215 @ 2550 RPM
IGNITION SYSTEM	DUAL MAGNETO
Spark Timing	22° BTC
Firing Order	1-6-3-2-5-4
DIMENSIONS AND WEIGHT	
Length (inches)	36.86
Width (inches)	33.56
Height (inches)	23.79
Basic Engine Dry Weight (lb)	430
Total Weight of Basic Engine and Accessories (lb)	472
FUEL SYSTEM	Teledyne Continental Motors Continuous Flow Fuel Injection
MINIMUM OCTANE REQUIREMENT	100/130 Avgas

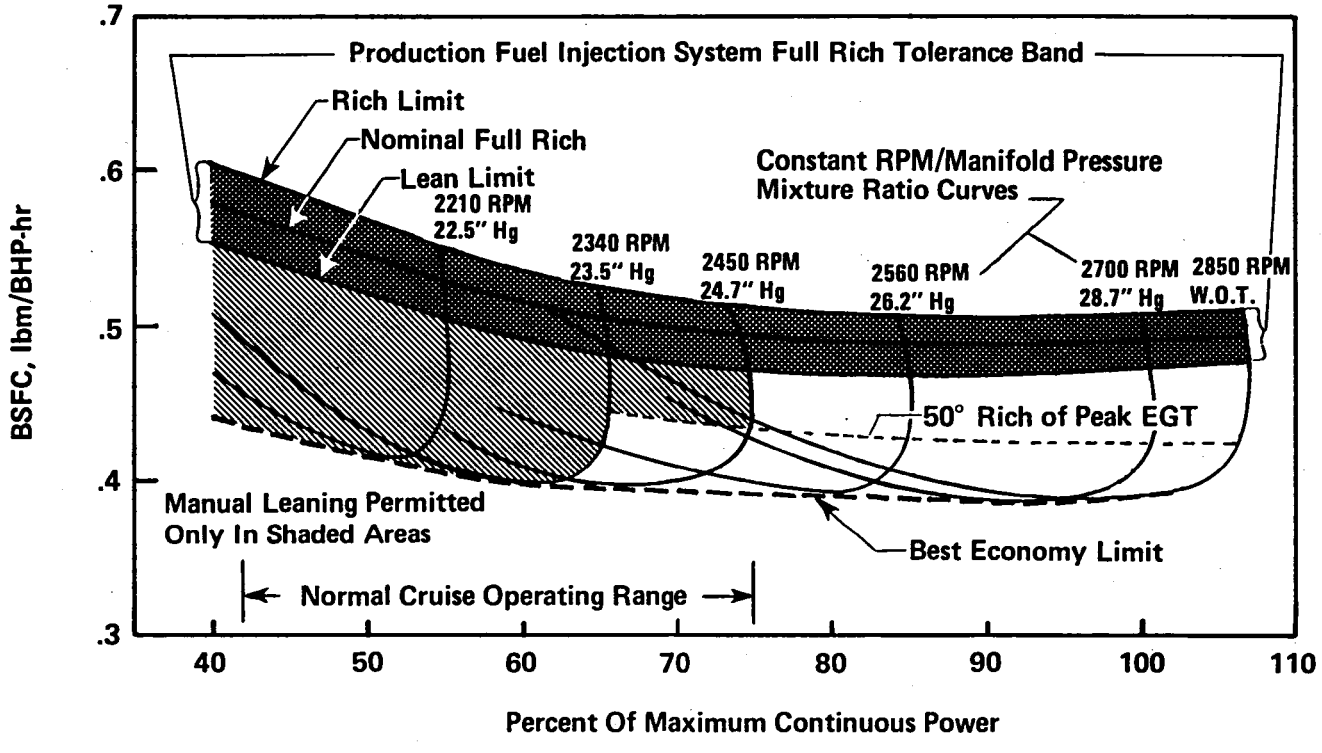

Fig. 2 - IO-520 engine propeller load fuel economy and operating range limitations at sea level.

by operating in accordance with the previously postulated maximum economy fuel schedule. In this region, operation at best economy fuel-air ratio is desirable. There are several practical considerations which must be dealt with. Near idle, the fuel system must be set rich enough to give consistent cold starting and cold idle operation. Since no acceleration pump is used on the TCM fuel injection system, fuel flow must be sufficient to provide acceptable engine transient response to wide open throttle from all part throttle operating points.

Another effect of lean operation at low powers which is more difficult to quantify is the reduction in cylinder head durability due to low cycle thermal stress superimposed upon the high cycle mechanical stress of combustion pressure. This low cycle thermal stress is caused by the normal aircraft operating cycle - high cylinder head temperatures during take off and climb modes of operation and low temperatures during high speed descent modes. Leaning to best economy in descent at low powers results in cylinder head temperatures which are lower than at best power or even full rich fuel flow (see Figure 1). This overcooling effect can have an impact on cylinder head life.

The following list summarizes the limitations that presently exist which prevent maximum possible fuel economy from being realized for the IO-520 engine.

1. Rich operation in all operating modes except cruise, to accommodate fuel injection system insensitivity to changes in ambient pressure and temperature.
2. Rich operation in all low power modes to allow smooth engine transient response.
3. Rich operation at high powers for cylinder head cooling and detonation suppression.
4. Restricted leaning between 65 - 75% because of material limitations (valves, valve guides, and cylinder heads).
5. Pilot manual mixture control technique

SECTION 4.0
EXHAUST EMISSIONS AND THE AIRCRAFT PISTON ENGINE

Once the fuel-air ratio mixture requirements are understood as being a function of engine operational considerations for the model IO-520 aircraft piston engine, the exhaust emission characteristics are more easily put into perspective. Table 2 is an example flight profile for a single engine, General Aviation aircraft which will be used as the basis for the discussion of both fuel economy and exhaust emissions. This flight profile involves a flight of 328.8 statute miles over a total time of 2 hours and 14 minutes using 26.14 gallons of fuel.

The first four modes - Idle, Taxi Out, Takeoff, Climb and the last three modes - Approach, Taxi In, Idle - comprise a landing/takeoff (LTO) cycle of operation below 3,000 feet above mean sea level (MSL). All operation in the LTO cycle is at full rich mixture. While 20% of the total time is spent in the LTO modes, only 6% of the total distance is covered using 13% of the fuel consumed during the trip.

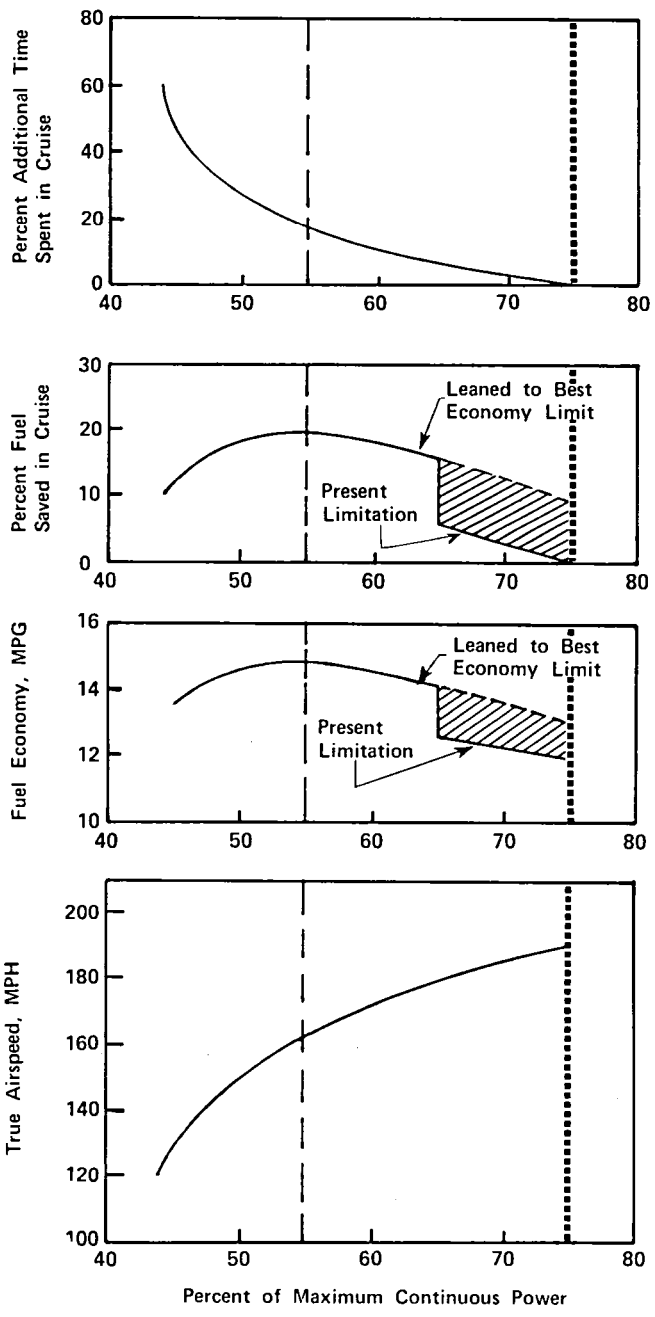

Fig. 3 - Cruise performance and fuel economy of typical single-engine aircraft powered by IO-520 engine, 7500 foot density attitude.

Table 2 - Example flight profile for a single-engine General Aviation airplane powered by a TCM IO-520 engine

	MODE OF OPERATION	TIME IN MODE (minutes)	% MAX CONTIN-UOUS POWER	TRUE AIRSPEED (stat. mi/hr)	DISTANCE TRAVELED PER MODE (statute mi)	FUEL RATE PER MODE (lbm/hr)	FUEL USED PER MODE (Gallons)	ALTITUDE (feet ASL)	MIXTURE LEVER POSITION
*	IDLE	1.0	0.5	–	–	6.0	.02	S.L.	FULL RICH
*	TAXI OUT	11.0	2.8	–	–	14.0	.44	S.L.	FULL RICH
*	TAKEOFF	0.3	105.3	–	–	148.0	.13	S.L.	FULL RICH
*	CLIMB	5.0	75.0	108	9.0	105.8	1.52	S.L.→3000'	FULL RICH
	ENROUTE CLIMB	7.5	75.0	108	13.5	93.0	2.00	3000→7500'	PART LEAN
	CRUISE	90.0	65.0	179	268.5	73.7	19.06	7500'	BEST ECONOMY
	CRUISE DESCENT	9.0	55.0	179	27.0	64.0	1.65	7500→3000'	BEST ECONOMY
*	APPROACH	6.0	40.0	108	10.8	68.2	1.18	3000'→S.L.	FULL RICH
*	TAXI IN	3.0	2.8	–	–	14.0	.12	S.L.	FULL RICH
*	IDLE	1.0	0.5	–	–	6.0	.02	S.L.	FULL RICH
	TOTALS	133.8	–	–	328.8	–	26.14	–	–

AVG. TRIP FUEL ECONOMY (mi/gal) - 12.58
AVG. TRIP SPEED (mi/hr) - 147.44
PERCENT FUEL USED DURING LTO CYCLE - 13.12
PERCENT TIME SPENT IN LTO CYCLE - 20.40
PERCENT DISTANCE TRAVELED DURING LTO CYCLE - 6.02

* EMISSIONS LANDING/TAKEOFF (LTO) CYCLE MODES

Table 3A - EPA five-mode landing /takeoff (LTO) cycle requirements

MODE NO.	MODE NAME	TIME-IN-MODE (min.)	POWER (%)	ENGINE RPM (%)
1	TAXI/IDLE OUT	12.0	***	***
2	TAKEOFF	0.3	100	100
3	CLIMB	5.0	75 to 100	***
4	APPROACH	6.0	40	***
5	TAXI/IDLE IN	4.0	***	***
	TOTAL CYCLE	27.3		

*** Manufacturer's Recommended

Table 3B - IO-520 five-mode landing/takeoff (LTO) cycle
Power and engine RPM are in percent of maximum continuous (285 BHP/2700 RPM)

MODE NO.	MODE NAME	TIME-IN-MODE (min.)	POWER (%)	ENGINE RPM (%)
1	TAXI/IDLE OUT	12.0	2.8	44.4
2	TAKEOFF	0.3	105.3	105.6
3	CLIMB	5.0	75.0	92.6
4	APPROACH	6.0	40.0	77.8
5	TAXI/IDLE IN	4.0	2.8	44.4
	TOTAL CYCLE	27.3		

The EPA five-mode LTO cycle is presented in Table 3A. Note that the separate Idle and Taxi modes of Table 2 are combined into Taxi/Idle Out and Taxi/Idle In modes in Table 3A. The power level of these modes, as permitted by the EPA, may be recommended by the manufacturer. For this engine, the Taxi/Idle mode will be 1200 RPM engine speed (about 3.0% power). The climb mode was selected at 75% maximum continuous power as shown in Table 3B.

The EPA standards for emission of CO, HC and NOx are shown in Table 4, where emissions of each pollutant for the five-mode LTO cycle are calculated as follows:

$$P_c = \frac{\sum_{i=1}^{5} \left(\dot{m}_{P_i}\, t_i\right)}{\text{BHP (maximum rated)}} \quad \text{(lbm P /BHP - cycle)} \qquad (1)$$

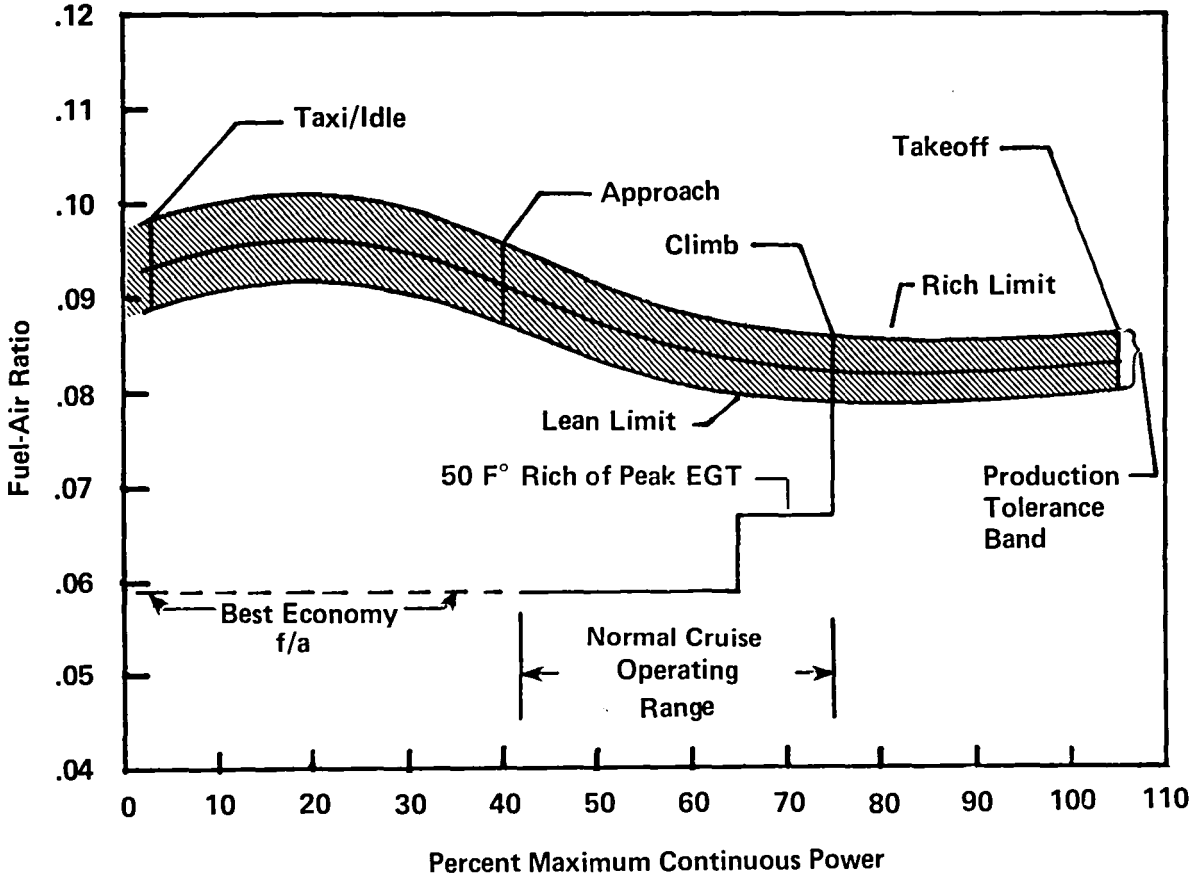

Fig. 4 - IO-520 full-rich production tolerance fuel-air ratio limits vs. percent maximum continuous power for 60° F, 60% relative humidity, 29.92 in. Hg ambient air.

Table 4 - EPA aircraft piston engine exhaust emissions standards for the five-mode LTO cycle.

POLLUTANT	EPA STANDARD
CO	.042 lbm CO/BHP - cycle
HC	.0019 lbm HC/BHP - cycle
NOx	.0015 lbm NOx/BHP - cycle

where P_c is the total mass of pollutant P per brake horsepower over the five-mode cycle, $\dot{m}_{p_i}$ is the mass rate of the pollutant in the i^{th} mode and t_i is the time-in-mode for the i^{th} mode.

During operation of an aircraft below 3,000 feet MSL, it is common practice to leave the mixture in the full-rich position. Since exhaust emissions are a principal function of power and fuel-air ratio, the full-rich mixture schedule is the determining factor in emission levels during LTO cycle operation. Figure 4 shows fuel-air ratio variation limits based on the production fuel flow tolerance band for the IO-520 engine as a function of percent maximum continuous power. Variations in power and fuel-air ratio due to non-standard day conditions are not included, since all emissions testing is done at standard sea level conditions (60° F, 60% relative humidity, 29.92 in. Hg pressure). Full rich fuel-air ratios can vary from 0.0785 to 0.1010 over the power range. The tendency is for fuel-air ratios to be near best power at high powers and slightly rich of that at lower powers to promote suitable transient response even at adverse ambient conditions.

The exhaust emissions of this engine operated over the LTO cycle are shown in Figure 5, as a percent of EPA standard. The emissions at the rich limit and lean limit of the production fuel flow tolerance band for the LTO cycle show the large variability which might exist in production IO-520 engines. Carbon monoxide could vary from 156 to 208 percent of the EPA limits, hydrocarbon variations from 107 to 129 percent of the standard are possible and a range of oxides of nitrogen from 12 to 8 percent could occur. From this it seems clear that any attempts to

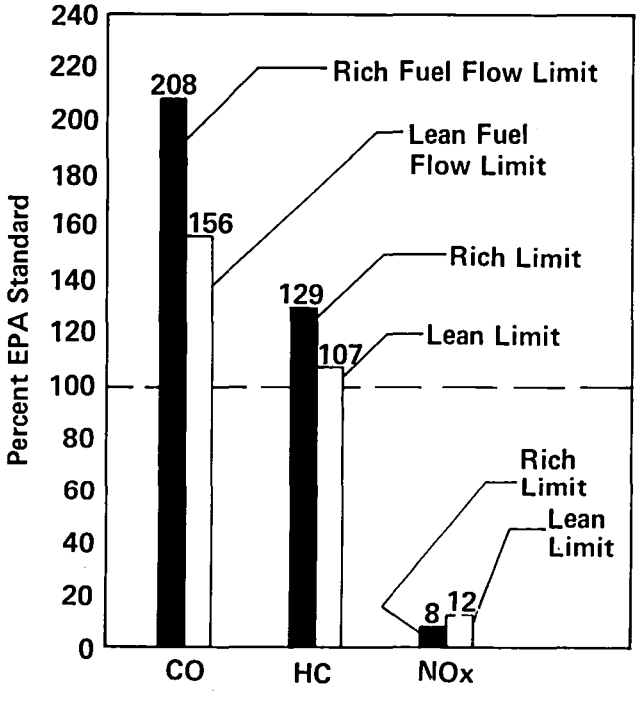

Fig. 5 - IO-520 exhaust emissions as a percent of EPA standards for rich and lean limit production fuel flow over the LTO cycle

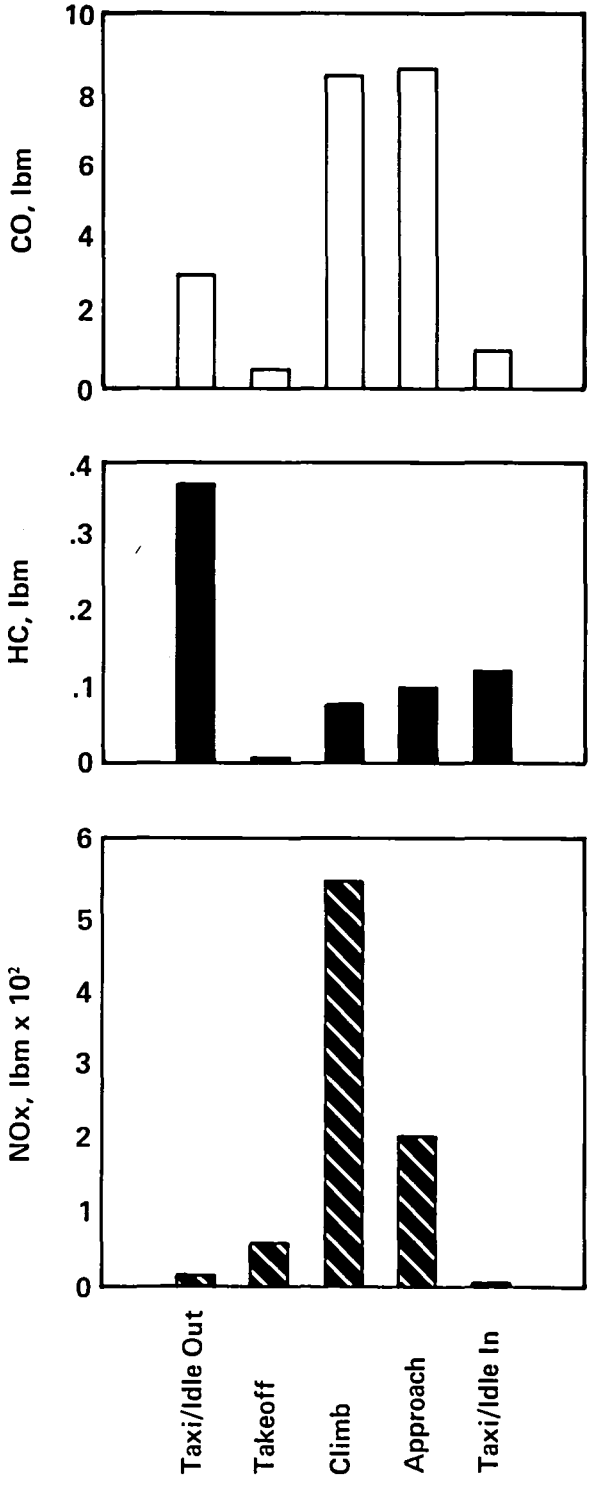

Fig. 6 - Individual mode contributions to total LTO cycle emissions levels of the IO-520 engine at nominal production schedule fuel flows.

control emissions should begin by reducing this wide variability through improved fuel injection system design. The next step would be to address individually each item which forces the fuel system to be richer than necessary over the entire operating range. Items such as engine transient response from low powers, cylinder head cooling at higher powers and exhaust valve guide and valve durability at moderate powers must be maintained at least at present levels.

Figure 6 shows the contribution of each of the five LTO modes to the total emissions of CO, HC, and NOx. The Takeoff mode does not contribute significantly to any of the three pollutant totals because it comprises only one percent of the LTO cycle time of 27.3 minutes. Concentrating efforts on the control of CO in the Climb and Approach modes, and HC in the Taxi/Idle modes will produce the most beneficial results. While NOx remains well below the EPA standard levels for full rich operation of the engine (Figure 5), attempts to control CO and HC by lean operation will result in increases in the NOx levels.

SECTION 5.0
CHOOSING THE THREE CONCEPTS

At the outset of this study an extensive literature search was conducted to choose a list of concepts which would be applied to the aircraft piston engine for the purpose of reducing exhaust emissions and improving fuel economy. Fourteen promising concepts, shown in Table 5, were selected for further evaluation.

Also, a set of cost-effectiveness criteria was selected by which the relative merits and benefits of the fourteen concepts could be evaluated. Table 6 is a list of these criteria.

A decision model that incorporates a computational algorithm (8, 9) was used to take the quantitative and qualitative judgements of a team of four engineers and provide a consensus ranking of the criteria. The criteria were assigned weighted values (emphasis coefficients) and an associated uncertainty factor (absolute certainty equals zero) as shown in Table 7. Then the concepts were ranked using the weighted criteria. The decision algorithm gave a final ranking of the concepts in order of importance and assigned weighted values (merit coefficients) and the associated uncertainties, as listed in Table 8.

Table 9 shows a matrix of concepts and criteria which indicates the relative rank of each of the concepts for each criterion. The three highest ranking concepts were thus chosen to be the most promising of the fourteen candidates in the effort to reduce exhaust emissions and improve fuel economy:

- Improved Cooling Cylinder Head
- Improved Fuel Injection System
- Exhaust Air Injection

Table 5 - Selected Emission Reduction Concepts

- Stratified Charge Combustion Chambers:
  - Honda Compound Vortex Controlled Combustion
  - Texaco Controlled Combustion System
  - Ford Programmed Combustion
- Improved Cooling Cylinder Head
- Diesel Combustion Chambers:
  - Four-Stroke, Open Chamber
  - Two-Stroke, McCulloch
- Variable Camshaft Timing
- Improved Fuel Injection Systems
- Ultrasonic Fuel Atomization – Autotronics System
- Thermal Fuel Vaporization – Ethyl Turbulent Flow System
- Ignition Systems:
  - Multiple Spark Discharge
  - Variable Timing
- Hydrogen Enrichment
- Exhaust Air Injection

Table 6 - Selected cost-effectiveness criteria used to evaluate the engine exhaust emission reduction design concepts

- COST
- RELIABILITY
- SAFETY
- TECHNOLOGY
- PERFORMANCE
- COOLING
- ADAPTABILITY
- OPERATIONAL CHARACTERISTICS
- MATERIALS
- INTEGRATION
- PRODUCIBILITY
- FUEL ECONOMY
- WEIGHT & SIZE
- MAINTAINABILITY & MAINTENANCE
- EMISSIONS

Table 7 - Engine exhaust emission reduction criteria emphasis coefficients and ranking - optimized

CRITERIA	EMPHASIS COEFFICIENT	UNCERTAINTY
Emissions	0.10952	0.00138
Safety	0.09676	0.00750
Performance	0.08714	0.00701
Cooling	0.07695	0.00707
Weight and Size	0.07238	0.01159
Fuel Economy	0.06990	0.01020
Cost	0.06771	0.01192
Reliability	0.05933	0.00903
Technology	0.05548	0.00658
Operational Characteristics	0.04200	0.01059
Maintainability and Maintenance	0.04029	0.00924
Integration	0.03324	0.00295
Materials	0.03029	0.00305
Producibility	0.02933	0.00210
Adaptability	0.02781	0.00267

Table 8 - Engine exhaust emission reduction concept final ranking

CONCEPT	RANK	MERIT COEFFICIENT	UNCERTAINTY
Improved Cooling Cylinder Head	1	0.07294	0.02391
Improved Fuel Injection Systems	2	0.07084	0.02165
Exhaust Air Injection	3	0.06540	0.02096
Multiple Spark Discharge System	4	0.06485	0.02201
Ultrasonic Fuel Atomization, Autotronic	5	0.05822	0.02018
Variable Timing System	6	0.05761	0.02024
Thermal Fuel Vaporization, Ethyl	7	0.05390	0.01986
Hydrogen Enrichment, JPL	8	0.04974	0.01641
Texaco CCS	9	0.04397	0.01657
Two-Stroke Diesel, McCulloch	10	0.04374	0.01691
Ford PROCO	11	0.04210	0.01549
Variable Camshaft Timing	12	0.04081	0.01659
Honda CVCC	13	0.04057	0.01548
Four-Stroke Diesel, Open Chamber	14	0.03471	0.01432

Table 9 - Concept rank ordering versus criteria importance

CONCEPT	CRITERIA														
	DOMINANT							SECONDARY				MINOR			
	EMISSIONS	SAFETY	PERFORMANCE	COOLING	WEIGHT AND SIZE	FUEL ECONOMY	COST	RELIABILITY	TECHNOLOGY	OPERATIONAL CHARACTERISTICS	MAINTAINABILITY AND MAINTENANCE	INTEGRATION	MATERIALS	PRODUCIBILITY	ADAPTABILITY
IMPROVED COOLING CYLINDER HEAD	9	1	6	1	1	6	6	3	2	1	1	6	3	2	4
IMPROVED FUEL INJECTION SYSTEM	3	2	1	14	2	5	7	4	1	6	2	4	2	7	6
EXHAUST AIR INJECTION	4	5	8	9	6	14	1	5	3	3	5	2	6	1	1
MULTIPLE SPARK DISCHARGE SYSTEM	14	3	5	7	3	12	2	6	4	2	3	1	1	5	2
ULTRASONIC FUEL ATOMIZ, AUTORONIC	12	4	9	11	5	10	4	1	5	5	4	10	4	4	7
VARIABLE TIMING IGNITION SYSTEM	13	6	3	8	4	11	5	7	7	9	6	3	5	6	3
THERMAL FUEL VAPORIZATION, ETHYL	11	7	10	13	7	9	3	2	6	4	7	9	7	3	5
HYDROGEN ENRICHMENT, JPL	1	14	7	4	8	1	12	8	9	12	8	7	14	8	8
TEXACO CCS	5	8	12	2	10	2	10	12	13	10	13	11	13	11	11
TWO STROKE DIESEL, McCULLOCH	7	11	2	6	13	4	13	9	11	13	9	13	12	13	14
FORD PROCO	6	9	13	3	11	3	9	11	14	11	14	12	9	12	12
VARIABLE CAMSHAFT TIMING	10	13	4	10	9	13	8	14	8	8	10	5	8	9	9
HONDA CVCC	2	12	11	12	12	8	11	13	10	7	11	8	10	10	10
FOUR-STROKE DIESEL, OPEN CHAMBER	8	10	14	5	14	7	14	10	12	14	12	14	11	14	13

SECTION 6.0
IMPROVED FUEL INJECTION

As indicated previously, cooling requirements, detonation limits and transient response characteristics are some of the operating limitations that constrain engine performance. Differences in fuel metering and distribution methods (10) such as carburetor venturi or injector nozzle delivery, injector location, fuel blend and vaporization characteristics are important considerations that significantly affect engine start-up, idle and transient response. Functional differences between continuous flow and timed fuel injection systems can affect engine performance and exhaust pollutants. Depending on the engine operating mode, the above constraints can be quite subtle or dramatic for a selected fuel metering approach. Also, ambient temperature, pressure and humidity (11) influence fuel metering unit design and ultimately, engine performance.

6.1 FUEL INJECTION SYSTEM SELECTION — Six fuel injection systems were evaluated for application to the aircraft piston engine. Table 10 presents a listing of timed, pulsed and continuous flow fuel injection systems and their attributes. The TCM continuous flow fuel injection system is certified for aircraft application and is presented for reference. Based on Table 10 and other performance information, it was possible to make a rational choice among the contending fuel injection systems. Table 11 shows the results of a study conducted for evaluating the most promising fuel injection concepts and how each ranked in comparison to the criteria.

A modified Simmonds Precision timed fuel injection system, designated DTU (Development Test Unit), was selected because it contained the necessary design features that are required to control the mixture ratio, while providing the capability of exploring variable injection timing. Also, the Simmonds system has proven reliability in aircraft and military applications. The Simmonds DTU is shown in Figure 7.

Table 10 - Fuel injection comparison chart.

PARAMETER		SYSTEM						
		BENDIX	BOSCH D	BOSCH L	BOSCH K	LUCAS	SIMMONDS	TCM
TYPE OF SYSTEM		ELEC.	ELEC.	ELEC.	MECH.	ELEC.	SERVO-MECH.	MECH.
TYPE OF INJECTION		PULSED (2)	PULSED (2)	PULSED (2)	CONTIN-UOUS	PULSED (2)	TIMED	CONTIN-UOUS
INJECTION PRESSURE (PSI)		30	30	40	48	30	90	4-18
FUEL METERING CONTROL		SPEED DENSITY +	SPEED DENSITY +	AIR FLOW METER +	AIR FLOW METER	SPEED DENSITY +	SPEED DENSITY	SPEED DENSITY
ALTITUDE COMPENSATION DEVICE		DIA-PHRAGM	DIA-PHRAGM	NONE	NONE	DIA-PHRAGM	ANEROIDS	ANEROID
SIZE	L*W*H (inches)				12*6*8*		3.7dia*8.7	5*7*3.5
	Volume (cubic inches)	~400	~400	~600	576	~400	94	123
WEIGHT (lbs)		~ 16	~ 16	~ 18	24	~ 16	12	8
MIXTURE CONTROL DEVICE		NONE	NONE	NONE	NONE	NONE	NONE/570 LEVER/580	LEVER
CALIBRATION & ADJUSTMENT		COMPLEX	COMPLEX	COMPLEX	SIMPLE	COMPLEX	RELA-TIVELY SIMPLE	SIMPLE
APPLICATION		AUTO-MOTIVE	AUTO-MOTIVE	AUTO-MOTIVE	AUTO-MOTIVE	AUTO-MOTIVE	AUTO-MOTIVE AIRCRAFT BOAT	AIRCRAFT INDUS-TRIAL

Table 11 - Fuel injection system concept rank ordering versus criteria importance.

CONCEPT	DOMINANT CRITERIA							
IMPROVED FUEL INJECTION SYSTEMS	EMISSIONS	SAFETY	PERFORMANCE	COOLING	WEIGHT & SIZE	FUEL ECONOMY	COST	CRITERIA WEIGHTED RANKING
BOSCH D JETRONIC	1	4	2	5	3	3	4	3
BOSCH L JETRONIC	4	5	4	4	5	4	5	5
BOSCH K JETRONIC	5	3	5	3	4	5	3	4
SIMMONDS INJECTION	2	2	1	2	2	1	2	1
TCM INJECTION (Modified for density compensation)	3	1	3	1	1	2	1	2

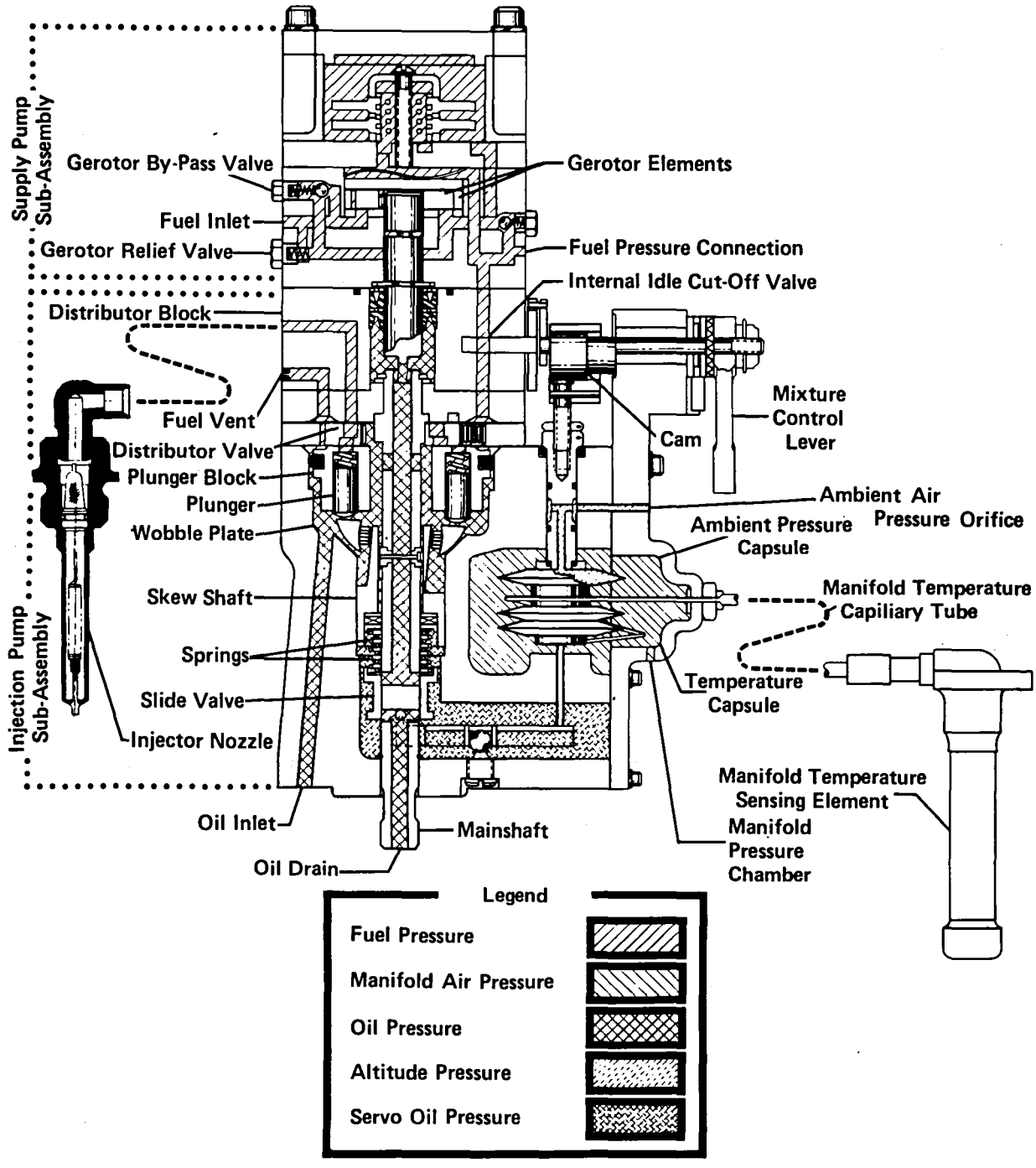

Fig. 7 - Simmonds DTU timed fuel injection system.

In this system the fuel injection pump is driven by the engine at crankshaft speed. A wobble plate is connected to the pump mainshaft and imparts a reciprocating motion to three fuel plungers when rotated. An oil operated servo system responding to manifold pressure, temperature and pressure altitude, varies the plunger stroke.

Fuel distribution from the individual plungers to the proper injection nozzle is coordinated by a rotating distributor valve that permits each plunger to deliver fuel to two different cylinders on alternate crankshaft revolutions. This is necessary on this particular unit because the pump is driven at engine crankshaft speed and injects over a 180-degree period. On a six-cylinder engine, for instance, each of the three plungers supplies fuel to two different cylinders.

Table 12 - Initial engine operating test conditions, IO-520-D

Mode	Horsepower (BHP)	Speed (rpm)	Manifold Pressure (in. Hg abs.)	Percent Horsepower (%)	Percent Speed (%)
Take Off	300	2850	28.9	105	105.5
Climb	214	2500	25.0	75	93
Approach	114	2100	20.7	40	78
Taxi/Idle	7	1200	13.5	3	44
* * * *	* * * *				
Cruise 1	165	2200	24.2	58	81
Cruise 2	194	2400	24.5	68	89
Cruise 3	214	2500	25.0	75	93

6.2 TESTING - Tests were conducted to determine what advantage could be obtained by using a timed, density-compensated fuel injection system in comparison to the TCM low pressure continuous flow system. The following parameters were investigated:

1) Effect on Maximum power.
2) Effect on exhaust emissions due to injection timing.
3) Effect on exhaust emissions due to density compensation.
4) Effect on fuel economy.
5) Effect on transient response.

Table 12 defines the engine test conditions which include the LTO cycle and three cruise conditions. Both the TCM and Simmonds DTU were assessed over the same operating conditions.

6.3 EFFECTS OF INJECTION TIMING - With injection duration fixed at 180 crankshaft degrees, the beginning of injection timing was varied such that total injection would occur at various times during the engine cycle. These changes in timing could only be accomplished manually when the engine was shut down, therefore direct comparisons of timing variations could not be made while the engine was running.

The region of greatest interest was established between 180-degrees BTC and TDC on the intake stroke. Starting injection during this interval meant that the 180-degree fuel spray duration would overlap the intake valve event (32° BTC - 246° ATC). Figure 8 shows the effect on CO and HC emissions with injection timing for the LTO cycle. Fuel flows were held constant at the nominal full rich production values. Best results were established when the injection period took place just before the valve opening event.

During this period the HC and CO emission levels were comparable to the TCM continuous fuel injection system. Starting injection after the intake valve began to open resulted in considerable increase in hydrocarbons while the carbon monoxide remained unchanged.

The reasons for such a dramatic change in hydrocarbons is unclear. Since the fuel charge is injected over a 180-degree crankshaft period and the effective intake valve opening period is 278 degrees, it is obvious that all the fuel charge should be injected into the combustion chamber even if the injection period starts shortly after the valve begins to open. However, the dynamics of the system, such as fuel injection pump piston displacement time, fuel line pressure rise and decay time, fuel nozzle opening time and induction manifold tuning all affect the fuel charge timing and type of charge (droplet size) captured by the combustion chamber.

A more detailed investigation of the injection periods between 30° and 90° BTC was undertaken by establishing mixture ratio variation data for both the TCM and the Simmonds DTU injection systems. The results of leaning did not change the above conclusions, that is, the Simmonds DTU system emission levels were equivalent to the TCM continuous flow system when compared at identical fuel-air ratios.

Varying the injection timing had no significant effect on maximum engine power which repeated within a few percent of its rated 300 BHP at 2850 RPM and wide open throttle. Also, fuel economy was not changed when compared at identical fuel-air ratios.

6.4 EFFECTS OF DENSITY COMPENSATION - Transient response was investigated for both the TCM and Simmonds DTU system. The test engine was operated at three steady-state modes; Idle, Taxi, and Approach. At each of these modes, an attempt was made to accelerate to wide open throttle conditions. If the engine did not reach full power operation within a three second time limit, the mixture ratio was considered unacceptable.

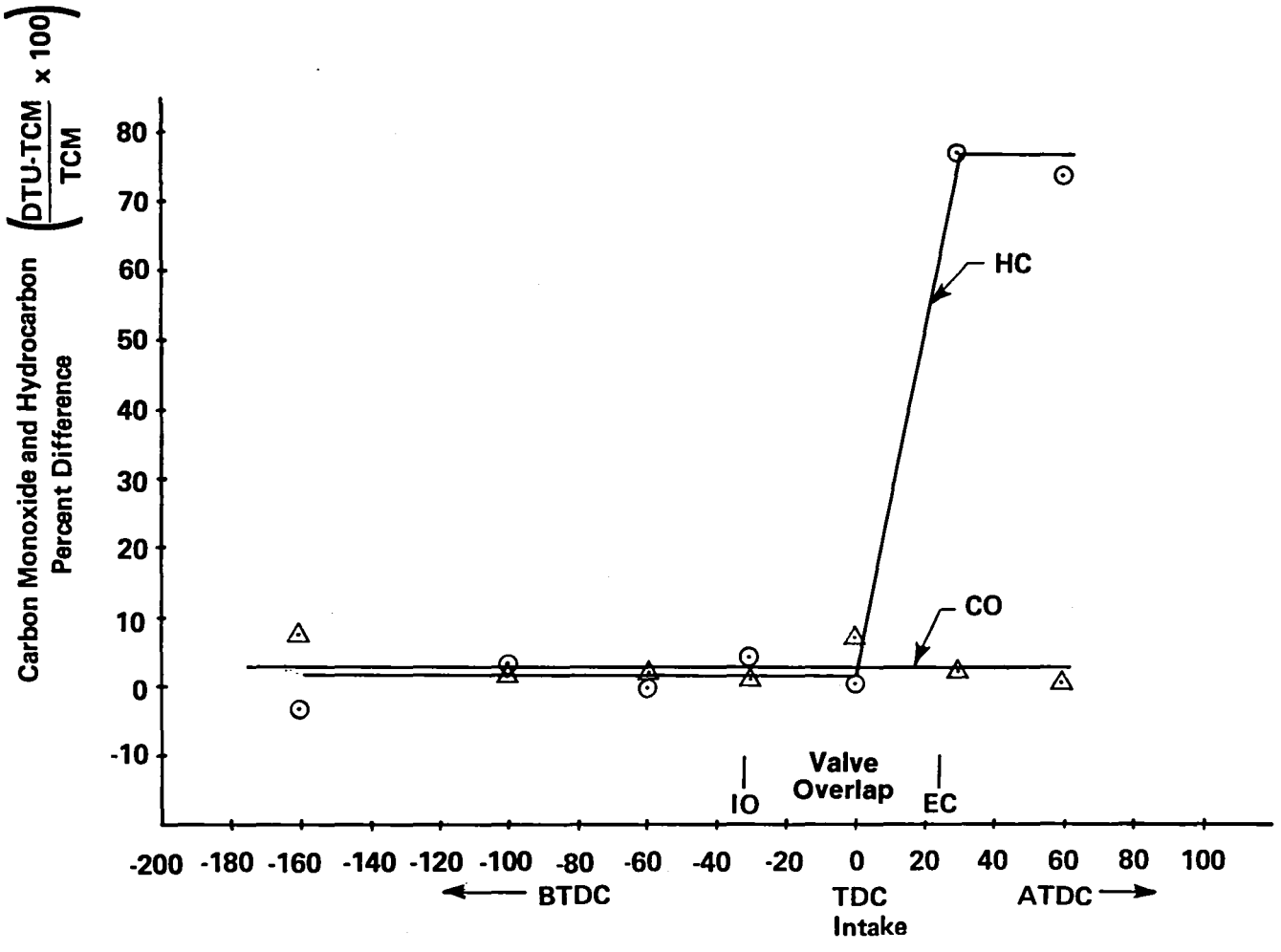

Fig. 8 - Comparison of IO-520 CO and HC emissions with TCM and Simmonds fuel injection systems.

For the TCM system, rich mixtures are required at the low power regime to provide adequate fuel distribution to all cylinders,and to insure adequate engine transient response. The Simmonds system, which senses changes in air density and engine speed, is capable of accelerating from much leaner fuel-air ratios.

A comparison between the TCM and Simmonds DTU fuel injection systems lean limit acceleration response is shown in Figure 9. The minimum acceptable fuel-air ratio for the TCM fuel injection system was 0.0685 in the Approach mode, compared to 0.0420 for the Simmonds DTU. Likewise, the Taxi/Idle mixture ratios could also be considerably reduced, 49% and 56% respectively.

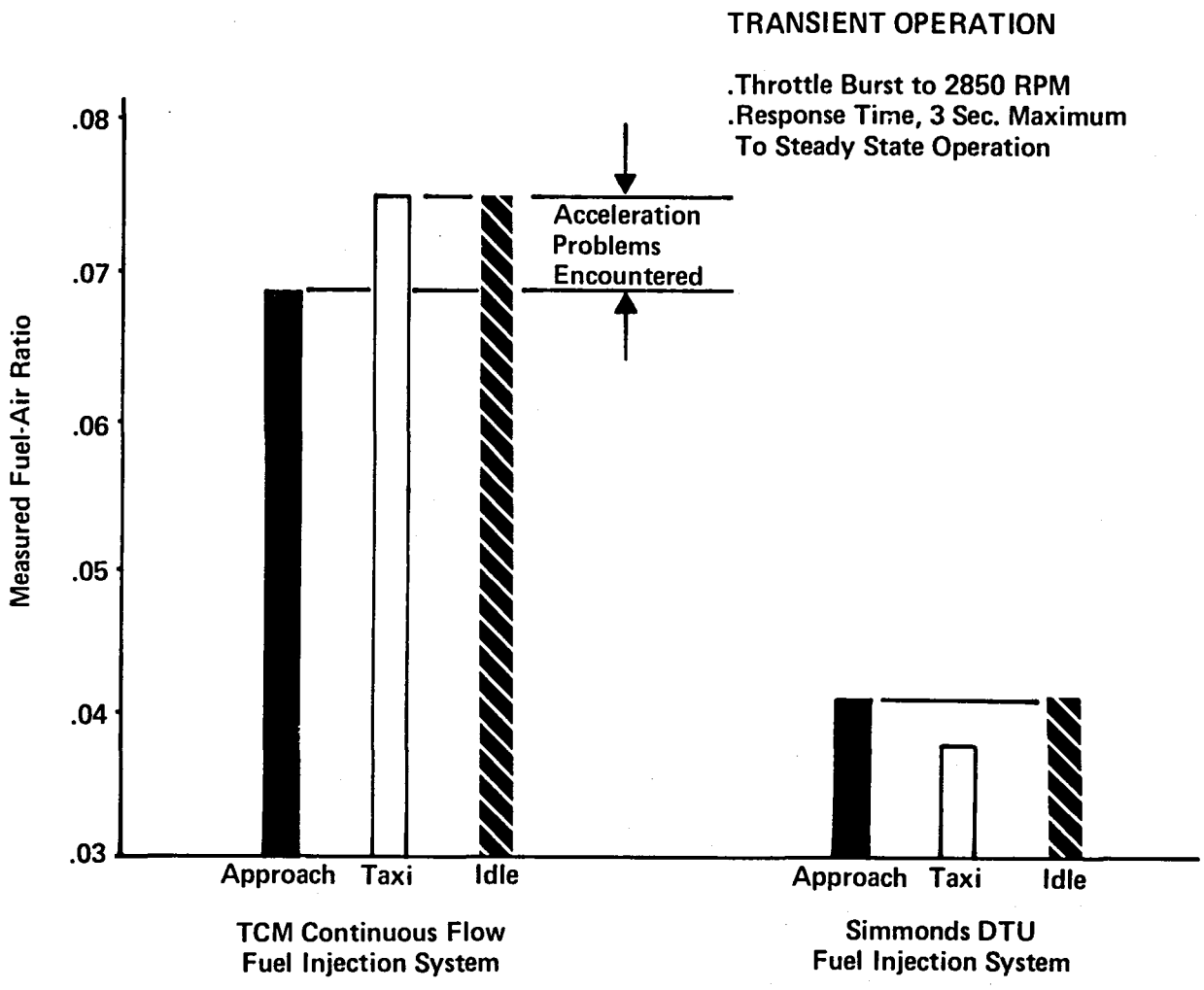

Fig. 9 - Comparision of minimum initial fuel-air ratios for acceleration from Approach, Taxi and Idle with TCM and Simmonds DTU fuel injection systems.

In order to fully explore both the TCM and the Simmonds DTU systems as to their potential for reducing emissions and fuel consumption, it is necessary to define the minimum acceptable fuel-air ratios for the LTO cycle. Table 13 summarizes the minimum acceptable mixture ratios for the two injection systems. The Takeoff and Climb modes are identical because the limiting fuel flows are cooling related. In the lower power modes, however, the limiting fuel flows are acceleration related.

Since the present TCM IO-520 fuel system is not density compensating, the fuel flow required for the Taxi/Idle and Approach modes are dependent on the fuel-air ratio required for cold day operation (O° F). As the induction air temperature increases, the resultant fuel-air ratio enrichens. For emission purposes therefore, the minimum acceptable fuel-air ratios were defined at an induction air temperature of 60° F and the fuel flow necessary to accelerate the engine at cold day conditions.

Table 13 - Fuel-Air Ratio Differences
TCM continuous flow vs. Simmonds DTU timed fuel injection systems

MODE	FUEL - AIR RATIOS			LIMITATION TO LEAN OPERATION
	TCM		SIMMONDS DTU	
	NOMINAL	MINIMUM ACCEPTABLE		
TAKEOFF	.0831	.0800	.0800	Cylinder Head Cooling
CLIMB	.0824	.0789	.0789	Cylinder Head Cooling
APPROACH	.0918	.0727	.0637	Engine Acceleration
TAXI/IDLE	.0929	.0800	.0634	Engine Acceleration

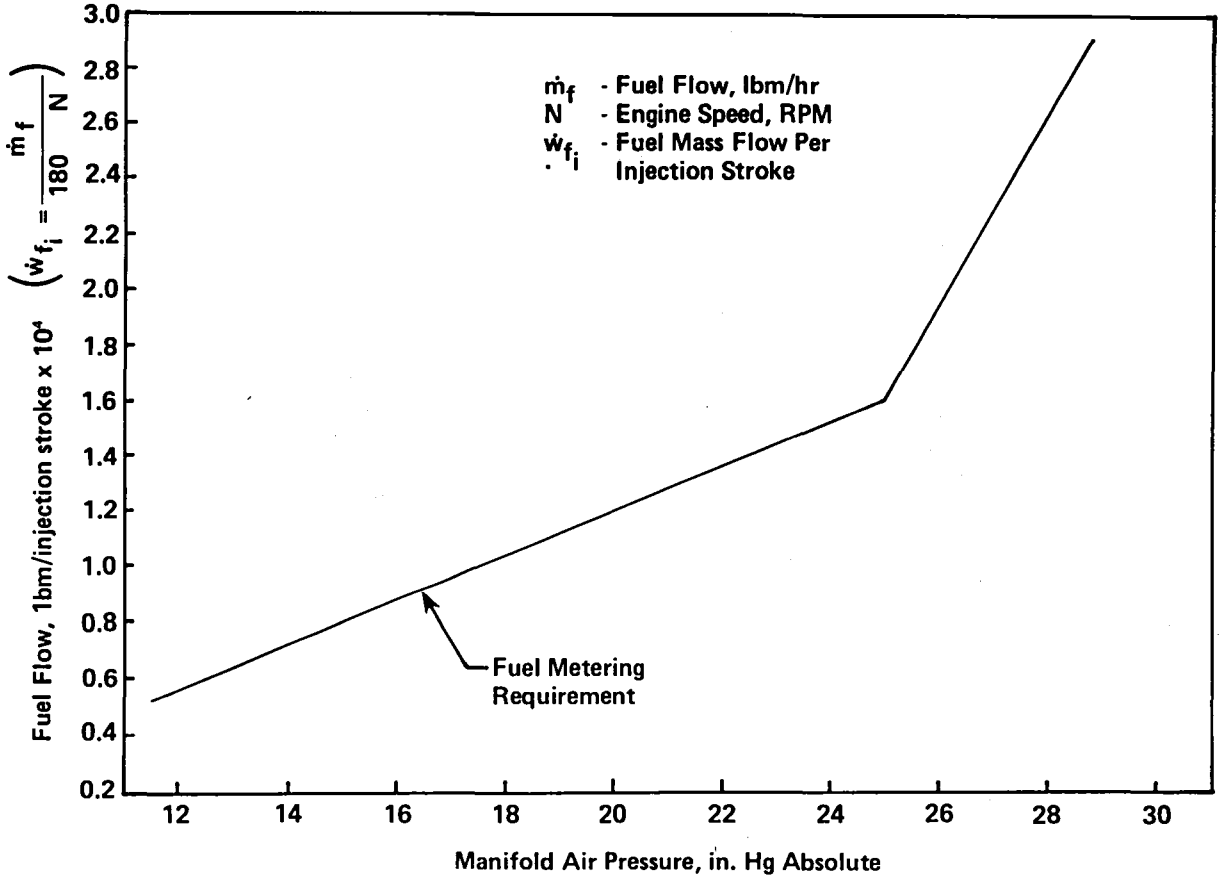

Fig. 10 - Simmonds DTU fuel metering schedule for IO-520 engine.

For the Simmonds DTU system the low power fuel-air ratios were determined by the linear fuel metering characteristics of the Simmonds DTU design, Figure 10. The slope of the 3 - 75% power regime is dictated by the cruise performance expected for the three combined concepts. The low power fuel-air ratios were then calculated based on the scheduled fuel flows at the respective manifold pressures. The resultant fuel-air ratios were well above the minimum acceptable for acceleration.

Based on the mixture schedules shown in Table 13, a 79% reduction in HC and a 58% reduction in CO is accomplished with a corresponding increase in NOx, as shown in Figure 11. The above reductions are with respect to the standard IO-520 nominal fuel schedule. In addition 62% and 42% reductions for HC and CO were accomplished compared to the minimum acceptable standard IO-520 fuel schedule. All pollutants were below the EPA standard for the Simmonds DTU system. Fuel consumption in the LTO cycle was likewise reduced, as

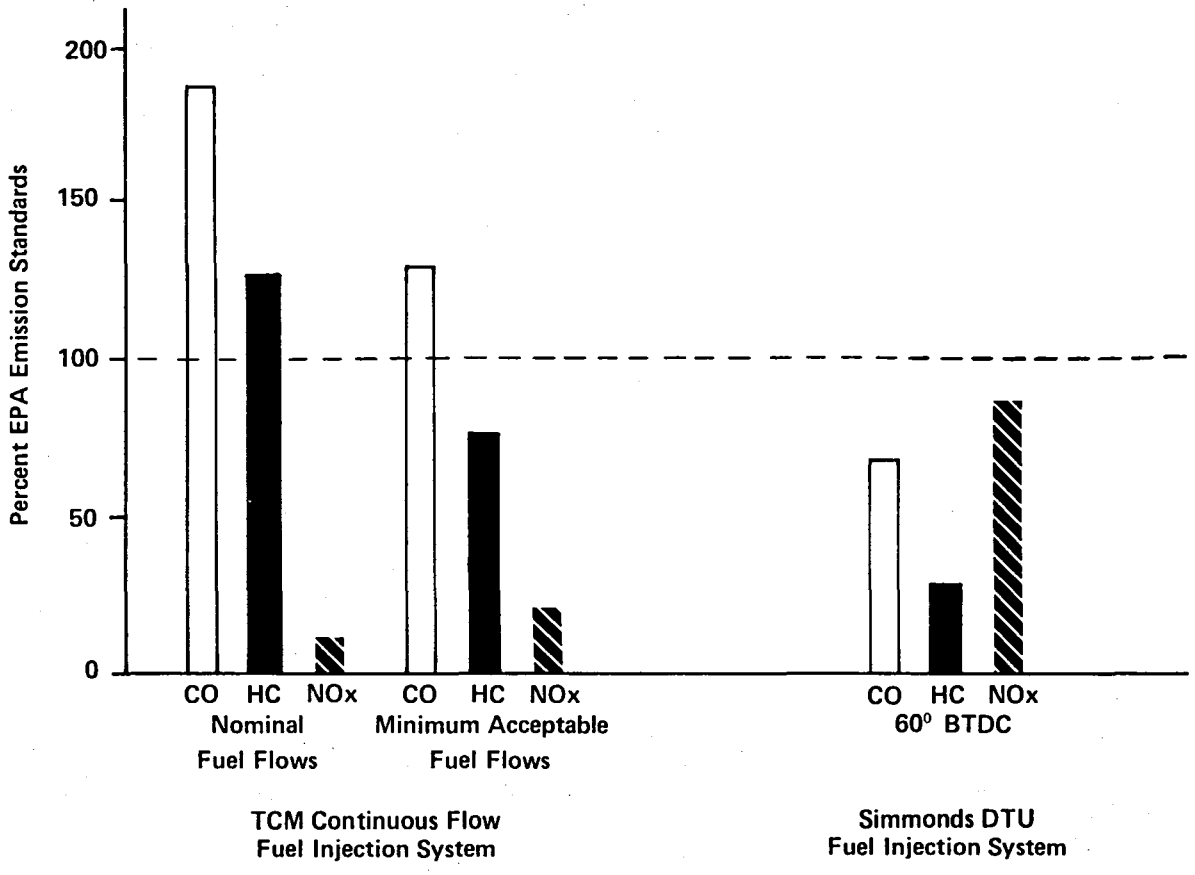

Fig. 11 Comparisons of five-mode LTO cycle emissions for IO-520 engine with TCM and Simmonds DTU fuel injection systems.

shown in Figure 12. The Simmonds DTU results in a 20% reduction in fuel consumed over the nominal fuel schedule and an 11% reduction over the TCM minimum acceptable fuel schedule.

6.5 PROTOTYPE DESIGN - The prototype Simmonds system is the same basic design as the DTU system. The major difference is in the metering fuel schedule requirements. Figure 10 presents the finalized fuel schedule for the Simmonds system based on integration with the other two concepts. Fuel flows in the takeoff (high power) regime were reduced based on the results of the improved cooling cylinder head, and a cooling scheme utilizing exhaust air injection. Likewise the cruise (moderate to low power) range was reduced to provide automatic leaning of the mixture in the 40 to 75% power range. No reduction in fuel consumption is envisioned in the cruise mode due to the Simmonds system, but rather the possible elimination of the mixture control lever.

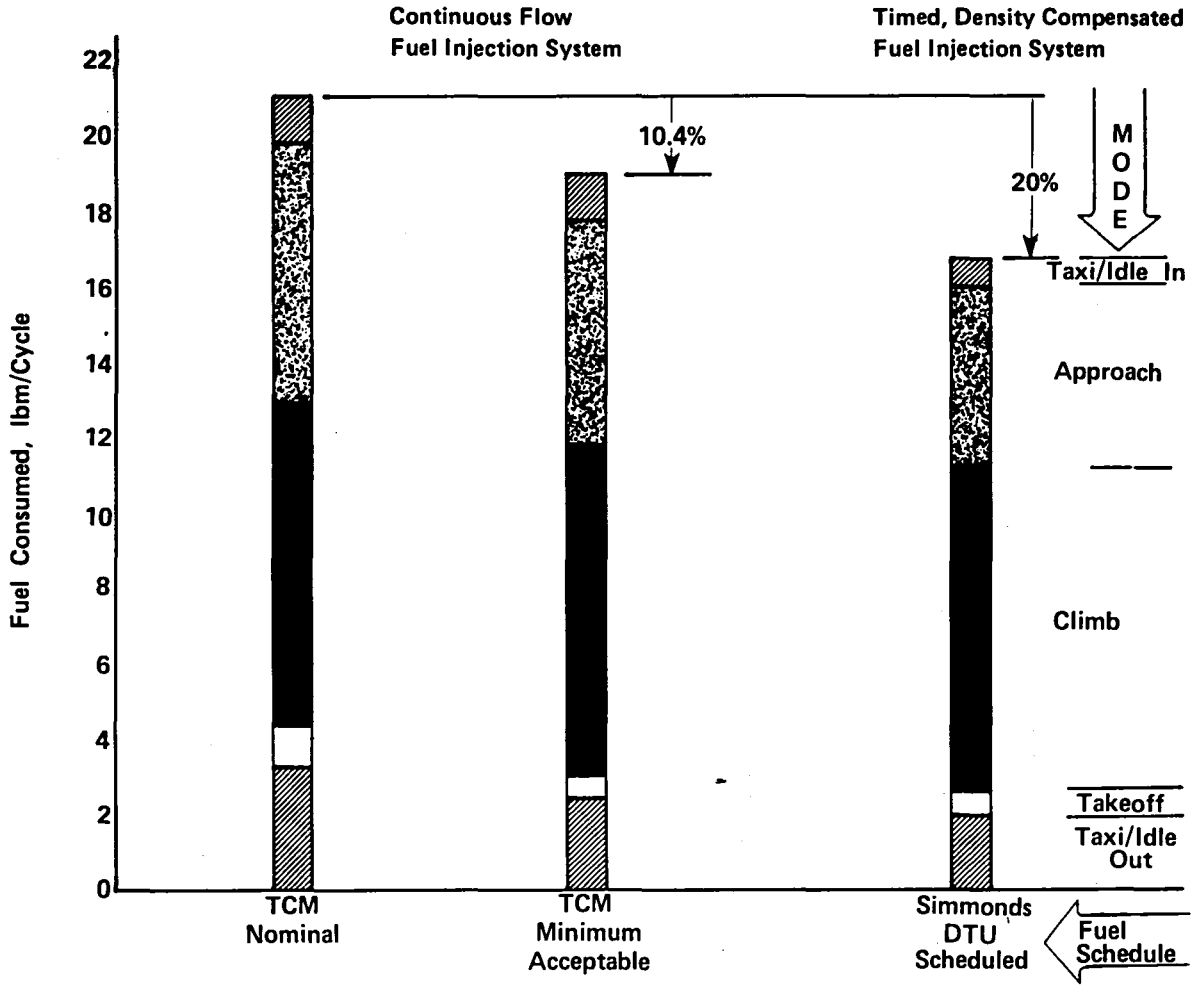

Fig. 12 - Comparison of five mode LTO cycle fuel economy for IO-520 engine with TCM and Simmonds DTU fuel injection systems. The contribution of each mode is also illustrated.

SECTION 7.0
IMPROVED COOLING CYLINDER HEAD

When an improved cooling cylinder head was being considered as one of the concepts for development, the primary objective was exhaust emissions reduction and the secondary objective was fuel economy improvement. The major effect on exhaust emissions would be through leaner operation during the Climb and Takeoff modes made possible by reducing thermal load on the cylinder head while maintaining the cylinder head temperature (CHT) within limits. A maximum allowable CHT of 460° F is the limiting criteria for leaning the IO-520 in those modes. For some of the improved cooling methods considered, a secondary emissions benefit could be realized through increased thermal oxidation of CO and HC resulting from higher exhaust gas temperatures. Any effect the concept was to have on fuel economy other than from leaning would be through reduced cooling air requirements resulting in lower cooling drag. The magnitude of this effect was not easily predictable, however, since it was not known at that time what method would be employed to gain the cooling improvement or, moreover, how much that method would allow cooling air to be reduced. To compound the problem, very little information on the heat rejection patterns of air-cooled engines was available. It was conjectured, however, that an improved cooling cylinder head would permit a significant reduction in exhaust emissions through leaner operation while allowing at least a modest improvement in fuel economy through leaner operation and reduced cooling drag. Based on this potential and other cost-effective merits, the improved cooling cylinder head was ultimately chosen as one of the three concepts for further development.

The next task was to determine the best technique for improving cylinder head cooling. Three possibilities were considered:

1. Cooling fin geometry redesign.
2. Ceramic coated exhaust ports
3. Exhaust port liners.

The effect of cooling fin geometry (size, shape, separation, etc.) on finned surface overall heat transfer coefficient was estimated through use of a TCM computer program based on techniques developed by Biermann and Pinkel (12). The other two methods involve thermal barriers in the exhaust port to promote exhaust gas heat retention. The relative benefit of the three improved cooling techniques was compared through an analysis based on the above computer program and an extensively modified version of a mathematical model of exhaust gas heat loss within an engine exhaust port developed by Hires and Pochmara (13). Based on these analyses as well as other considerations such as durability, complexity, cost and weight, an exhaust port liner featuring an enclosed air space between the liner and port walls was chosen as the most viable method for improved cylinder head cooling. An additional merit of such a liner design is its versatility. The potential existed for adding air injection which would maintain or improve the cooling potential for the cylinder head and exhaust valve while increasing CO and HC oxidation in the exhaust.

7.1 DESIGN CONSIDERATION - Liners that could be installed in the cylinder head after casting or even after maching, called "push-in liners", are attractive from a production standpoint, but due to the complex exhaust port geometry that characterize all TCM cylinder head designs, a cast-in version was chosen as the more practical. The basic design called for 0.035 inch Inconel 601 to be hydroformed in two pieces and welded to provide exhaust gas flow passage geometry that duplicated the geometry of the standard cast port to preclude any effect on volumetric efficiency. The shape of the liner is such that the forward end would be cast into the aluminum around the exhaust valve seat insert and the aft end would float (Figure 13), to minimize liner-to-head contact area. Rush (14) conducted experiments with exhaust port liners in water-cooled cylinder heads and found that heat transfer through the contact areas, even though small in surface area, can be significant. Of course, heat may also be conducted along the liner to any contact areas.

It was further deemed necessary to seal the air space to minimize exhaust flow into that region. Sealing the aft end of the liner was accomplished with the seal shown in Figure 13 that fits tightly around the liner outer diameter and is bolted to the head between the exhaust flange and an asbestos gasket reducing heat flow from the liner to the head. Unfortunately, a seal had to be custom made for

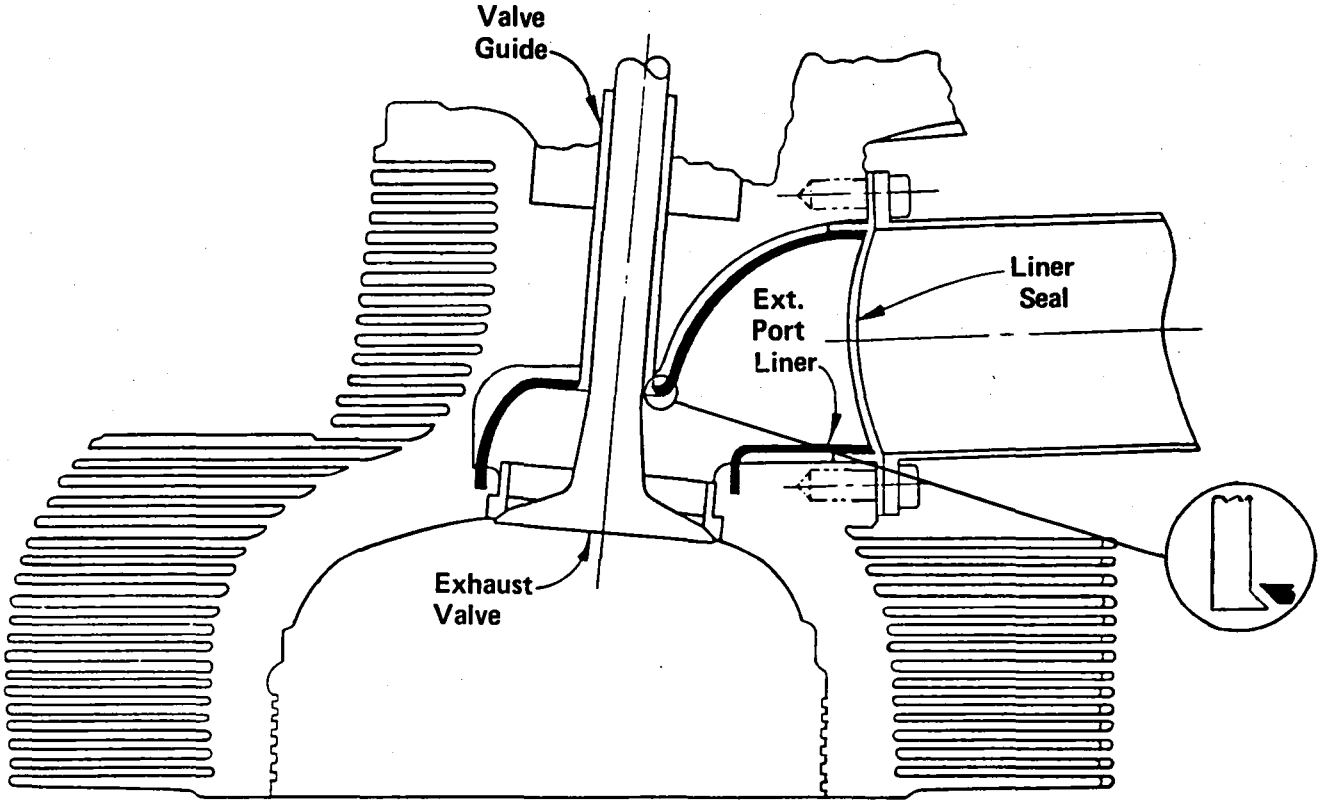

Fig. 13 - Cross-sectional view of exhaust port liner as cast in IO-520 cylinder head.

each head to account for liner position variation from head to head that occurred during casting.

To insure a good seal between the liner and exhaust valve guide the initial design called for welding the guide to the liner and casting the head around them as a unit. This was actually done on the prototype heads, but misalignment of the valve guide caused by liner shifts during casting required the guides be drilled out and a more conventional approach be employed as this technique would likely be too difficult to implement in production. An adequate seal was obtained by maching a 45° bevel on the valve guide and a corresponding seat on the liner (Figure 13), and pressing the guide into the head through the valve seat opening.

To form the 0.125 inch air gap around the liner a special core box was fabricated to accept the liner and allow sand to be blown into and around the outside of the liner in those areas where the air gap was needed. The cylinder heads were then cast using the sand coated liner in place of a standard exhaust port sand core. All the sand was removed after casting, leaving an air gap between the liner and port walls. Wall thicknesses around the exhaust port were maintained at the expense of slightly shorter cooling fins and 0.125 inch shorter exhaust valve springs.

7.2 INSTRUMENTATION - To determine the effect of exhaust port liners two IO-520 cylinder heads, a standard or baseline (B/L) head and an exhaust port liner (EPL) head were extensively instrumented. In the region of the exhaust port eight chromel-alumel thermocouples were installed at the locations shown in Figures 14A, B, and C. Another thermocouple was installed in the combustion chamber dome of each head between the lower spark plug and the exhaust valve seat insert because this is known to be a highly stressed area. This instrumentation is in addition to the normal cylinder head bayonet thermocouple and the exhaust gas thermocouple.

7.3 TESTING - An extensive matrix of data points were obtained by performing mixture ratio curves (varying fuel-air ratio) for both of the heads at the conditions cited in Table 14 for cooling air pressure drops across the cylinders of 3.0, 5.0 and 7.0 inches of water. Each head was tested at all combinations of the three cooling air pressures at cylinder position 2 and again at cylinder position 4 to allow consideration for the effects of cylinder-to-cylinder variations in induction air, cooling air, and fuel flow.

Table 14 — Exhaust port liner test matrix
engine operating points

MODE	%POWER @ RPM
Takeoff	W.O.T. @ 2850
Climb	84% @ 2565
Cruise - 2	68% @ 2400

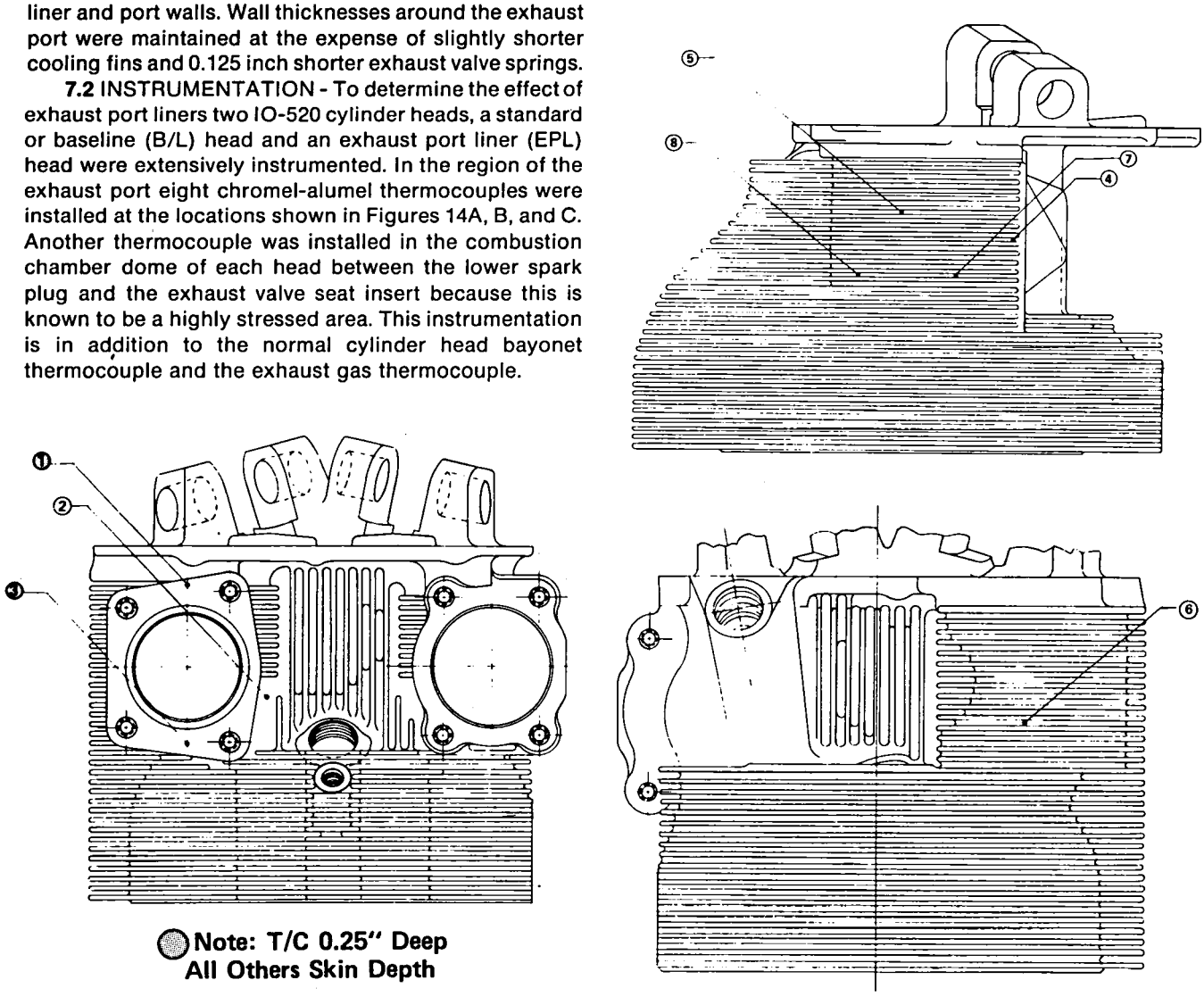

Fig. 14 A, B, C - Location of thermocouples for comparison of IO-520 exhaust port temperature profiles with and without exhaust port liners.

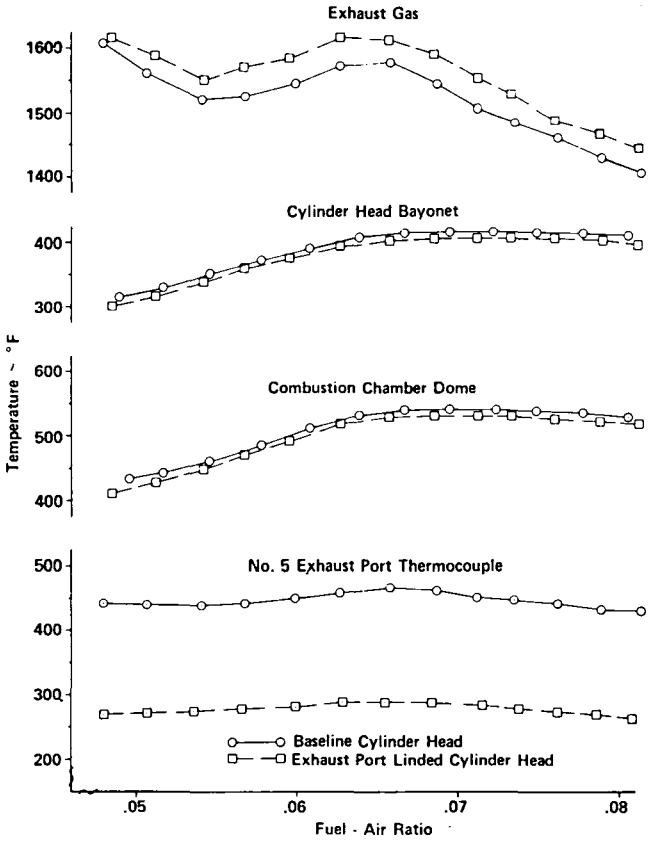

Fig. 15 - Effect of exhaust port liner on various operating temperatures.

Table 15 - Change in average exhaust port and exhaust gas temperatures due to exhaust port liner

	EXHAUST PORT Temperature Reduction, F°	EXHAUST GAS Temperature Increase, F°
CRUISE - 2		
CYL. POS. 2	80	20
CYL. POS. 4	95	25
CLIMB		
CYL. POS. 2	90	25
CYL. POS. 4	115	30
TAKEOFF		
CYL. POS. 2	110	35
CYL. POS. 4	125	40

NOTE: 1. Cylinder Head Bayonet - No Change
2. Combustion Chamber Dome - No Change

Figure 15 presents a typical example of the data obtained at one power setting (Takeoff) over the mixture ratio range investigated for one cooling air pressure at cylinder position 4. Only one of the eight exhaust port temperatures is presented in this figure, however the other temperatures follow the same trend as Figure 16 indicates. Conclusions drawn from other combinations of power level, cooling air flow and cylinder position are the same as those conclusions from the data presented in Figures 15 and 16, except the magnitudes differ. The liners appear to have little effect on the bayonet temperature or the combustion chamber dome temperature. The reasons for this are twofold. First, since the thermocouples are located closer to the combustion chamber than to the exhaust port, the effect of reducing exhaust port heat transfer is small. Second, the heat transferred along the liner to the end cast into the combustion chamber dome could have been quite significant as Rush (14) suggested. The liners did reduce exhaust port wall temperatures significantly while increasing EGT's. The magnitude of these effects in terms of temperature differentials was found to be independent of the cooling air flow, all other things being equal. Table 15 summarizes these findings by presenting the average exhaust port temperature and EGT differences for power level and cylinder position. The effect of the liners improved with increasing power as shown by the increasing temperature differences with power. The maximum exhaust port temperature reduction of 125 F° and the 40 F° EGT increase at Takeoff reflects an 18% reduction in exhaust port heat transfer to the cylinder head based on a simple energy balance and the exhaust port heat transfer computer simulation.

The benefit of liners appeared to be much greater at cylinder position 4 than at cylinder position 2. This is thought to be due to cylinder-to-cylinder induction airflow variation. In addition, testing was performed with exhaust valves constructed of a temperature-sensitive material that allowed determination of the maximum temperature attained at various points on the valve during a specified test procedure. The exact location of the points examined are shown in Figure 17. There are fifteen peripheral locations on the head and thirty-one profile locations divided into three regions, "Underhead", "Face" and "Top of Head". Both B/L and EPL heads with the temperature-sensitive valves installed were run at Takeoff and Climb in both cylinder positions 2 and 4 with 5.0 inches of water cooling air pressure. Fuel flow in all cases was set for maximum EGT, the most severe condition and one that is not recommended above 65% power.

In general, the results indicated that in the Climb mode the valve temperatures in the EPL head were equivalent to or slightly higher than for the B/L head, but for the Takeoff mode the EPL valve temperatures were significantly higher than for the B/L valves. Table 16 summarizes the maximum and average temperatures at the peripheral and profile locations for both Climb and Takeoff at both cylinder positions. The largest differences were at Takeoff in the underhead region where valves in cylinder positions 2 and 4 were , respectively, 121° F and 242° F hotter in the EPL head than in the B/L head.

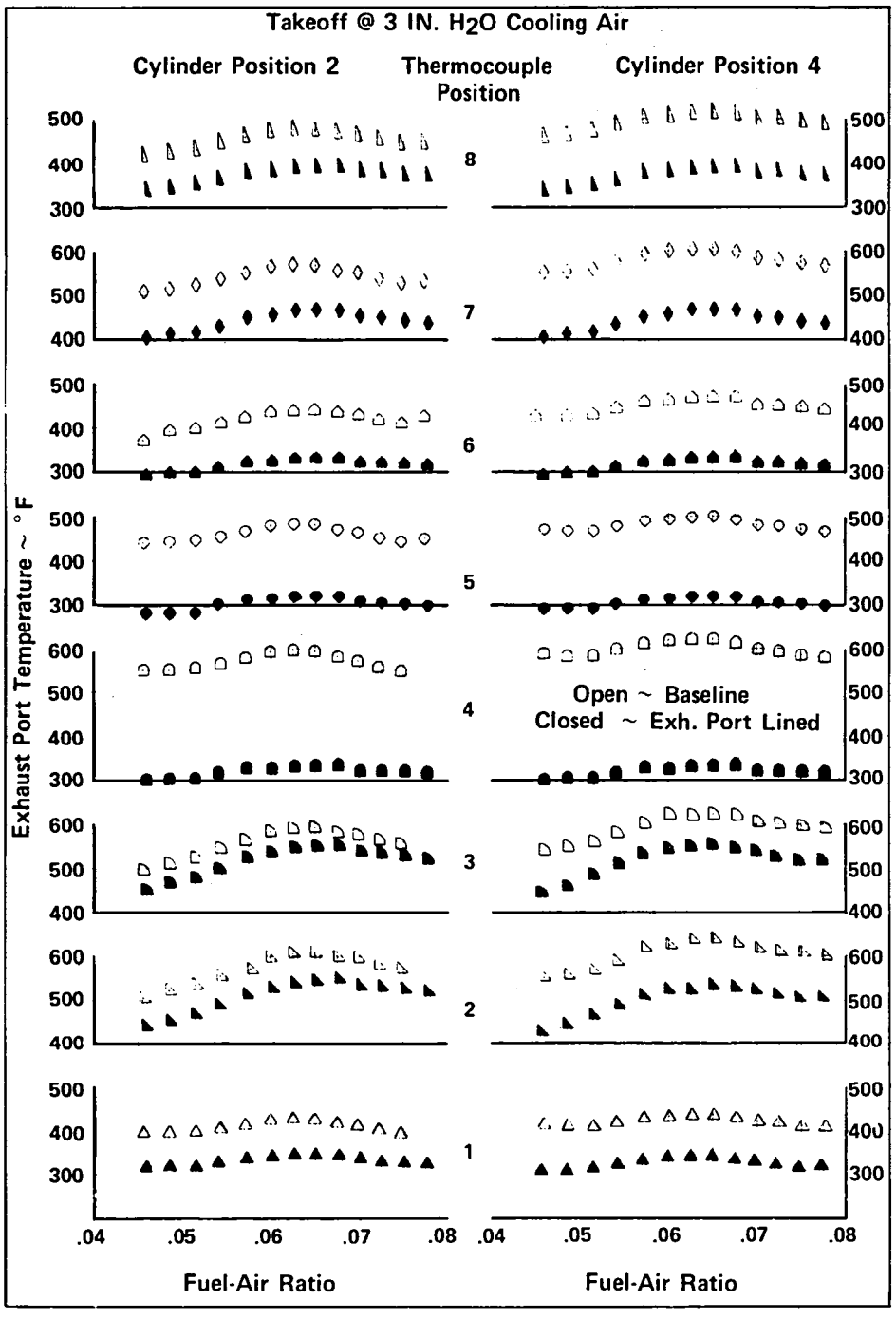

Fig. 16 - Effect of liners on exhaust port temperatures.

Maximum underhead temperatures were located at point 8 (Figure 17), in every case except one, where the maximum occurred at point 9, one position nearer the face. The importance of this area is presented graphically in Figures 18A, B which show the EPL and B/L valve temperature differences as a function of location at Takeoff power for cylinder position 4. The EPL valve temperatures were higher in almost every case but the maximum differences occurred at or near this underhead region near the contact point of the valve, liner and valve guide. Thus, if valve guide/port liner contact could be reduced or eliminated then valve temperatures would likely be reduced in the EPL head. Sodium cooled valves could be used to improve valve cooling but this would increase valve guide heat flow. Another method is to incorporate some type of air-cooling scheme using air injection behind the liner. The results of incorporating the latter method will be discussed under exhaust air injection.

Additional testing was done to establish the

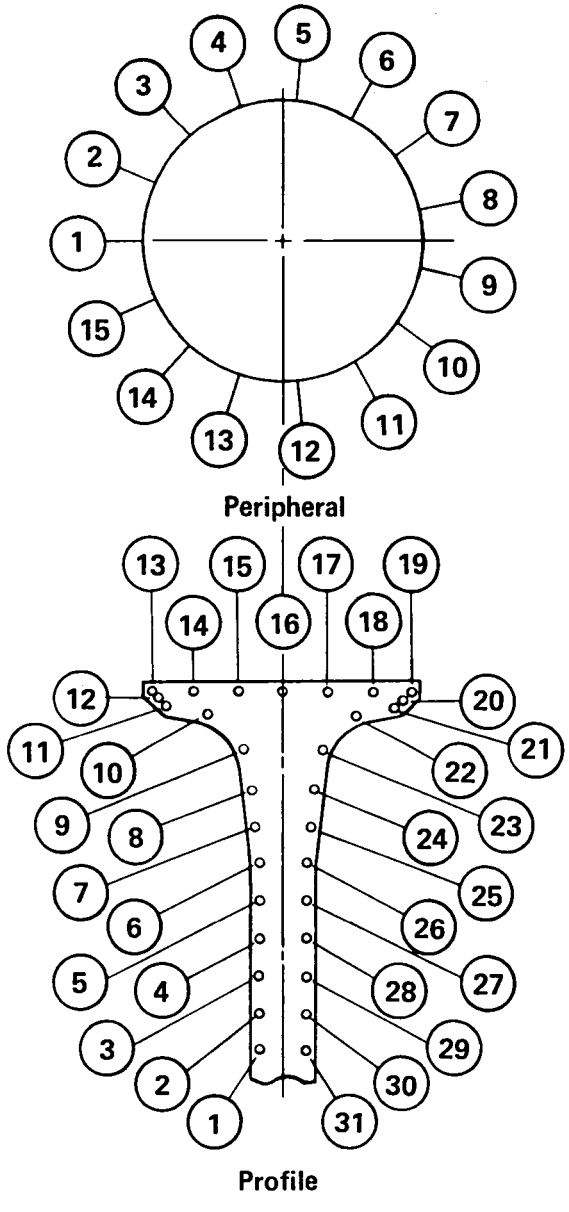

Fig. 17 - IO-520 exhaust valve temperature data point locations.

feasibility of deleting cooling air flow external to the exhaust port of the EPL head since this would be a step in the right direction if significant fuel economy improvement is to be realized from the use of exhaust port liners. All cooling air was blocked off to the exhaust port segment of the head by putting a sheet metal shroud on the EPL head. The results of this testing at Takeoff power are compared to similar data for the B/L head and the EPL head without the shroud in Figure 19. The exhaust port temperatures without cooling air were higher than with cooling air but still considerably below those for the B/L head. Other temperatures were about the same as for the EPL head with cooling air. Therefore exhaust port liners will allow that portion of the cooling air to be deleted.

The next step was to determine how much of the total cooling air was required by the exhaust port sector. This was accomplished by using a TCM single-cylinder research engine configured with a standard IO-520 cylinder assembly. Various combinations of cooling air flow areas were flowed to define the distribution

Table 16 - Effect of exhaust port liners on exhaust valve temperatures

POWER	TEMPERATURES (°F)	CYLINDER HEAD @ POSITION 2			CYLINDER HEAD @ POSITION 4		
		EPL	BASELINE	ΔT	EPL	BASELINE	ΔT
CLIMB	PERIPHERAL						
	MAXIMUM	1223	1223	0	1278	1217	67
	AVERAGE	1117	1121	−4	1216	1148	68
	PROFILE						
	MAXIMUM	1421	1380	41	1428	1421	7
	AVERAGE	1213	1222	−9	1305	1279	26
TAKEOFF	PERIPHERAL						
	MAXIMUM	1417	1340	77	1385	1385	0
	AVERAGE	1360	1285	75	1355	1310	45
	PROFILE						
	MAXIMUM	1650	1529	121	1750	1508	242
	AVERAGE	1445	1378	67	1432	1371	61

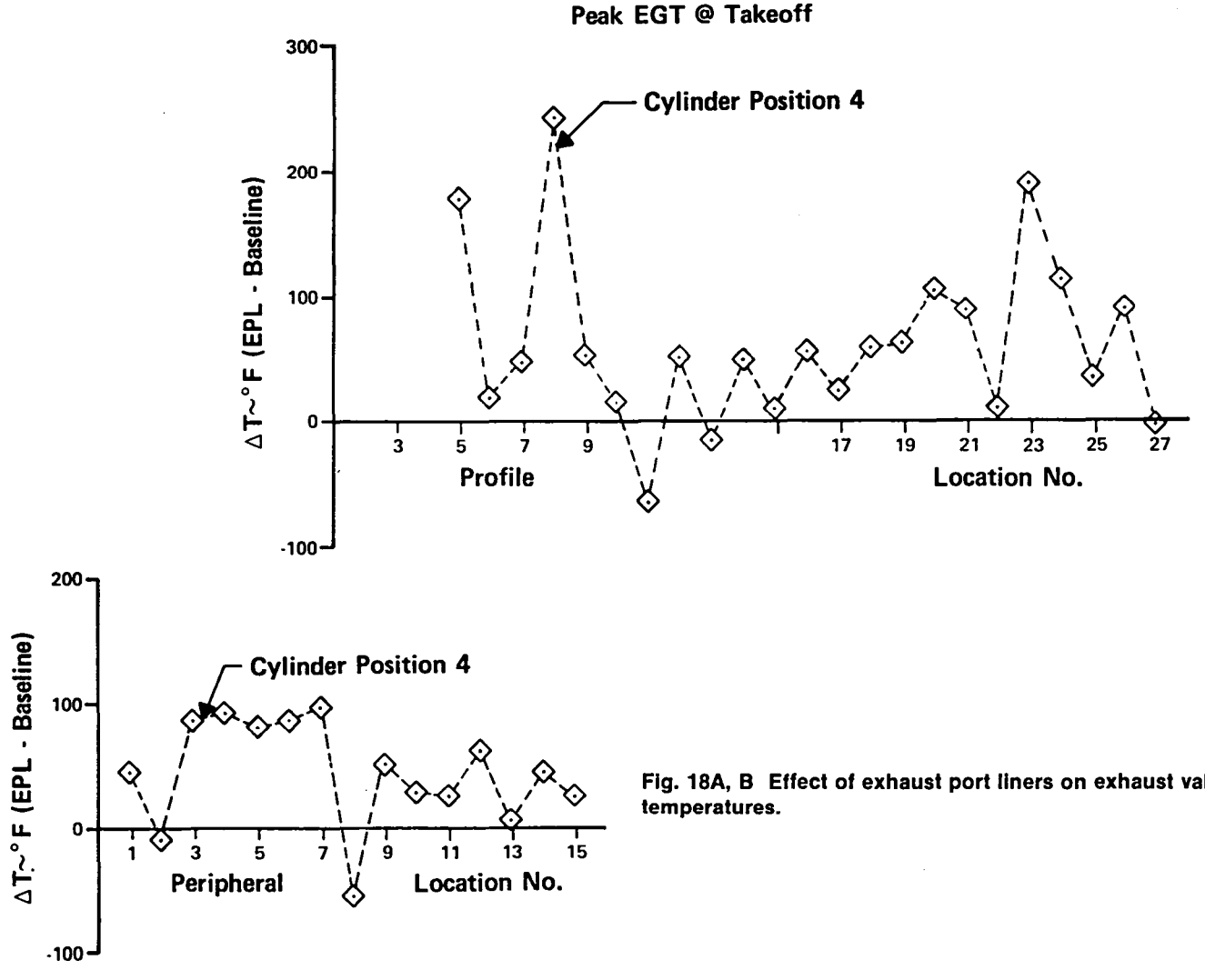

Fig. 18A, B Effect of exhaust port liners on exhaust valve temperatures.

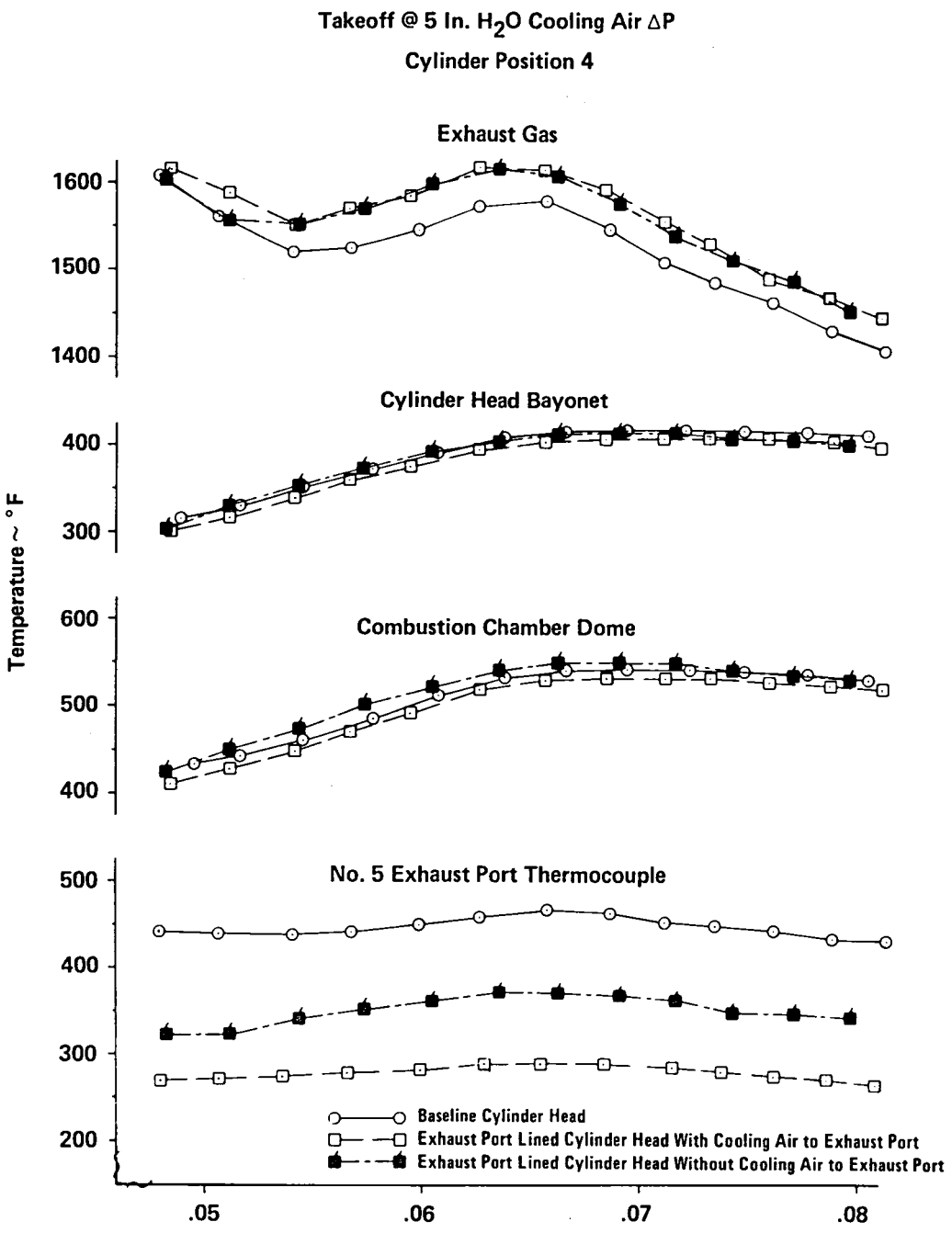

Fig. 19 - Effect of exhaust port liners on various operating temperatures.

presented in Figure 20. Based on this testing it was concluded that exhaust port cooling air for the area defined by this study accounts for 11% of the total IO-520 engine cooling air (excluding oil cooler).

Even though cylinder head bayonet and combustion chamber dome temperatures were not significantly reduced through the use of exhaust port liners as initially designed, the large reduction in exhaust port temperatures did merit further consideration of the liner as a viable method for improving cylinder head cooling. The reduced exhaust port sector temperatures tend to reduce the temperature gradient across the cylinder head between the exhaust and intake ports. This could reduce the thermally induced stresses in the head, allowing higher bayonet temperatures to be attained for the same level of stress. Proof of this supposition would of course require considerable durability testing.

7.4 EFFECTS ON EMISSIONS - Leaning in the Climb and Takeoff modes is currently limited by the maximum allowable cylinder head bayonet temperature of 460 F°. With the use of exhaust port liners this limit might increase enough to allow leaning to the minimum fuel

flows for the Takeoff and Climb modes while maintaining power. Based on emission characteristics of the IO-520 engine for the LTO cycle, this leaning would result in 35% and 12% decreases in CO and HC, respectively, along with a significant increase in NOx. The resulting levels of CO, HC and NOx with an improved cooling cylinder head alone would be 118%, 112%, and 132% of the EPA standard, respectively.

7.5 EFFECTS ON FUEL ECONOMY - Cooling power, P, may be approximated by the following expression:

$$P \propto \dot{m}\, \Delta h \qquad (2)$$

where, $\dot{m}$ is the cooling air mass flow, and Δh is the total head loss. The IO-520 finning is of a geometry such that,

$$\Delta h \propto \dot{m}^{1.76} \qquad (3)$$

and the additive effect of cooling air mass flow reduction on cooling power is,

$$\Delta P = \left[1 - \left(\frac{100 - \Delta\dot{m}}{100}\right)^{2.76}\right] \times 100\% \qquad (4)$$

where ΔP and $\Delta\dot{m}$ are expressed in percent change.

In the case of exhaust port cooling air, for instance, the 11% reduction in mass flow becomes a 27.5% reduction in cooling power by the above equation. If cooling power for a particular installation is 5% to 6% of the total shaft power the 11% reduction in cooling air flow represents an improvement of approximately 1.5% in propulsive power. This can be converted into fuel savings by taking less flying time at the same fuel flow (at the expense of increased airframe drag) or the same flying time at less fuel flow. This 1.5% is considered the minimum possible with an improved cooling cylinder head. Additional leaning capability in Climb and Takeoff will provide slight additional fuel economy improvement for a typical mission, but time spent in these modes represents a small percentage of the total time. Exhaust port liners also offer the possibility of improving the durability of exhaust valves and guides through the addition of an air cooling scheme and may permit leaning to best economy between 65% and 75% power in Cruise. This could produce substantial fuel consumption reductions since fuel used in Cruise and Cruise Descent accounts for 79% of the total fuel used during the example flight profile of Table 2.

7.6 DURABILITY - After completing the extensive testing outlined above plus additional testing to be highlighted in the following section, no durability problems associated with the liners were noted. A hairline stress relief crack was observed in one liner about midway through the above testing but no further growth or leakage was observed for the remaining testing.

7.7 PROTOTYPE DESIGN AND FABRICATION - The basic prototype liner design differs very little from the original design. The same material, Inconel 601 is hydroformed in two pieces and welded together to form

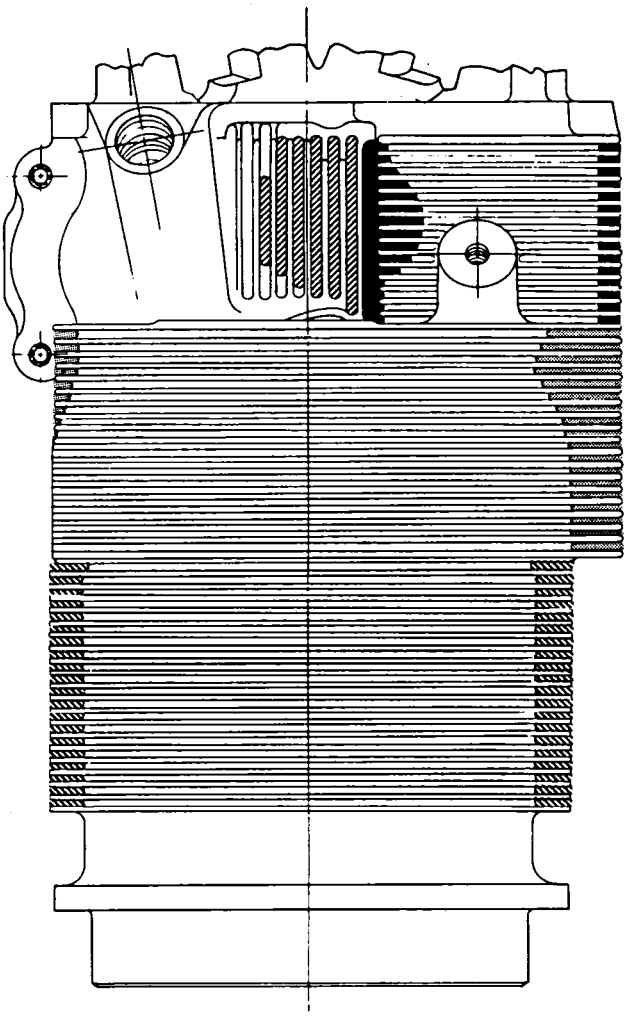

FLOW AREA	% TOTAL HEAD FLOW	% TOTAL CYLINDER ASSEMBLY FLOW
▨	18.	10.
■	20.	11.
▩	62.	34.
▨	—	45.
TOTAL	100.0	100.0

Fig. 20 - IO-520 cylinder assembly cooling air distribution.

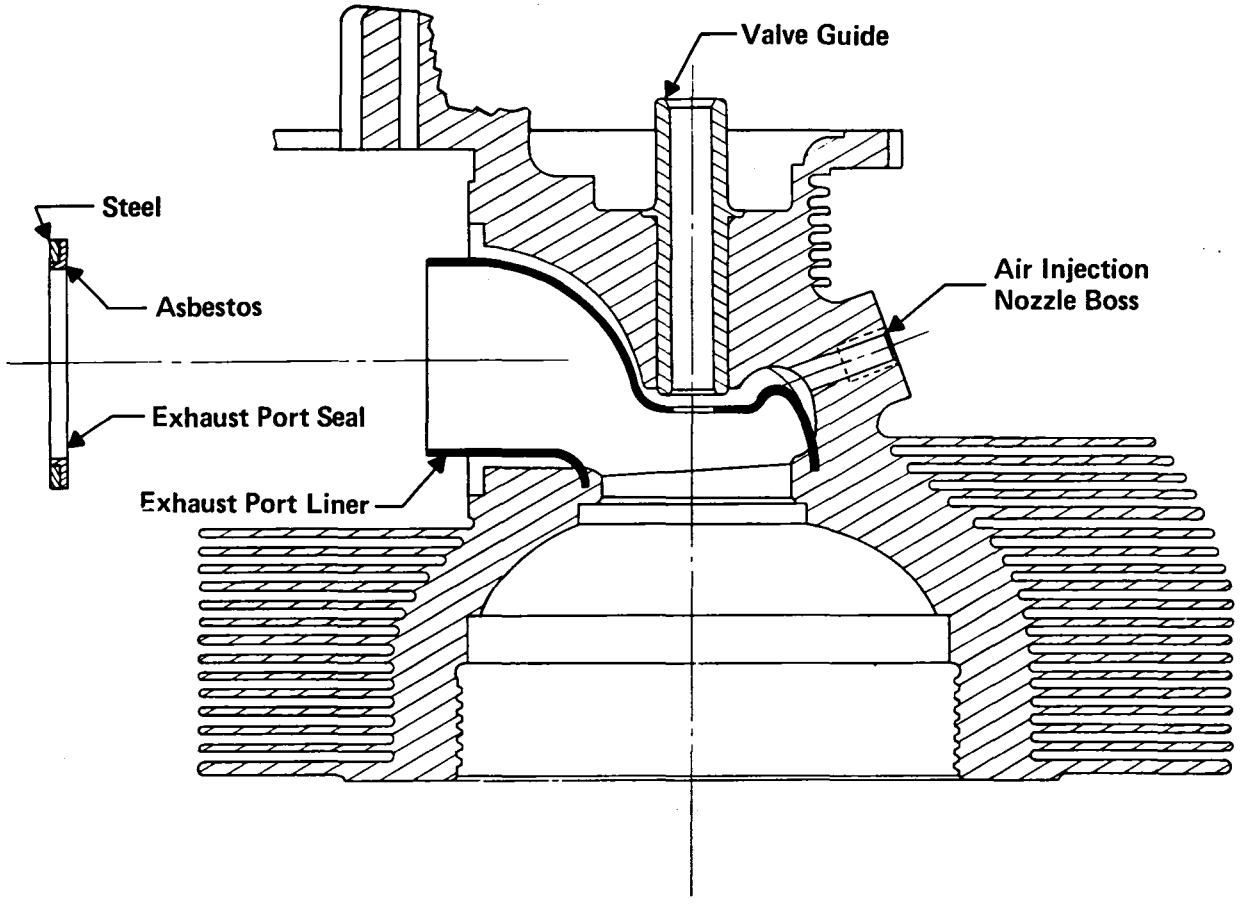

Fig. 21 - Cross sectional view of IO-520 cylinder head with prototype exhaust port liner cast in.

the same flow geometry as the standard cast port. Figure 21 shows how the aft end of the liner has been extended 0.375 inch beyond the exhaust flange surface to permit use of the redesigned seal which is intended to preclude custom fitting a seal to each head. The seal will be form fitting around the liner outer diameter (O.D.) and will utilize a low conductivity material in conjunction with stainless steel to reduce the flow of heat from the liner to the head. A circular recess with an O.D. larger than the O.D. of the seal will be machined in the cylinder head exhaust flange surface and will house the seal. The difference in the two diameters will be large enough to compensate for liner misalignment. The forward end of the liner is again cast in the aluminum around the exhaust valve seat. Contact between the liner and valve guide will be eliminated to reduce valve temperatures and to permit addition of air injection.

SECTION 8.0
EXHAUST AIR INJECTION

The role of exhaust air injection as a means of chemically oxidizing exhaust pollutants to help meet strignent automotive emissions standards is well established (15 - 20). More recently however, air injection has been relegated to the job of providing additional oxygen content to the exhaust gas stream for the purpose of aiding catalytic conversion which has become necessary with ever increasing emission control demands.

Simply, the oxidation of exhaust pollutants through air injection is intended to convert hydrocarbons and carbon monoxide to carbon dioxide and water vapor as in Equations (5) and (6):

$$C_xH_y + O_2 \longrightarrow CO + CO_2 + H_2O \quad (5)$$

$$CO + O_2 \longrightarrow CO_2 \quad (6)$$

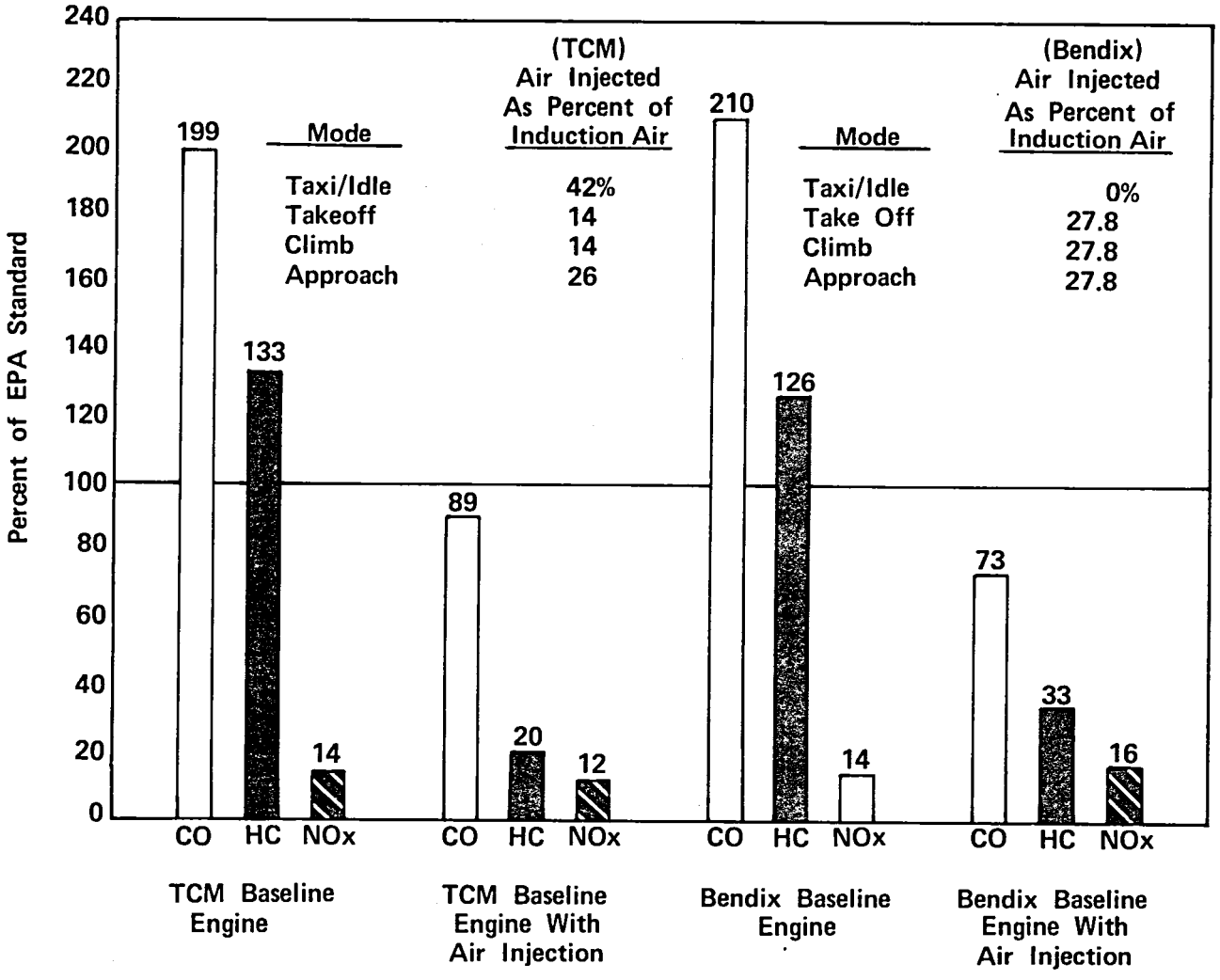

Fig. 22 - The effect of secondary air injection on exhaust emissions of TCM 0-200-A engine. Comparions between Bendix (15) and TCM data.

8.1 FEASIBILITY STUDIES - The first noteworthy application of exhaust air injection to an aircraft piston engine was conducted in late 1972 by The Bendix Corporation under contract to the EPA (21). Secondary air was supplied to the exhaust manifolds of a Teledyne Continental Motors 0-200-A engine by a pair of engine-driven air pumps. The results of this testing showed that the exhaust emissions of this engine could be reduced to values below the proposed EPA standards by simple secondary air injection.

A comparison of the Bendix work and subsequent air injection testing at TCM on the 0-200-A engine is shown in Figure 22. Baseline emissions for both engines are nearly the same and air injection results are similar. Both show that air injection alone is capable of reducing exhaust emissions to levels below the EPA standards. The two tests differ, however, in the quantities of air injected. The Bendix test was run with an amount of air added to the exhaust (27.8% of the induction air) giving equivalent stoichiometric mixture to the exhaust gas composition, starting with an induction fuel-air ratio of 0.087 for the Takeoff, Climb and Approach modes. No air injection was added in the Taxi/Idle modes due to difficulty in "lighting off" the reaction. The TCM testing overcame this difficulty by injecting air much closer to the exhaust valves in quantities which could reasonably be supplied by an engine driven air pump. The result of successful "light off" in the Taxi/Idle mode is seen in the lower value of total LTO cycle hydrocarbons (20% of the EPA standard) compared to the Bendix test (33% of the EPA standard). The higher quantities of air injected during the Climb mode in the Bendix tests account for the lower emissions

of carbon monoxide (73% versus 89%) for the LTO cycle.

In all, air injection feasibility studies have been conducted on four aircraft piston engines at TCM to determine the effects of air injection on exhaust emissions. The four engines tested were the 0-200-A (carbureted, 100 BHP), the TSIO-520-L (turbocharged, 310 BHP), the GTSIO-520-K (geared, turbocharged, 435 BHP) and the IO-520-D. The results of these studies indicate that each engine has the potential for meeting the EPA standards with air injection alone.

Several tests were also conducted using the General Motors "Pulsair" scheme (18), but the quantities of air induced into the exhaust manifolds were not sufficient to reduce emissions at the higher power LTO cycle modes.

The effect of air injection on the individual modes, in Figure 23, was investigated using regulated, dry shop air, which allowed a maximum of 86 lbm/hr of air flow to be injected into the exhaust gas stream. In the Taxi-Idle mode, if an amount of air equal to 45% of the induction air is injected into the exhaust, then CO and HC emissions are reduced to only 20% of the original value.

Two phenomena are shown in Figure 23 which deserve comment. As injection air is added, initially in small amounts, the CO mass emissions increase slightly. This is due to the fact that HC is being converted at a rapid rate into CO and CO_2. The rate of production of CO, being dominant in the low oxygen content exhaust products, is faster than the oxidation of CO to CO_2, so that a net gain in CO is observed.

The second phenomenon involves the decrease in NOx emissions for all modes below about 20% injected air. In work done by D. J. Pozniak (19), it was demonstrated that a chemical reduction of NO occurred when additional hydrocarbons in the form of ethane (C_2H_6) were injected into the exhaust manifold near the exhaust valve. A simplified example of one mechanism suggested by Pozniak involves the gas phase reduction of NO in the presence of thermally dissociated hydrocarbons:

$$C_2H_6 \longrightarrow H + \text{Hydrocarbon radicals} \quad (7)$$

$$H + NO \longrightarrow N + OH \quad (8)$$

$$N + NO \longrightarrow N_2 + O \quad (9)$$

Further, it was found that small amounts of air injection promoted the NO reducing reactions, coinciding with previous results cited by the paper which concluded that reduction of NO by hydrocarbons is influenced by the amount of oxygen present.

Apparently, the chemical kinetics of this reduction process are exceedingly complex and measurements of exhaust composition far downstream, both in time and distance, tend to mask the dynamic nature of the reactions taking place near the exhaust valve.

This process is thought to be responsible for the lower levels of NOx observed in Figure 22 and where NOx went from 14% to 12% of the EPA standard with air injection. An increase in NOx was noted, however, in the Bendix air injection results due to the larger quantities of air which were injected during the high power modes (27.8% of induction air). Figure 22 shows this increase in

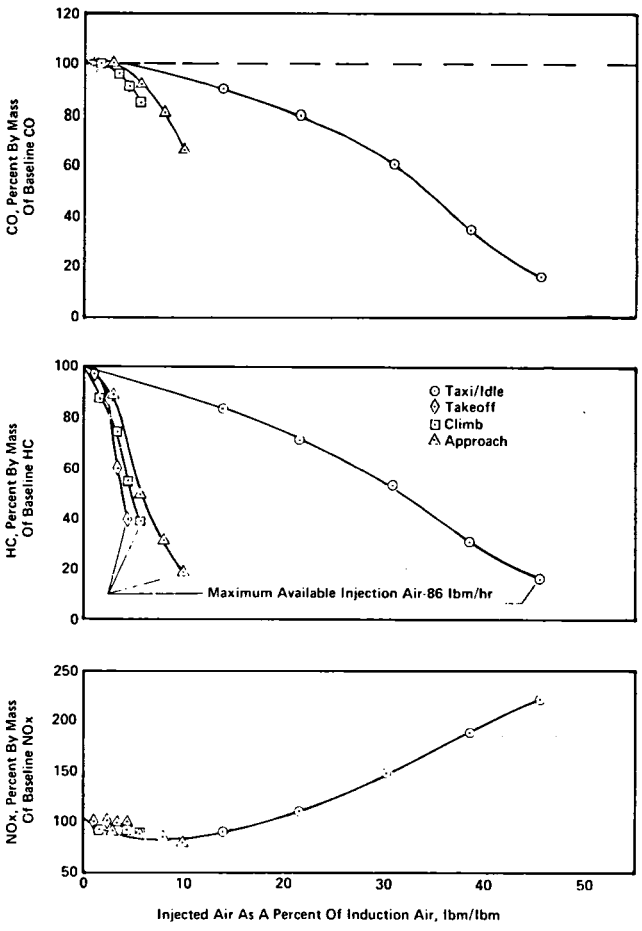

Fig. 23 - Effect of air injection on exhaust emissions of CO, HC and NOx in the Taxi/Idle, Takeoff, Climb and Approach modes using regulated shop air supply. Maximum available injection air flow - 86 lbm/hr. IO-520 engine with baseline (nominal full rich) fuel flows.

NOx for the LTO cycle from 14% ot 16% for the Bendix results.

The conclusion is, that a careful tailoring of injected air quantities can result in lower levels of all three pollutants.

During early testing of the IO-520, sufficient injection air was not available to determine the potential reduction of emission possible with air injection alone. A logical extrapolation of the data available, however, gives an estimate of exhaust emissions of CO, HC and NOx using air pump performance data. Figure 24 shows that if air injection was applied to the baseline engine, the levels of CO, HC and NOx would be reduced to well below the EPA standard levels (29%, 10% and 15% respectively).

8.2 AIR INJECTION WITH EXHAUST PORT LINERS - The use of air injection in combination with exhaust port liners is a relatively new concept. The benefits are almost immediately obvious from Figures 25A, B which show two designs where the injected air is introduced behind the exhaust port liner into the air gap region. In Figure 25A, the air exits at the exhaust flange through an annular gap, thereby scavenging the majority of the gap volume. A second design (Figure 25B) shows the injected air exiting the liner gap volume through an annular gap which is designed to cool the exhaust valve stem.

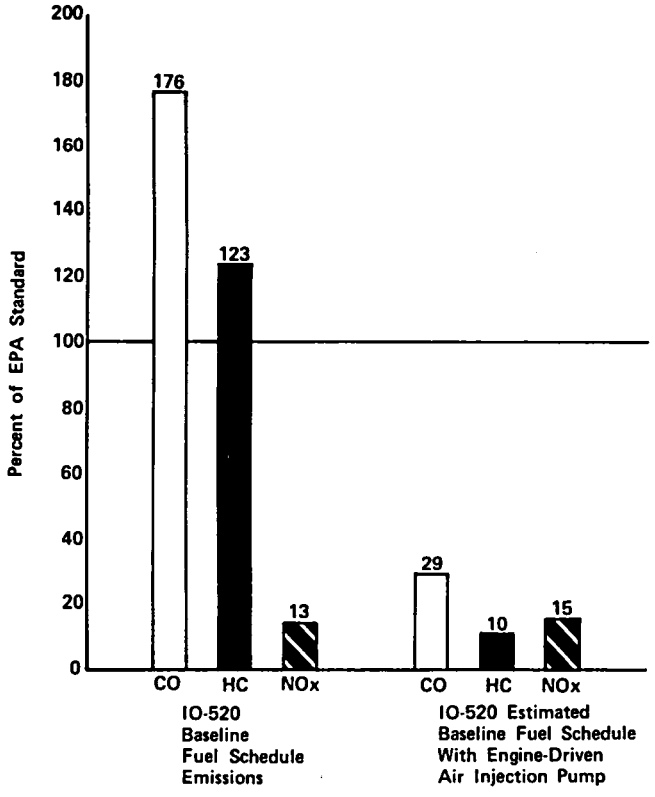

Fig. 24 - Estimated reduction of IO-520 emissions from baseline with engine - driven exhaust air injection pump.

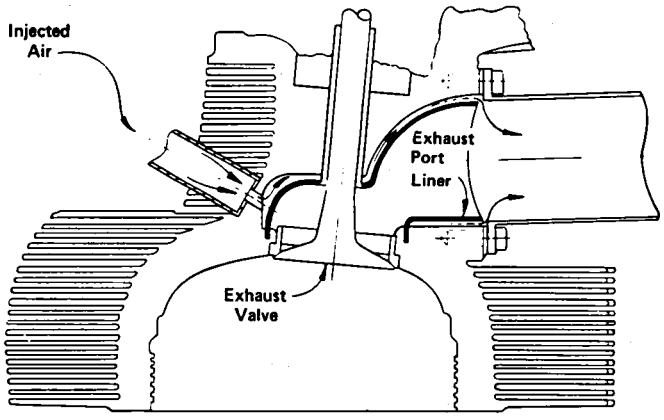

Fig. 25 A - Cross sectional view of IO-520 cylinder head with exhaust port liner scavenging design.

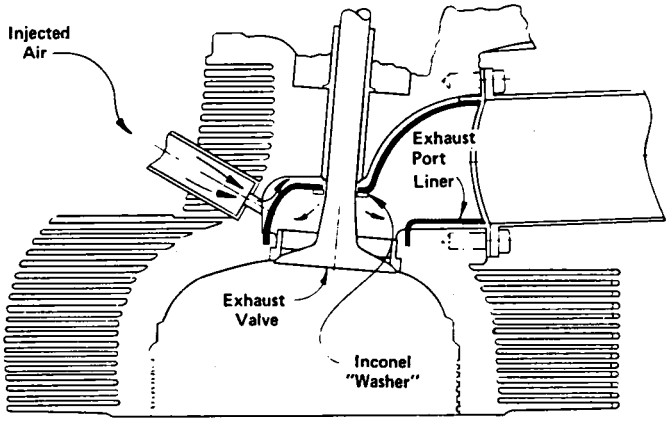

Fig. 25 B - Cross sectional view of IO-520 cylinder head with exhaust port liner valve stem cooling design.

The injected air, whose ultimate purpose is to oxidize HC and CO in the exhaust is employed in these two design to provide additional cooling to the cylinder head and the integrally cast, Inconel exhaust port liner. In turn, the injected air is heated, which aids in the oxidation of HC and CO.

The two proposed designs were chosen for their ability to provide additional cooling to the exhaust port, port liner, valve guide and valve, rather than for minimum emissions. In flow tests it was found that, for a given injected air pressure, the exhaust port liner scavenging design provided about 8-10% more air mass flow than the more restrictive valve stem cooling design.

Exhaust emissions were not measured during this series of tests because only two cylinders were equipped with air injection. Cylinder number 2 had the exhaust port liner scavenging design and cylinder number 4 had the valve stem cooling design. Temperature sensitive exhaust valves were used in both, at an air injection rate of 22 lbm/hr. The results of the valve temperature survey compared with basline and a port lined cylinder head with no air injection, are shown in Figure 26A, B. The valve cooling, air injection design (Figure 26B) was run in cylinder position number 4 only, and is compared with the exhaust port liner and the baseline cylinder head valve temperature profiles. The exhaust port liner by itself had a mean temperature profile difference ($\overline{Y}$) of +53.2 F° higher than baseline while the exhaust port liner with the valve cooling air injection design showed a mean value of -51.3 F° or 51.3 F° cooler than the baseline valve temperatures. The largest temperature differences appear in the valve stem and underhead region, as expected.

Figure 26B compares the exhaust port liner and exhaust port liner scavenging air injection design with baseline exhaust valve profile temperatures in cylinder position number 2. A similar effect is demonstrated, where the exhaust port liner, by itself, gives higher valve profile temperatures than the baseline cylinder head ($\overline{Y}$= +67.2 F°), and lower temperatures ($\overline{Y}$ = —26.3 F°) with the liner scavenging air injection design.

Comparing Figures 26A and 26B, the mean temperature difference below baseline for the two air

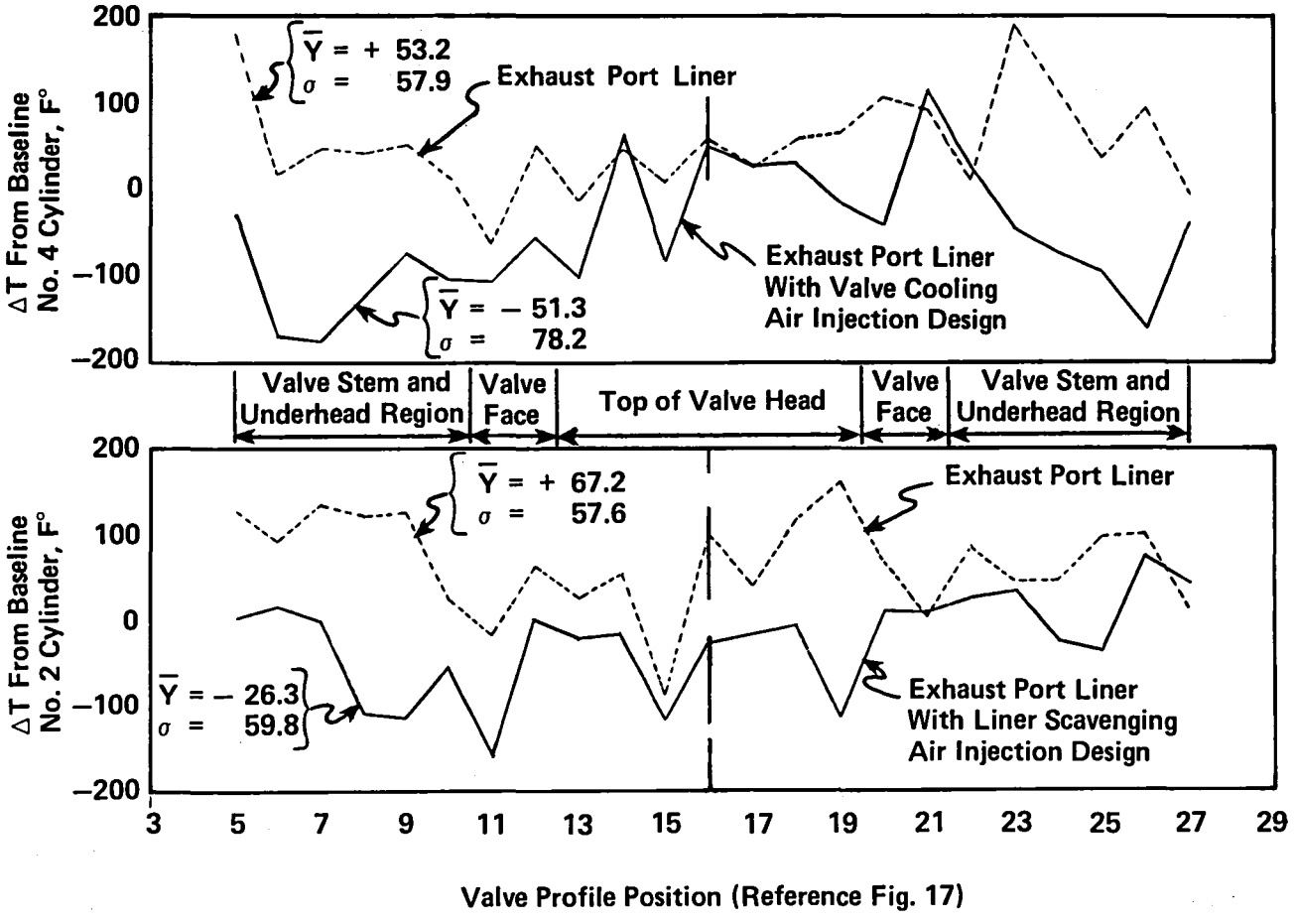

Fig. 26 A, B - Comparison of maximum exhaust valve profile temperatures to baseline cylinder head of; A) exhaust port liner alone versus exahust port liner with valve cooling design in cylinder No. 4 position, and; B) exhaust port liner alone versus exhaust port liner with liner scavenging design in cylinder No. 2 position.

injection designs indicates that, for the same mass flow of injected air (22 lbm/hr), the valve cooling design is more effective in cooling the valve ($\bar{Y}$ = -51.3 F°) than the liner scavenging design ($\bar{Y}$ = —26.3 F°).

On this basis, a modified valve cooling design was chosen as the best compromise.

8.3 PROTOTYPE DESIGN AND INSTALLATION - During engine testing with an engine-mounted, belt-driven air pump, a Saginaw automotive air pump was used. Its counter-clockwise rotation, making compact installation difficult, and unknown durability led to the use of a spline-driven clockwise rotation Airborne aircraft air pump for the final integrated design. The Airborne pump capacity is about 240 pounds of air per hour at 4000 RPM compared to 210 pounds per hour at 6000 RPM for the Saginaw pump. Since both pumps are of the carbon vane type, the Airborne pump should provide longer life due to its lower vane tip speed. Also, the fact that the Airborne air pump has been certified for aircraft use would make engine certification easier.

The Airborne pump is directly mounted to an existing drive pad on the rear of the engine (Figure 27) and is driven at 1.5 times engine crankshaft speed and would use about 6 HP at Takeoff (2% of engine power). Pump inlet air is taken from the air filter box and distributed by means of two log manifolds, each feeding air to three cylinders. Individual air injection lines conduct the air to each cylinder from the manifolds through Delco "Pulsair" check valves which prevent backflow of exhaust gases and reduce required pump work.

SECTION 9.0
INTEGRATION OF THE THREE CONCEPTS

As a final proof of the practical applicability of the work which has been accomplished, TCM conducted verification testing of all three concepts integrated into an airworthy package based on the IO-520 engine. The testing consisted of power calibration, transient response, emission measurement, and flight test. Figure 27 shows how these concepts were combined into a compact airworthy package. The largest single change to standard engine hardware was the new cylinder head casting and machining. The liner, of course, had to be cast-in with attendant modifications to preserve structural integrity of the cylinder head. The improved fuel injection system required that the nozzle boss be

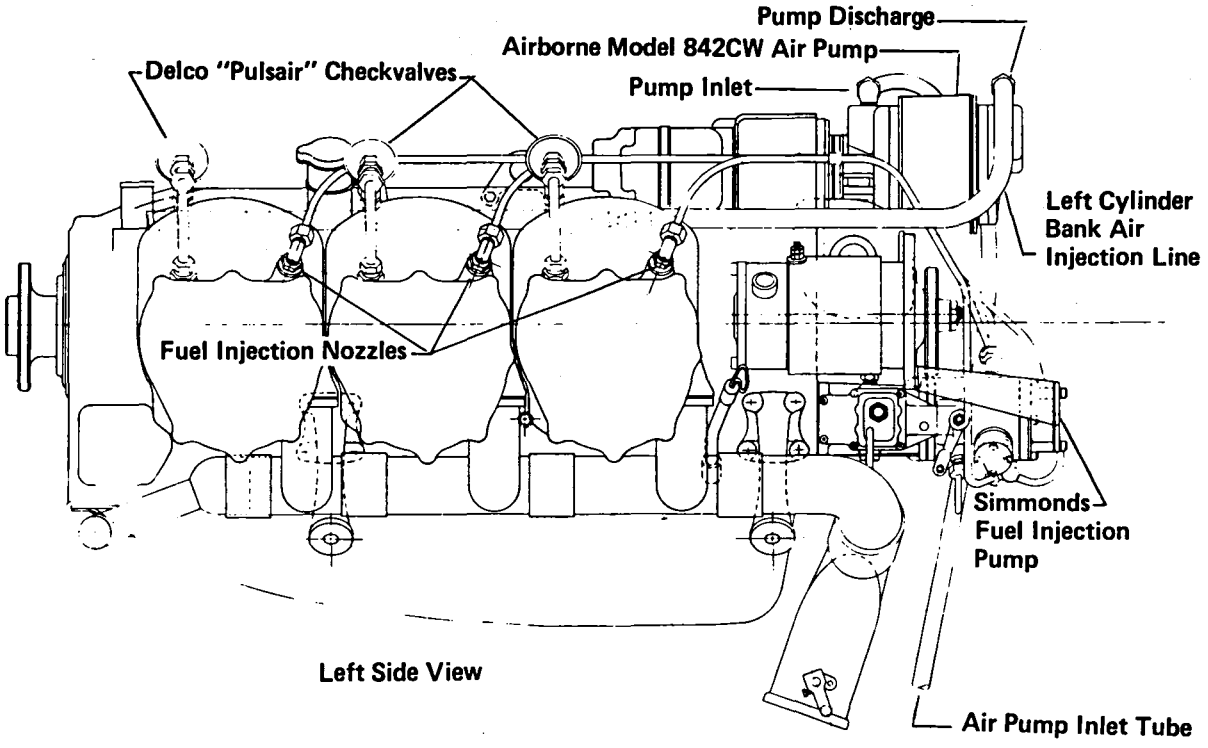

Fig. 27 - IO-520-D engine with Simmonds fuel injection and air injection.

relocated and redesigned to accept the Simmonds nozzle. An additional boss was cast on the exhaust port for the air injection nozzle. These casting changes required the cylinder head machining procedure be modified accordingly.

Table 17 presents an estimated fuel economy comparison between the standard IO-520 engine and the IO-520 with the three integrated concepts. The comparision is based on the example single-engine airplane flight profile of Table 2, and shows that the IO-520 prototype would use 4.6% less fuel than an IO-520 baseline engine.

Average trip fuel economy (miles traveled per gallon of fuel) increased by 4.8%. Table 18 breaks the profile into two segments where the LTO cycle is one segment and Enroute Climb, Cruise, and Cruise Descent comprise the second segment. This table points out that of the fuel consumption 4.6% improvement, 3.7% came from gains made in the LTO cycle while only 0.9% was derived from the remaining three modes. This is because fuel consumption was reduced by 27.4% in the LTO cycle while the reduction in the other three modes was only 1.0%. Estimated LTO cycle fuel economy improvements result from:

1. Leaner operation in Climb and Takeoff due to the improved cooling cylinder head and air injection, which permit operation at near best economy in Climb and considerably lean of the current TCM full-rich fuel flow at Takeoff.

2. Leaner operation at Apporach while maintaining good transient response with the improved fuel injection system.

Leaning to best economy in Enroute Climb alone accounted for the 1.0% improvement in the remaining modes since both the standard TCM fuel injection system and the improved fuel injection system permit leaning to best economy at 65% and 55% power in Cruise and Cruise Descent, respectively.

Figure 28 presents an estimated fuel economy comparison between the standard IO-520 engine and the prototype IO-520 with the three integrated concepts for non-stop flight distances up to 600 statute miles. The curve is truncated at 19.8 miles as that corresponds to the distance assumed covered during the five-mode LTO

Table 17 - Fuel economy comparison of a typical single-engine aircraft flight profile with baseline and prototype IO-520 engines.

	IO-520 BASELINE	IO-520 PROTOTYPE	% CHANGE
TOTAL DISTANCE TRAVELED (STAT. MILES)	329.	329.	0.
TOTAL TIME (HOURS)	2.23	2.23	0.
TOTAL FUEL CONSUMED (GALLONS)	26.3	25.1	-4.6
AVERAGE TRIP FUEL ECONOMY (MPG)	12.5	13.1	+4.8

Table 18 - Fuel economy comparison of a typical single-engine aircraft over five-mode LTO cycle with baseline and prototype IO-520 engines.

	% OF TIME	TOTAL DISTANCE	FUEL CONSUMED (Gallons) IO-520 BASELINE	IO-520 PROTOTYPE	% CHANGE	CONTRIBUTION TO TOTAL FUEL CONSUMTPION REDUCTION
LTO CYCLE	20.4	6.0	3.6	2.6	-27.4	3.7%
ENROUTE CLIMB, CRUISE, CRUISE DESCENT	79.6	94.0	22.7	22.5	- 1.0	0.9%
TOTALS	100.0	100.0	26.3	25.1	-	4.6%

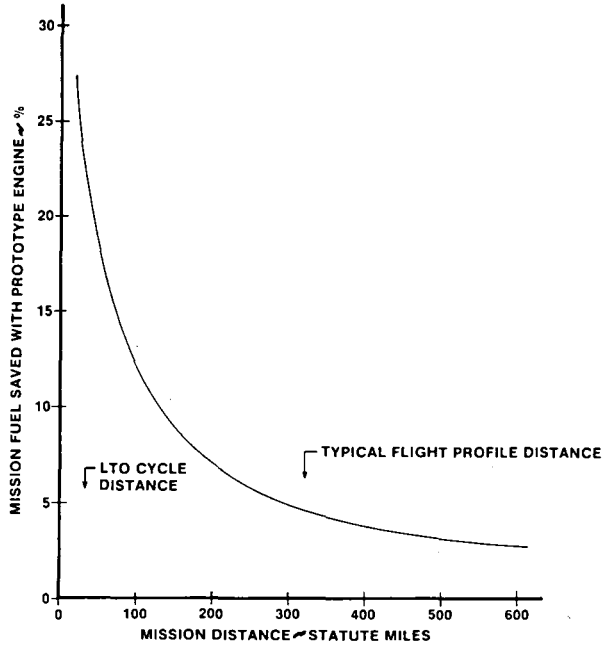

Fig. 28 — Fuel economy comparison of a typical single engine aircraft with baseline and prototype IO-520 engines as a function of distance traveled.

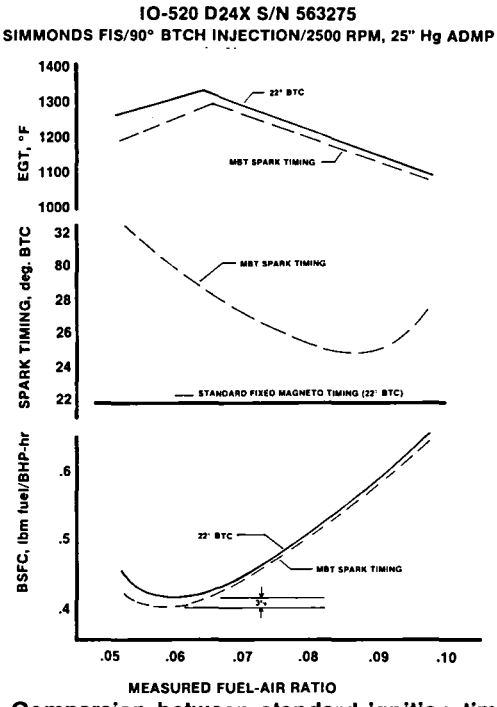

Fig. 29 - Comparsion between standard ignition timing and MBT timing, and the effect on EGT and BSFC.

portion of the typical flight profile of Table 2. The figure illustrates that the IO-520 prototype would use 27.4% and 4.6% less fuel than the baseline for the LTO cycle and typical flight profile of Table 2, respectively. Since very little of the fuel economy improvement is attributable to modes other than the LTO cycle the fuel saving from the prototype engine decreases markedly with distance, which indicates that significant reductions in overall fuel economy require improvements in the cruise mode.

A comparison of the emissions for the standard engine configuration and the engine configured with improved fuel injection system, improved cooling cylinder head, and air injection is presented in Table 19. The comparison is made for the 5-mode LTO cycle as

Table 19 - Comparison of IO-520 emission levels for five-mode LTO cycle

CONFIGURATION	% EPA STANDARD CO	HC	NOx
IO-520 BASELINE	182	127	10
IO-520 PROTOTYPE (CONCEPTS A+B+C)	20	1	79

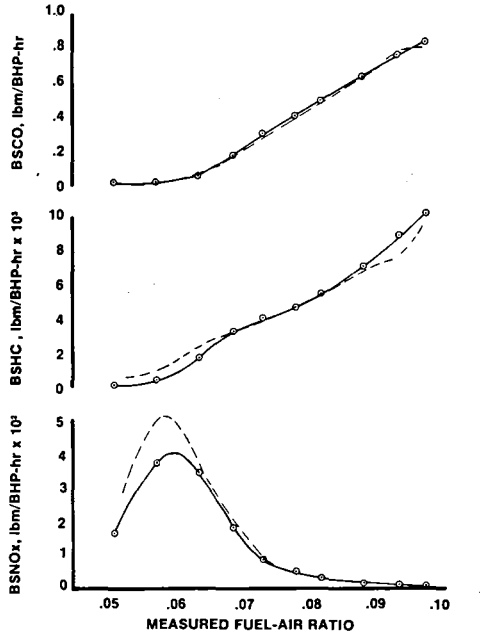

Fig. 30 — The effect on emissions of Co, HC and NOx, of MBT timing compared with standard fixed timing.

defined in Table 3B, and baseline emissions are based on nominal production fuel flows.

The prototype IO-520 emissions of Table 19 are based on the leanest possbile fuel flows for each of the five modes which results in the lowest fuel use for the LTO cycle. See Appendix A., for detailed data on exhaust emissions measurements and calculations.

SECTION 10.0
VARIABLE IGNITION TIMING STUDY

In Table 9, the various concepts being considered in this study were ranked in order of importance. One of the easiest concepts to implement into a new engine design is variable ignition timing which ranked third in both adaptability and integration. Its effect on NOx emission, however, was known to be negative while at the same time having a positive effect on fuel economy. Although variable ignition timing was not chosen as one of the three principal candidate concepts, its value was considered sufficient to warrant further investigation for the sake of improved fuel economy.

As an addition to the original contract scope of work, variable ignition timing was explored independently of the three principal concepts. Using the IO-520 engine, a performance map was run over the entire range of engine speeds, manifold pressures and fuel-air ratios for power levels from 26 to 76% of maximum continuous power (285 BHP). For each point, minimum spark advance for best torque (MBT) timing was recorded along with exhaust emissions and other engine operating parameters. In all, 556 individual operating points were recorded for the engine map matrix.

Figure 29 is typical of the results of the testing. The standard fixed magneto timing for the IO-520-D engine is 22° BTC. MBT timing varies from a minimum of 25° BTC at best power fuel-air ratio to 30° BTC at best economy fuel-air ratio. The conclusions of the testing showed that for this engine a fixed timing setting further advanced than the standard 22° BTC would provide fuel savings close enough to that obtained with MBT timing provided a sufficient detonation margin could be demonstrated. The compromise timing selected was 27° BTC which is MBT timing for a fuel-air ratio midway between best power and best economy fuel-air ratios, which results in a 2% fuel economy improvement for cruise operation. No detonation was detected at any of the MBT timing settings for the sea level testing which was conducted. Detonation margin was not determined for any of these points however.

As expected, MBT timing had no effect on emissions of CO, a small effect on HC, and caused increased oxides of nitrogen at the leaner fuel-air ratios as shown in Figure 30.

SECTION 11.0
FLIGHT TESTING

Flight testing was conducted at TCM, from Brookley Airport in Mobile, Alabama. The test airplane was a 1979 Cessna 210N Centurion II, registration number N5525A.

The airplane was instrumented (see Appendix B) in its original condition and baseline flight tests were conducted with the production engine. Upon completion of the emissions testing on the prototype engine, it was installed in the air-frame and comparison testing was done.

Qualitatively, the airplane flew and handled well with the prototype engine and the only problem was backfiring in the exhaust after rapid throttle closing. This problem could easily be fixed by using a manifold pressure controlled valve to shut off air injection at lower than normal manifold pressures.

A comparison was made between the baseline and prototype flight test engines over a typical flight profile identical to that in Table 2, for the fictional airframe used for illustrative purposes in Section 4.0 of this report. The distance 328.8 statute miles remains the same and all the times-in-mode remain the same except for time spent in the Cruise mode. This time was adjusted so that the distance traveled came out to 328.8 statute miles at the actual measured true air-speed in both cases. The results, presented in Appendix C., show that the prototype engine with standard fixed magneto timing of 22° BTC got 6.3% better fuel economy over the flight profile than the baseline production engine.

The majority of the fuel savings came during the Climb, Enroute Climb and Approach modes as expected. Of the nearly 10 pounds of fuel saved during the flight schedule, about 17% was saved during the Climb mode, 46% during the Enroute Climb mode and 27% during the Approach mode. During both Climb and Enroute Climb, cylinder head temperatures for both the baseline and prototype engines remained comfortably below the 460° F limit, in most cases by at least 100° F.

Some flight testing was conducted with the prototype engine magneto timing advanced to the 27° BTC selected as the best compromise from the variable ignition timing study. Detonation margins at this setting were not defined so takeoff and climb were performed at power/speed conditions less severe than those specified in Table 3A to minimize the possiblity of detonation. Test stand data indicate that a fuel economy improvement of 2% would be expected. Although no detonation was detected, the anticipated reduction in fuel consumption could not be absolutely confirmed. This is attributed to difficulty in consistently setting up equivalent baseline and prototype test conditions and accurately measuring small fuel flow differences in a flight test environment.

Appendix D., shows photographs of the prototype engine and installation in the Cessna 210, as well as the cockpit flight test instrumentation.

SECTION 12.0
CONCLUSIONS

A methodical study has been conducted to select and apply items of known technology to an aircraft piston engine for the purpose of reducing exhaust emissions while at the same time improving fuel economy.

The use of an improved fuel injection system along with exhaust port liners and exhaust air injection has been shown to be a means of achieving these goals safely.

It is clear that efforts aimed at significant reductions in overall fuel consumption must be applied to the Cruise mode where the majority of the fuel is used.

The following conclusions were reached as a result of this work:

1. The EPA standards for CO, HC and NOx can be met by a combination of improved fuel injection, exhaust port liners and exhaust air injection for the IO-520 engine.
2. The baseline IO-520 engine can meet the EPA

standard for Co, HC and NOx using air injection alone, with no improvement in fuel economy.

3. The EPA standards for Co, HC and NOx can be met by using only the Simmonds improved fuel injection system to provide a leaned fuel schedule for the IO-520 engine.

4. Fuel economy of the IO-520 engine can be improved up to 6.3% over a typical single-engine airplane flight profile.

5. The use of exhaust air injection in combination with exhaust port liners reduces exhaust valve stem temperatures to levels below that of the baseline engine, which could result in longer valve guide life.

6. The use of exhaust port liners alone, can reduce engine cooling air requirements by at least 11% which is the equivalent of a 1.5% increase in propulsive power.

7. A fixed ignition timing of 27° BTC (5° advancement over the standard timing) provided a test bed fuel economy improvement of 2% for cruise operation, however this improvement could not be substantiated during the flight tests.

In a more general sense it can be concluded that the work accomplished satisfied the basic purpose of the contract, to produce the technology necessary to meet the above objectives. That technology included three approaches:

1) Improving fuel metering for better fuel - air ratio control.

2) Reducing heat transfer from exhaust gases to cylinder heads.

3) Oxidation of exhaust pollutants.

The particular hardware or means utilized for this program may not necessarily represent the most cost-effective means of incorporating this technology; an in-depth cost analysis being outside the scope of work. For instance, the fuel injection system selected served well as a tool to demonstrate the benefits of improving fuel-air ratio control but could prove to be too expensive for production. It should not be concluded from this that incorporating technology Item 1 above into a production engine is too expensive but rather the particular fuel injection system in question is too expensive and some less costly means of integrating this technology should be incorporated into the production design. A closed-loop electronic system monitoring EGT or exhaust oxygen level, for example, might be combined with a less expensive fuel injection system to produce a more cost effective system to control fuel-air ratio. Similarly, in reducing heat transfer from exhaust gases to cylinder heads, the use of thermal barrier coatings and/or improved exhaust port design might produce benefits similar to those obtained with port liners at less cost. A similar argument could be made for oxidation of exhaust pollutants by air injection.

REFERENCES

1. Evironmental Protection Agency, "Control of Air Pollution from Aircraft and Aircraft Engines", Federal Register, Volume 38, Number 136, Part 11, Tuesday, July 17, 1973.
2. A. A. Quader, "What Limits Lean Operation in Spark Ignition Engines - Flame Initiation or Propagation?" SAE Paper No. 760760.
3. A. A. Quader, "Lean Combustion and the Misfire Limit in Spark-Ignition Engines", SAE Paper No. 741055, 1974.
4. J. G. Hansel, "Lean Automotive Engine Operation-Hydrocarbon Exhaust Emissions and Combutsion Characteristics", SAE Paper No. 710164, 1971.
5. G. H. Shiomoto, R. F. Sawyer, B. D. Kelly, "Characterization of the Lean Misfire Limit", SAE Paper No. 780235, 1978.
6. "Continental Aircraft Engine Fuel Injection System Operator's Manual", TCM Publication, January, 1973.
7. "E. G. T. Recommendations", TCM Service Bulletin M76-19, 1976.
8. C. E. DeSanctis, "A Systems Engineering Decision Algorithm with Application to Appollo Applications Program Integration Problems," NASA TM X-53992, National Aeronautics and Space Administration, Marshall Space Flight Center, Alabama, February 2, 1970.
9. B. J. Rezy, J. E. Meyers, J. R. Tucker, and K. J. Stuckas, "Screening Anaylis and Selection of Emission Reduction Concepts for Intermittent Combustion Aircraft Engines," NASA CR-135074, National Aeronautics and Space Administration, Lewis Research Center, Cleveland, Ohio, November, 1976.
10. J. A. Bolt, "Fuel Metering by Engine, Speed and Manifold Density", SAE Quarterly Transactions, Vol. 1, No. 3, July, 1947, pp. 498-513.
11. E.E. Kempke, Jr., "Summary Report on Effects of Temperature, Humidity, and Fuel-Air Ratio on Two Air-Cooled Light Aircraft Engines", NASA CP-2005, Presented at The Aircraft Piston Engine Exhaust Emissions Symposium, National Aeronautics and Space Administration, Lewis Research Center, Cleveland, Ohio, September 14-15, 1976, pp. 85-119.
12. Biermann, Arnold E., and Pinkel, Benjamin, "Heat Transfer from Finned Metal Cylinders in an Air Stream", NACA Technical Report No. 488, 1934.
13. Hires, S. D., and Pochmara, G. L., "An Analytical Study of Exhaust Gas Heat Loss in a Piston Engine Exhaust Port", SAE Paper No. 760767.
14. Rush, James H., "Exhaust Port Heat Rejection in a Piston Engine-A Preliminary Report", SAE Paper No. 760766.
15. D. A. Brownson, R. F. Stebar, "Factors Influencing the Effectiveness of Air Injection in Reducing Exhaust Emissions", SAE Paper No. 650526, 1965.
16. W. K. Steinhagen, G. W. Niepoth, S. H. Mick, "Design and Development of the General Motors Air Injection Reactor System", SAE Paper No. 660106, 1966.
17. R. S. Ried, J. G. Mingle, W. H. Paul, "Oxides of Nitrogen from Air Added in Exhaust Ports", SAE Paper 660115, 1966.
18. R. A. Gast, "Pulsair-A Method for Exhaust System Induction of Secondary Air for Emission Control", SAE Paper No. 750172, 1975.
19. D. J. Pozniak, "Exhaust-Port Fuel Injection for Chemical Reduction of Nitric Oxide", SAE Paper 750174, 1975.
20. R. J. Herrin, "The Importance of Secondary Air Mixing in Exhaust Thermal Reactor Systems", SAE Paper 750174, 1975.
21. W. F. Datwyler, A. Blatter, S. T. Hassan, "Control of Emissions from Light Piston - Engine Aircraft", EPA Contract Report APTD-1521, May, 1973.
22. "Detail Specification for TCM Model IO-520-D Air-craft Engine", Teledyne Continental Motors, Mobile, Alabama, June 7, 1978.
23. "IO-520 Series Operation's Manual", X-30041, Teledyne Continental Motors, Mobile, Alabama, August, 1974.

APPENDIX A.

Exhaust emissions for 5-mode EPA cycle for the three combined concepts.

IO520D59X, SER# 174649R, NASA PROTOTYPE ENGINE. 01-24-80, 5 - MODEL LTO CYCLE EMISSION LEVELS.
CONCEPTS A, B PLUS C OPTIMIZED.

PBARO IN HG ABS	TDRY DEG F	TWET DEG F	FUEL HYDROGEN-CARBON RATIO	TAMB DEG F	RATED HP	CID INCH**3	EXHAUST C — H FORMULA	H20 IN AIR PERCENT
30.124	60.00	52.30	2.1250	88.00	300.00	520.00	3.000 5.550	0.650

	UNITS	MODE 2	MODE 3	MODE 4	MODE 5	MODE 6	TOTAL
RUN NUMBER	—	366.	362.	401.	365.	366.	
TIME IN MODE	MINUTES	12.00	0.30	5.00	6.00	4.00	27.30
FUEL FLOW	LB/HR	10.14	147.00	104.30	50.10	10.14	
INDUCTION AIR FLOW (W)	LB/HR	161.00	1843.00	1315.40	785.00	161.00	
EXH. AIR INJ. FLOW (D)	LB/HR	145.00	288.00	269.50	237.00	145.00	
HYDROCARBON CONC.	PPM-C W	120.00	40.50	18.00	15.00	120.00	
OXIDES OF NITROGEN CONC	PPM W	20.00	225.00	375.00	1700.00	20.00	
CARBON MONOXIDE CONC.	PERCENT	0.35	3.51	1.63	0.21	0.35	
CARBON DIOXIDE CONC.	PERCENT	9.40	12.50	13.40	11.89	9.40	
OXYGEN CONC.	PERCENT	10.50	0.31	0.25	5.80	10.50	
WET CORRECTION FACTOR	—	0.85403	0.85403	0.85403	0.86388	0.85403	
PROP. TORQUE	FT-LB	34.00	554.00	449.00	285.00	34.00	
PROP. SPEED	RPM	1200.00	2850.00	2500.00	2100.00	1200.00	
MFLD PRESSURE	IN HG ABS DRY	12.00	28.80	25.80	21.00	12.00	
INDUCTION AIR TEMP	DEG F	63.00	60.00	61.00	61.00	63.00	
COOLING AIR TEMP	DEG F	94.00	99.00	99.00	95.00	94.00	
COOLING AIR DELTA P	IN H20	0.70	1.80	1.00	0.90	0.70	
MAX CYL HEAD TEMP	DEG F	265.00	449.00	410.00	358.00	265.00	
EXHAUST GAS TEMP	DEG F	808.00	1652.00	1661.00	1265.00	808.00	
DESIRED F/A	LB/LB	0.06340	0.08000	0.07890	0.06370	0.06340	
INDUCTION F/A RATIO (D)	LB/LB	0.06339	0.08028	0.07981	0.06424	0.06339	0.06677 TA
IND. F/A EQUIV. RATIO (D)	—	0.95	1.20	1.19	0.96	0.95	1.00 TA
TOTAL F/A RATIO (D)	LB/LB	0.03325	0.06937	0.06617	0.04927	0.03325	0.04320 TA
ENGINE OBSERVED POWER	HP	7.77	300.63	213.73	113.96	7.77	
OBSERVED BMEP	PSI	9.86	160.66	130.21	82.65	9.86	
OBSERVED BSFC	LBM/BHP-HR	1.305	0.489	0.488	0.440	1.305	
CARBON BALANCE MASS EMISSIONS							
HC EMISSION RATE	LB/HR	0.01431	0.04268	0.01434	0.00705	0.01431	
BRAKE SPECIFIC HC	LBM/BHP-HR	0.00184	0.00014	0.00007	0.00006	0.00184	
HC MASS / MODE	LB	0.00286	0.00021	0.00119	0.00070	0.00095	0.00593
HC MASS / RATED HP	LB/HP						0.00002
HC - PERCENT OF EPA STANDARD							1.04
CO EMISSION RATE	LB/HR	0.71940	63.76755	22.38448	1.72070	0.71940	
BRAKE SPECIFIC CO	LBM/BHP-HR	0.09261	0.21211	0.10473	0.01510	0.09261	
CO MASS / MODE	LB	0.14388	0.31884	1.86537	0.17207	0.04796	2.54812
CO MASS / RATED HP	LB/HP						0.00849
CO - PERCENT OF EPA STANDARD							20.22
NOX EMISSION RATE	LB/HR	0.00791	0.78618	0.99046	2.64850	0.00791	
BRAKE SPECIFIC NOX	LBM/BHP-HR	0.00102	0.00262	0.00463	0.02324	0.00102	
NOX MASS / MODE	LB	0.00158	0.00393	0.08254	0.26485	0.00053	0.35343
NOX MASS / RATED HP	LB/HP						0.00118
NOX - PERCENT OF EPA STANDARD							78.54

APPENDIX B.

Flight test instrumentation equipment lists.

ITEM	RECORD
1. Elapsed time	Clock and Recorder Chart Speed, hr:min
2. Calibrated Crankshaft Speed	Electro-Optical Index, rpm
3. Indicated Crankshaft Speed	Aircraft Indicator, rpm
4. Crankshaft Torque	Digital Readout, 0-560 ft-lb.
5. Indicated Fuel Flow	Aircraft Indicator, lb/hr
6. Fuel Injection Pump Capsule Chamber Manifold Air Pressure	Pressure Gage, MAP-3 or CCMAP 0-40 in. Hg.
7. Manifold Pressure, Line Tee	Pressure Gage, MAP-2, O-40 in. Hg.
8. Peak Exhasut Gas Temperature	Digital Readout, CH No. 6, ° F
9. Engine Oil Temperature	Aircraft Indicator, 1/4 ot 1/2 of Green Arc.
10. Exhaust Gas Plume Temperature	Temperature Gage, EGPT, 0-600° F
11. Cowl Flap Position	Detent Location, 1-8
12. Calibrated Airspeed, Normal Pitot Static Source	Aircraft Airspeed Indicator, KIAS corrected to KCAS
13. True Airspeed, Probe Pitot Static Source	Installed Airspeed Indictor, Corrected MPH
14. Rate of Climb	Aircraft Indictor, Ft./min., @ 100 KIAS and Zero Wing Flaps
15. Rate of Descent	Aircraft Indicator, ft/min., @ 2300 RPM and Zero Wing Flaps
16. Outside Air Temperature (OAT)	Cabin Thermometer and Digital Readout (Ref. CH-23, Prime for LED)
17. Cabin Density Altitude	Absolute Prssure Gage, CPA, 0-30 in. Hg.
18. Indicated Altitude	Aircraft Altimeter, ft. ASL and Window Barometric Setting, in. Hg.
19. Cabin Vent Position	Control Locations, OPEN/CLOSE
20. Barometric Pressure	Mercury Barometer, in. Hg.
21. Vapor Pressure	Psychometric Chart, in. Hg.
22. Wet and Dry Bulb Temperature	Thermometer and Sling Psychrometer, ° F/° F
23. Cooling AirΔP, Upper	Pressure Gage, 0-20 in. H20
24. Cooling Air Static P, Lower	Pressure Gage, 0-20 in. H20
25. Cylinder Head Temperature, Reference	Temperature Gage, CHT-5 (Hot) 0-460° F
26. Fuel Injection Pump Flow Rate	Gage, Total Fuel Flow x10, lb/hr

APPENDIX B

STRIP CHART RECORDER (SCR2) — HONEYWELL RY 15303846, 24-CHANNELS

Measurement	Transducer	Channel No.
1. Cylinder Head Temperatures (6)	Thermocouple, Type J, Iron-constantan	1 - 6
2. Exhaust Gas Temperature (6)	Thermocouple, Type K, Chromel-alumel	7 - 12
3. Fuel Temperature, Flow Meter Inlet, S/N: 23022 (1)	Thermocouple, Type J, Iron-constantan	13
4. Cooling air Intake Plenum Temperature (2) — Lower (CH-14), Upper (CH-15)	Thermocouple, Type J, Iron-constantan	14 & 15
5. Cooling Air Cowling Exit Temperature (2) — R. H. Vent (CH-16), L.H. Vent (CH-17)	Thermocouple, Type J, Iron-constantan	16 & 17
6. Engine Induction Air Box Temperature, At Throttle Body (1)	Thermocouple, Type J, Iron-constantan	18
7. Air Injection Pump Discharge Temperature (1)	Thermocouple, Type J, Iron-Constantan	19
8. Exhaust Port Skin Temperature (2) — Cyl. Hd. No. 1 (CH-20), Cyl. Hd. No. 6 (CH-21)	Thermocouple, Type J, Iron-constantan	20 & 21
9. Outside Air Temperature (2)— R.H. Wing (Prime), Cowling Landing Light Instl. (Secondary)	Thermocouple, Type J, Iron-constantan	23

STRIP CHART RECORDER (SCR1) — ESTERLINE ANGUS, 910121, SPEED SERVO II, 2-CHANNELS

Measurement	Transducer	Channel No.	Range Setting
1. Fuel Injection Pump Flow Rate, Total (1)	Floscan, Turbine Transducers, Model 201B S/N: 23022 (Inlet) & S/N: 23023 (return), 0-200 lbm/hr	1 — Red	W X 2
2. Crankshaft Torque (1)	Lebow Torque Sensor & Signal Generator, 0 - 1000 ft-lb	6 — Green	Q X 10

RECORDING OSCILLOGRAPH (SCR3) — CONSOLIATED ELECTRODYNAMICS CORP., 5-124A, 8-CHANNELS

Measurement	Tranducer	Channel No.	Range Setting
1. Induction manifold Air Pressure (1)	Bourns Pressure Transducer, 0-15 psia, Model No. 4271, P/N: 200451006	Amp. No. 2	20mVdc, Galvanometer No. 8, 1 div. = 2 in. Hg.
2. Throttle Control Position (1)	Bourns Position Potentiometer, 0-80°, Model No. 2051085014, 2.25 in., 2K Ohms.	Amp. No. 3	100 mVdc, Galvanometer No. 9, 1 div. = 10°
3. Servo Oil Inlet Pressure (1)	Bourns Pressure Transducer, 0-100 psig, P/N: 200556101	Amp. No. 5	100 mVdc, Galvanometer No. 11 1 div. = 10 psi
4. Mixture Control Position (1)	Bourns Position Potentiometer, 0-80°, P/N: 2051085014 2.25 in., 2K Ohms.	Amp. No. 1	100 mVdc, Galvanometer No. 7, 1 div. = 10°
5. Air Injection Pump Discharge Pressure (1)	Bourns Pressure Transducer, 0-25 psig, P/N: 2055431003	Amp. No. 6	100 mVdc, Galvanometer No. 12, 1 div. = 1 psi
6. Crankshaft Speed (1)	Anadex P1-600 Frequency to Voltage Converter with Electro Products 3010 AN Magnetic Pickup, 0-3000 rpm	Amp. No. 4	5.0 Vdc, Galvanometer No. 10 1 div. = 200 rpm

APPENDIX C

Flight test comparison results — Baseline versus prototype engine.

		BASELINE ENGINE			PROTOTYPE ENGINE			
	MODE OF OPERATION	TIME IN MODE (MIN.)	DATA POINT NUMBER	FUEL FLOW (lbm/hr)	FUEL USED PER MODE (lbm)	PERCENT FUEL SAVED PER MODE	DATA POINT NUMBER	FUEL FLOW (lbm/hr)	FUEL USED PER MODE (lbm)
*	IDLE OUT	1.0	300.0	7.0	0.12	-0.3	1.0	8.9	0.15
*	TAXI OUT	11.0	301.0	18.0	3.30	1.5	2.0	17.2	3.15
*	TAKEOFF	0.3	302.0	152.0	0.76	0.3	3.0	145.4	0.73
*	CLIMB	5.0	303.0	114.0	9.50	16.9	4.0	93.9	7.83
	ENROUTE CLIMB	7.5	306.0	124.8	15.60	46.0	7.0	88.3	11.04
	CRUISE	83.2	57.0	78.0	108.16	7.0	68.0	77.5	107.47
	CRUISE DESCENT	9.0	22.0	64.6	9.69	3.0	83.3	62.6	9.39
*	APPROACH	6.0	309.0	81.0	8.10	26.9	83.5	54.3	5.43
*	TAXI IN	3.0	311.0	18.0	0.90	-0.8	87.0	19.6	0.98
*	IDLE IN	1.0	312.0	6.0	0.10	-0.5	88.0	8.9	0.15
	TOTALS	**127.0**	—	—	**156.23**	**100.0**	—	—	**146.32**

	BASELINE	PROTOTYPE
AVG. TRIP FUEL ECONOMY (mi/gal)	12.3	13.1
AVG. TRIP SPEED (mi/hr)	155.3	155.3
PERCENT FUEL USED DURING LTO CYCLE	14.6	12.6

*EMISSIONS LANDING/TAKEOFF (LTO) CYCLE MODES.

APPENDIX D

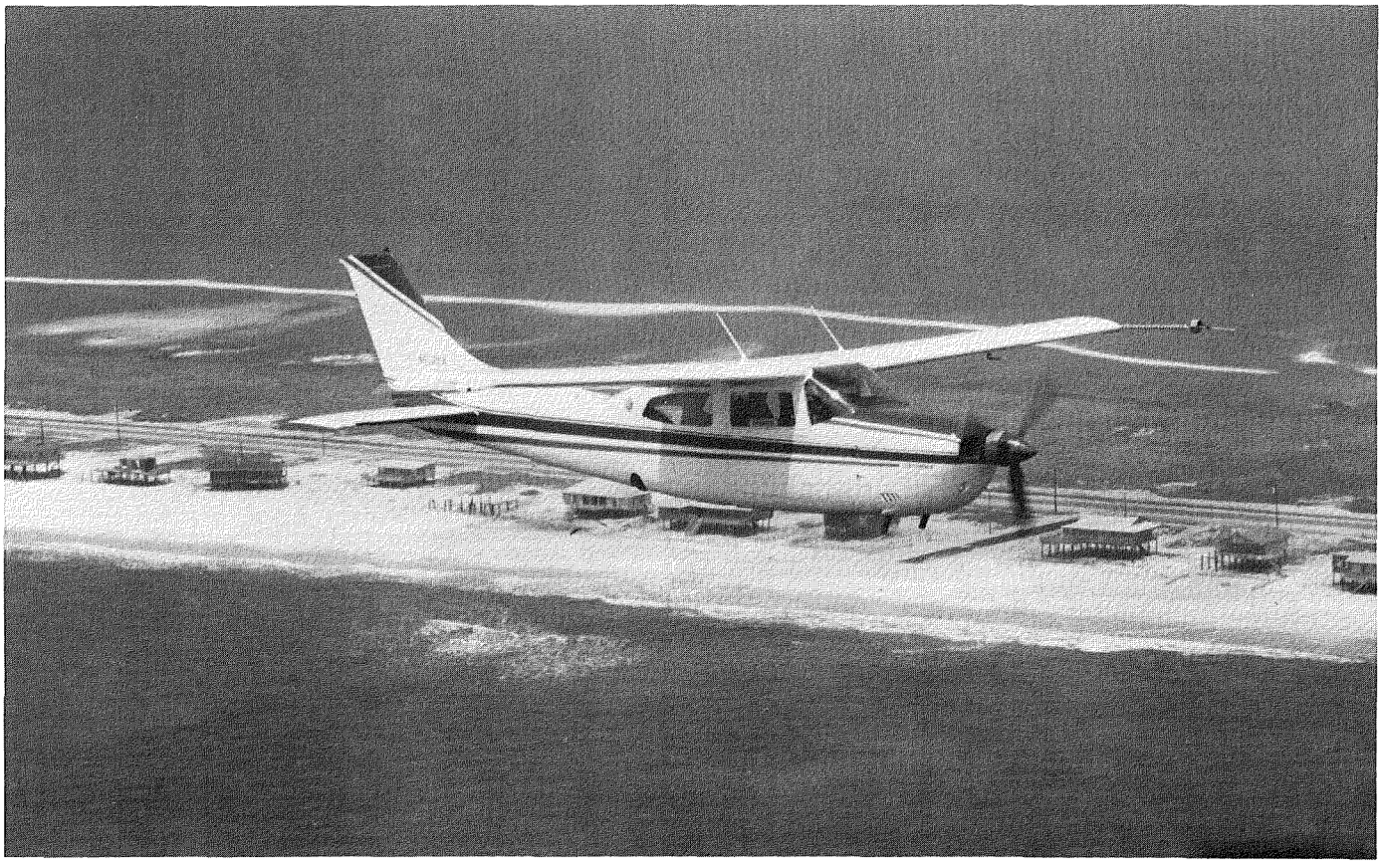

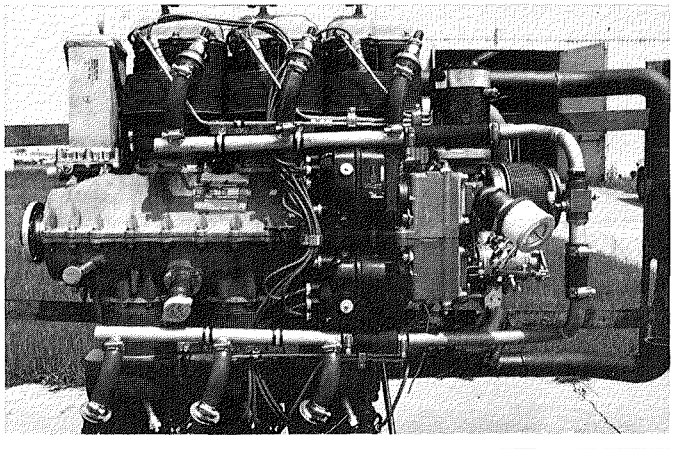

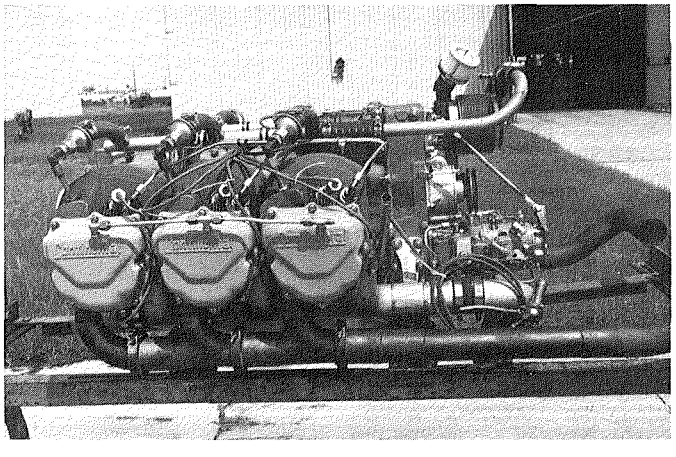

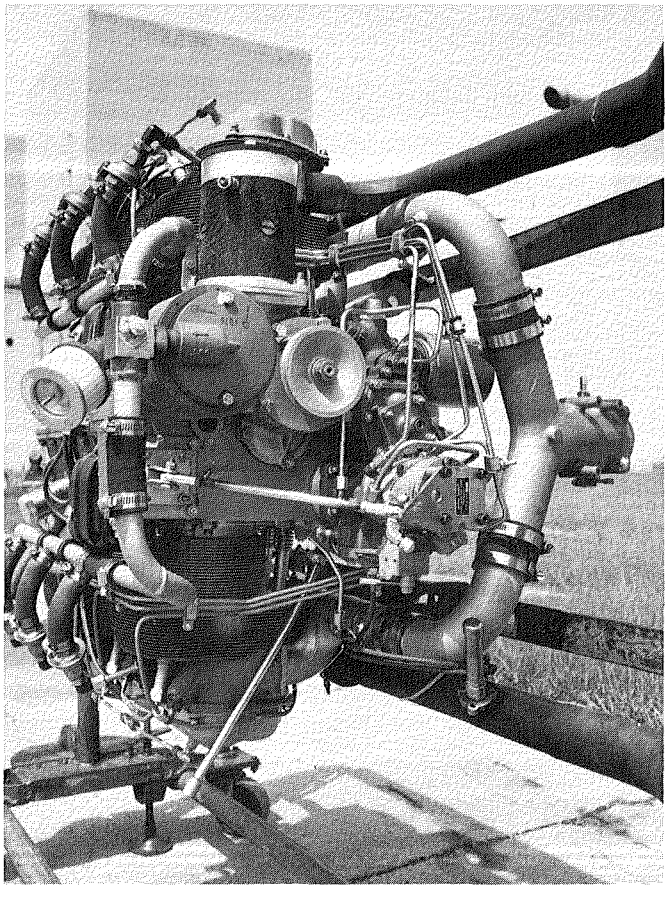

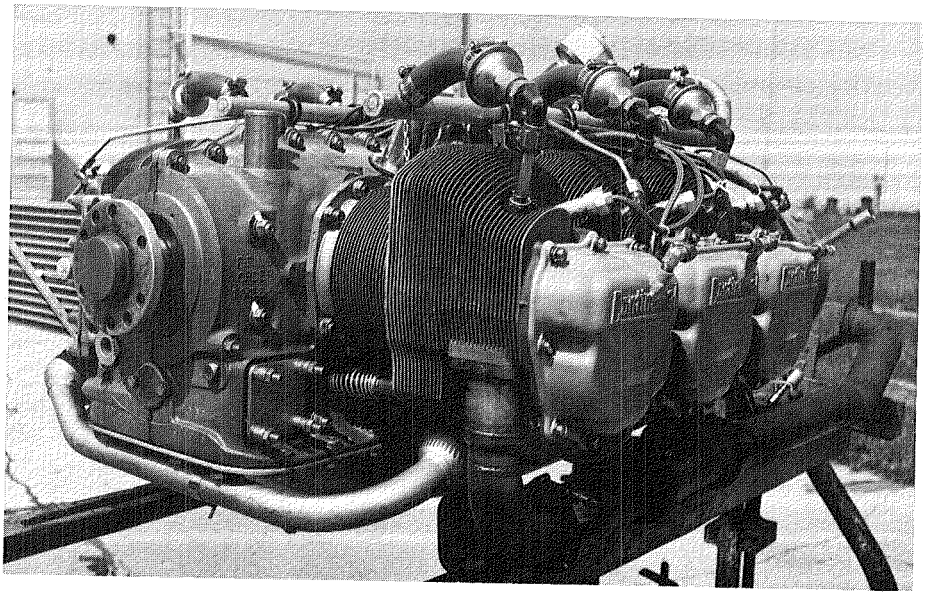

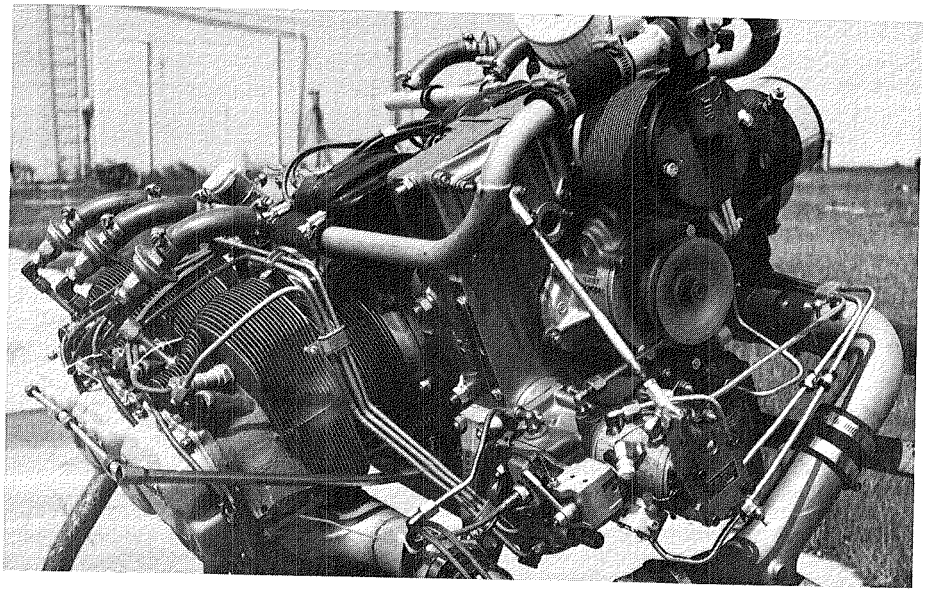

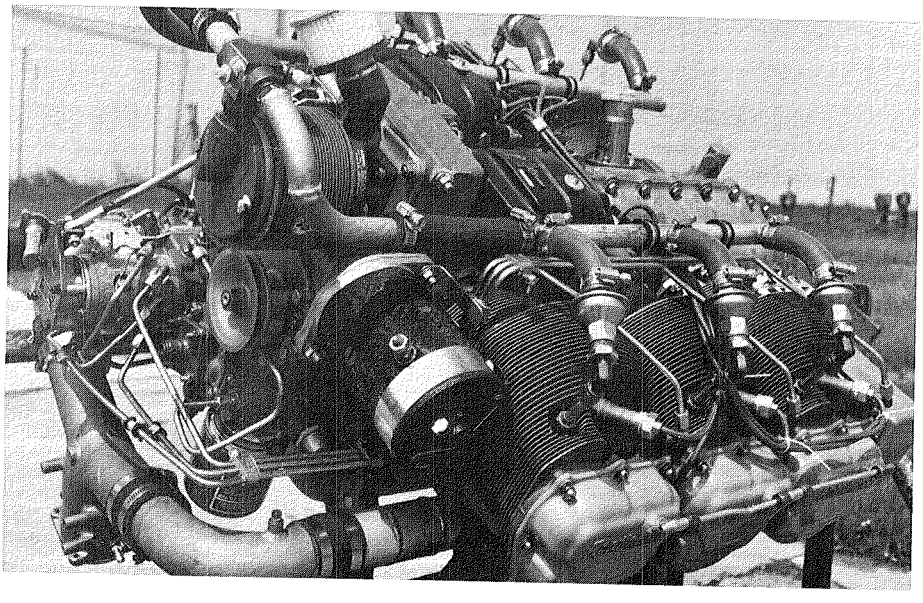

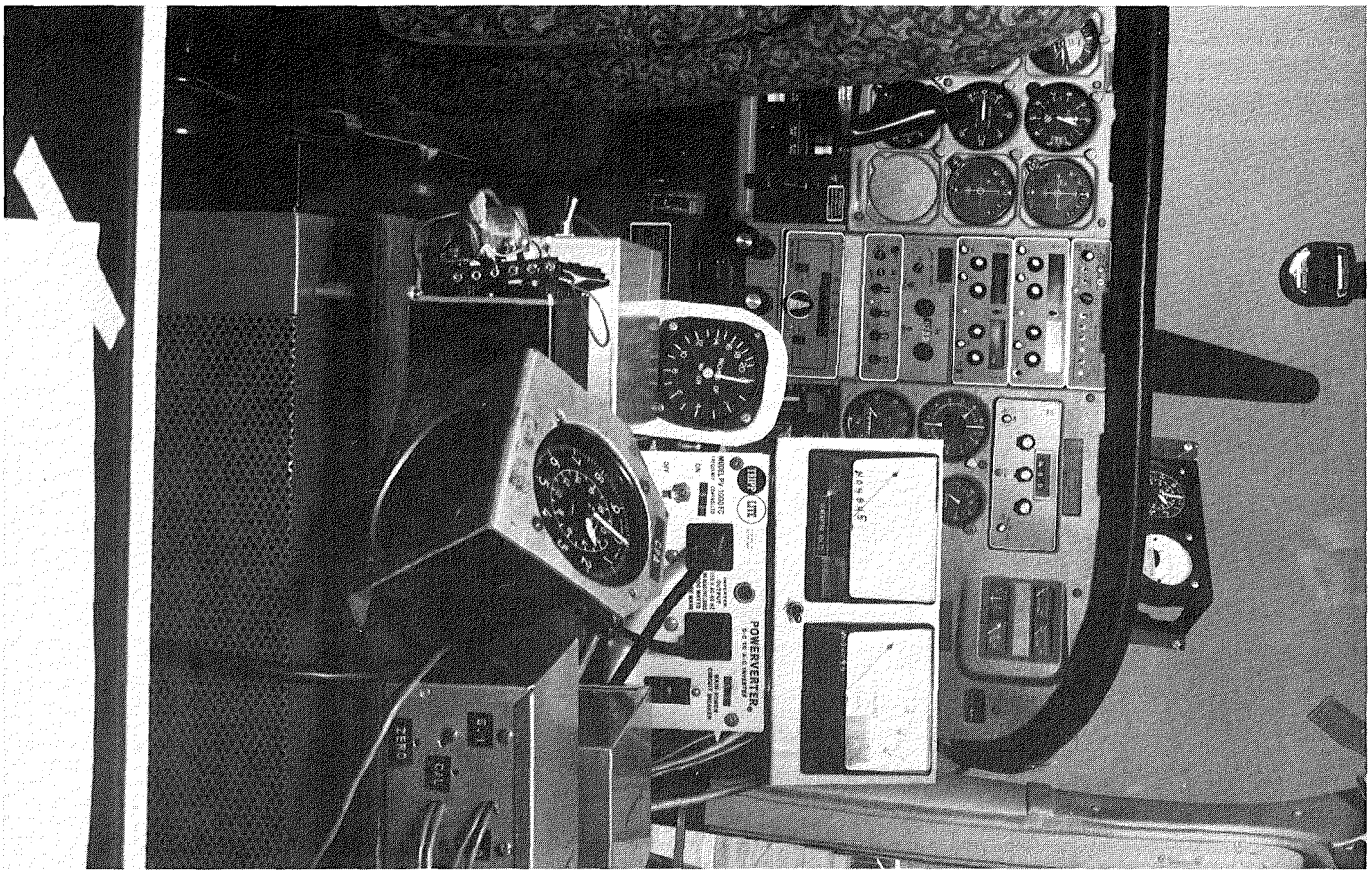
POWERVERTER

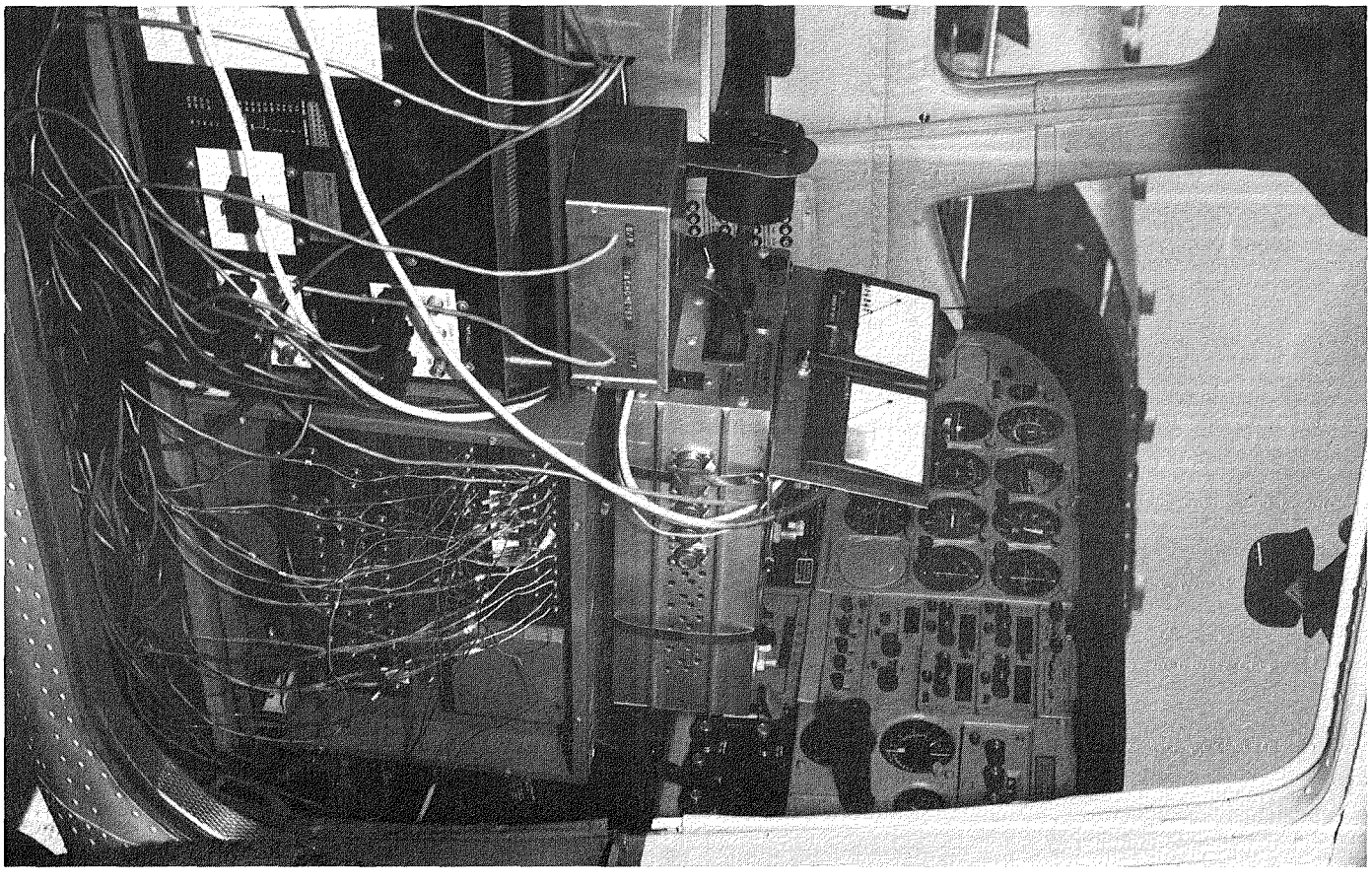


600
datagraph® 5-164
BELL & HOWELL

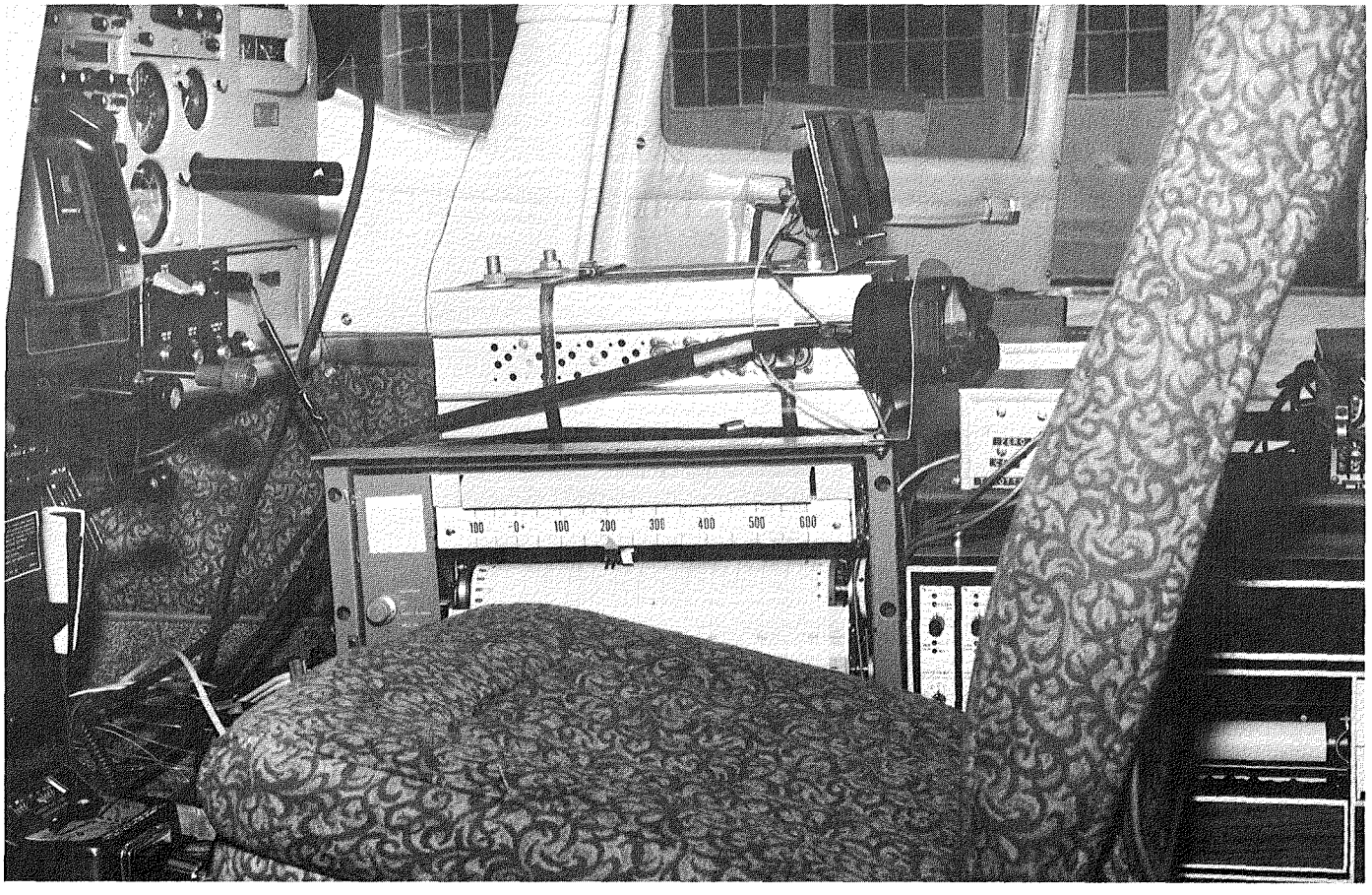
100 0 100 200 300 400 500 600

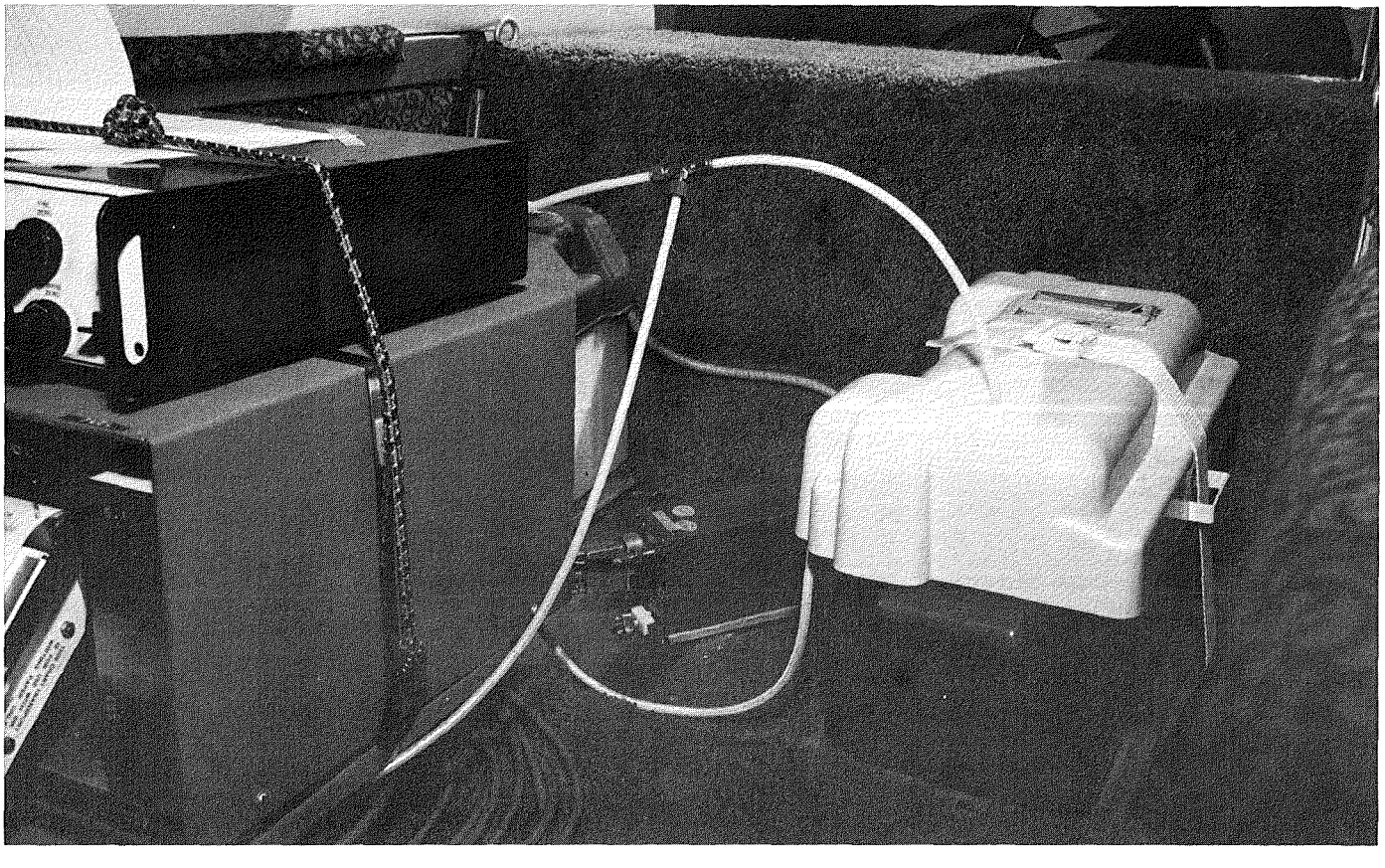


PHONE


CESSNA
N5525A

DISTRIBUTION LIST

Piper Aircraft Corp.
Lakeland Division
3000 Medulla Avenue
Lakeland, FL 33803
Attn: Harvey O. Nay (1)
Graham Gates (1)

Dr . Montgomerie C. Steele (1)
AiResearch Manufacturing Co.
of Arizona
402 South 36 Street
Phoenix, AZ 85034

George W. Westphal (1)
Grumman American Aviation
Corporation
318 Bishop Road
Cleveland, OH 44143

Max E. Bleck (1)
President and Chief Executive Officer
Piper Aircraft Corp.
Vero Beach, FL 32960

James Kirwin (1)
Bendix Corporation
717 N. Bendix Drive
South Bend, IN 46620

Professor J. A. Nicholls (1)
Department of Aerospace
Engineering
University of Michigan
Ann Arbor, MI 48109

Carl F. Bachle
Consultant
72 Moran Road
Grosse Point Farms, MI 48238

J. David Powell (1)
Aero/Astro Department
Stanford University
Stanford, CA

Beech Aircraft Corporation
9709 E. Central
Wichita, KS 67201
Attn: Mr. J. Terry (1)
Mr. R. Benefiel (1)
Mr. R. Tamlinson (1)
Mr. C. Rembleske (1)

Mr. E. Nichols (1)
Piper Aircraft Corp.
P. O. Box 1328
Vero Beach, FL 32960

L. Waters (1)
Senior Vice President of Engineering
Teledyne-Continental Motors
P. O. Box 90
Mobile, AL 36601

Bernard J. Rezy (14)
Vice President, Engineering
Teledyne-Continental Motors
P. O. Box 90
Mobile, AL 36601

Edward LaCouture
Naval Ship System Engineering Station
Code 031B
Philadelphia, PA 19112

Mr. Carmen DiGiandomenico
U.S. Marine Corps. Development
and Education Command
LVT(X) Directorate, D16
Quantico, VA 22134

AVCO-Lycoming
Williamsport Division
652 Oliver Street
Williamsport, PA 17701
Attn: A. Light (1)
S. Jedszowski (1)
L. Duke (1)
J. Masten (1)

William T. Westfield
Program Manager (1)
Environmental Research Branch
FAA-ARD-550
Washington, DC 20591

Professor Roger W. Van Gunst
Dept. of Aerospace
Engineering
University of Michigan
Ann Arbor, MI 48109

Professor Samuel S. Lestz (1)
Pennsylvania State University
208 Mechanical Eng. Building
University Park, PA 16802

NASA Scientific and Technical (25)
Information Facility
Accession Department
P. O. Box 8757
Balt./Wash. International
Airport, MD 21240

Department of Transportation (1)
Reference Library
Federal Aviation Administration
Washington, DC 20590

Environmental Protection (1)
Agency
Reference Library
2565 Plymouth Road
Ann Arbor, MI 48105

Environmental Protection (1)
Agency
Reference Library
Washington, DC 10460

Federal Aviation Administration (1)
Attn: AW455/G. D. Kittredge
NAFEC, ANA-410
Atlantic City, NJ 08405

Curtiss-Wright Corporation
One Passaic Street
Wood-Ridge, NJ 07075
Attn: Charles Jones (1)
Robert Mount (1)
Murray Berkowitz (1)
David Myers (1)
Irving Manning (1)
William Figart (1)
Larry Loeffler (1)

Advanced Technology Laboratory (1)
U.S. Army RTL
Attn: John White
Ft. Eustis, VA 23604

Headquarters U.S. Army Material (1)
Development and Readiness
Command
Attn: DRCLDC/Robert Langworthy
50001 Eisenhower Avenue
Alexandria, VA 22333

Naval Weapons Center
Attn: 128/George Handler
China Lake, CA 93555

NASA-Lewis Research Center
21000 Brookpark Road
Cleveland, OH 44135
Attn: W. Wintucky, 500-127 (1)
Lewis Library, 60-3 (2)
Report Control, 5-5 (1)
M. Beheim, 3-5 (1)
D. Poferl, 500-207 (1)
E. Willis, 500-127 (1)
J. McFadden, 500-127 (1)
R. Dezelick, 500-127 (1)
W. Strack, 501-10 (1)
T. Wickenheiser, 501-10 (1)
R. Plencner, 501-10 (1)
J. Eisenberg, 501-10 (1)
A. Willoughby, 501-1 (1)
J. Acurio, 302-2 (1)
P. Meng, 500-127 (25)

NASA Headquarters
600 Independence Avenue, SW
Washington, DC 20546
Attn: H. Johnson, RJG-2 (1)
P. Evanich, RJG-2 (1)
R. Rose, RJG-2 (1)
N. Mayer, RJL-2 (1)

NASA Langley Research Center
Hampton, VA 23365
Attn: R. Bower (1)
L. Williams (2)
J. Stickle (2)

NASA Ames Research Center
Moffett Field, CA 94035
Attn: L. Roberts (1)
T. Galloway (1)
P. Talbot (1)
H. Dean Wilstead (2)

NASA Dryden Flight Research Center
P. O. Box 273
Edwards, CA 93523
Attn: L. Gillam (1)

GAMA
1025 Connecticut Avenue, NW
Washington, DC 20036
Attn: Mr. Stanley Green (5)

Fairchild Republic Company
Farmingdale Long Island, NY 11735
Attn: Mr. C. Prokop (1)
Mr. Decker (1)

Swearingen Aviation Company
P. O. Box 32486
San Antonio, TX 78284
Attn: Mr. James Kirkpatrick (1)

Flying Magazine
P. O. Box 321
Basking Ridge, NJ 07920
Attn: Mr. J. Olcott (1)

DOT/FAA
800 Independence Avenue, SW
Washington, DC 20591
Attn: Mr. C. Blake (1)
Mr. T. Horeff (1)
Mr. R. Nugent (1)
Reference Library (1)

Gulfstream American Aviation
P. O. Box 2206
Savannah, GA 31402
Attn: Mr. R. Stewart (1)

Mooney Aircraft Corporation
P. O. Box 72
Kerrville, TX 78028
Attn: Mr. T. Smith (1)

Piper Aircraft Company
820 E. Bald Eagle Street
Lock Haven, PA 17745
Attn: Mr. F. Strickland (1)

National Air Trans. Association
1010 Wisconsin Avenue
Washington, DC 20007
Attn: Mr. W. Power (1)
Mr. L. Brian (1)

Mr. R. L. Maxwell
Transportation Program Manager
Office of Technology Assessment
United States Congress
Washington, DC 20510

University of Oklahoma
865 Ast Street
Norman, OK 73019
Attn: Prof. Carl Bergie (1)

Massachusetts Institute of Technology
Cambridge, MA 02139
Attn: 3-340/Prof. J. Haywood (1)
3-447/David Wilson (1)

Princeton University
School of Engineering and Applied Sciences
Dept. of Mech. and Aerospace Engrg.
Princeton, NJ 08540
Attn: Prof. S. Bogdonoff (1)
Prof. L. Sweet (1)

University of Kansas
Department of Aerospace Engineering
Lawrence, KS 66045
Attn: Prof. Jan Roskam (1)

Mr. H. J. Wood (1)
Consultant
14285 Valley Vista Blvd.
Sherman Oaks, CA 91413

Mr. Donald Weidhuner (1)
Consultant
Route 1, Box 333
Edinburg, VA 22824

Bell Helicopter
P. O. Box 482
Ft. Worth, TX 76101
Attn: Mr. R. May (1)

Hughes Helicopter
Centinela Avenue and Teale Street
Culver City, CA 90230
Attn: Mr. C. Perry (1)
Mr. F. Strible (1)

Mr. R. R. Brown
NAIR-330
Propulsion Administrator
Commander, Naval Air Systems Command
Washington, DC 20361

Lt. Commander H. Richardson (1)
NAIR-5362 C4
Energy Efficient Engines and Propellers
Commander, Naval Air Systems Command
Washington, DC 20361

Col. D. H. Smith
D.R. STS-X
U.S. Army Aviation Research and Development Command
St. Louis MO 63166

Defense Advanced Research Project Agency
1400 Wilson Blvd.
Arlington, VA 22209
Attn: Mr. S. Sigman, Jr. (1)

Mr. Roger L. Smith (1)
DRDAV-NC
CDR, AVRADCOM
4300 Goodfellow Blvd.
St. Louis, MO 63120

Naval Air Development Center
Code 605B
Warminster, PA 18974
Attn: Mr. David B. Bailey (1)

Institute of Defense Analysis
400 Army Navy Drive
Arlington, VA 22202
Attn: Dr. Donald Dix (1)
Dr. David Wilson (1)

Mr. Thomas Falatko (1)
Department of the Air Force
Pentagon
Washington, DC 20330

Mr. Jerry Turner (1)
AFWAL/POOC
Wright Patterson AFB, OH 45433

Mr. Everett Bailey
AFWAL/NASA
Wright Patterson AFB, OH 45433

Dr. Paul Glance
Department of Army
Headquarters U.S. Army TACOM
Warren, MI 48090

Mr. George Cheklich
U.S. Army Tank Automotive Command
Research and Development Center
DRSTA/GBA
Warren, MI 48090

U.S. Army Tank Automotive Command
Research and Development Center
Propulsion Systems Division
DRSTA/RGET
Warren, MI 48090
Attn: Ernie Schwartz (1)
Richard W. Munt (1)

Dr. Walter Bryzik (1)
U.S. Army Tank Automotive Command
Propulsion Systems Division
38111 Van Dyke
Warren, MI 48090

Department of the Army
Office of the Deputy Chief of Staff
for Research Development and
Acquisition
Washington, DC 20310
Attn: DAMA-ZE/Charles Church (1)

Department of the Navy
Naval Sea Systems Command
Washington, DC 20362
Attn: Code 5231/Dan A. Groghan (1)
Code 5231/Martin G. Kandl (1)

Teledyne Continental Motors
General Products Division
76 Getty Street
Muskegon, MI 49442
Attn: S. Berenyi (1)
A. Brouwers (1)

Avco Everett Research Laboratory,
Inc.
Attn: Fred Sheldon (1)
Everett, MA 02149

General Motors Research
Laboratories
Attn: Charles A. Amann (1)
Warren, MI 48090

Outboard Marine Corporation
Research Center
Attn: George G. Lassanske (1)
4109 N. 27th Street
P. O. Box 663
Milwaukee, WI 53201

Ceradyne, Inc.
Attn: Richard J. Palicka (1)
3030-A South Red Hill Avenue
Santa Ana, CA 92705

Defense and Space Systems Group of
TRW, Inc.
Attn: Dr. Robert J. Jones (1)
Building O-I, Room 2171
One Space Park
Redondo Beach, CA 90278

Eaton Corporation
Engineering and Research Center
Attn: Richard Chute (1)
26201 Northwestern Highway
P. O. Box 766
Southfield, MI 48037

Gould, Inc., Gould Laboratories
Attn: Dr. Lee A. Swanger (1)
540 East 105th Street
Cleveland, OH 44108

Wallace Murray Corporation
Attn: Robert C. Bremer, Jr. (1)
1125 Brookside Avenue
P. O. Box 80-B
Indianapolis, IN 46206

Department of Transportation
Technology
Attn: Curtis Swanson (1)

Western Michigan University
Kalamazoo, MI 49008

Bendix
Electric and Fluid Power Division
Attn: R. A. Elliott (1)
211 Seward Avenue
Utica, NY 13503

AiResearch Industrial Division
Garrett Automotive Products Company
Attn: Paul Craig (1)
3201 Lomita Boulevard
Torrance, CA 90505

Flying
Attn: Nigel Moll (1)
One Park Avenue
New York, NY 10016

AOPA
Attn: J. B. Hartranft, Jr. (1)
7315 Wisconsin Avenue
Washington, DC 20014

Automotive Engineering Magazine
SAE, Inc.
Attn: L. Givens
400 Commonwealth Drive
Warrendale, PA 15096

Cessna Aircraft Corporation
Pawnee Division
Wichita, KA 67201
Attn: D. Ellis (3)
G. Huggins (3)
A. Mueller (3)
J. Hembrey (3)
Everett A. Lake
Air Force Wright Aeronautical
Laboratories
Aerospace Power Division
Wright-Patterson AFB, OH 45433

End of Document